UNIVERSITY OF MANITOBA

ENERGY AUDIT OF A PASSIVE SOLAR RESIDENCE WITH EMPHASIS ON BASEMENT HEAT LOSSES AND SOLAR GAINS

by

Dharmendr Seebaluck

A Thesis

Submitted to the Faculty of Graduate Studies in partial

Fulfilment of the Requirements for the

Master of Science Degree in Mechanical Engineering.

Winnipeg, Manitoba

ENERGY AUDIT OF A PASSIVE SOLAR RESIDENCE WITH EMPHASIS ON BASEMENT HEAT LOSSES AND SOLAR GAINS

BY

DHARMENDR SEEBALUCK

A thesis submitted to the Faculty of Graduate Studies of the University of Manitoba in partial fulfillment of the requirements of the degree of

MASTER OF SCIENCE

Dedicated To My Father

I hereby declare that I am the sole author of this thesis.

I authorize the University of Manitoba to lend this thesis to other institutions or individuals for the purpose of scholarly research.

Dharmendr Seebaluck

I further authorize the University of Manitoba to reproduce this thesis by photocopying or by other means, in total or in part, at the request of other institutions or individuals for the purpose of scholarly research.

Dharmendr Seebaluck

ACKNOWLEDGEMENTS

The author of this thesis wishes to express his deepest gratitude to Prof. R.E Chant for his continuing interest, encouragement and professional guidance without which this thesis would have been impossible. Special thanks to Prof.J.D. Welch for providing his residence and continuous access for this study. The author is grateful to Manitoba Hydro for providing financial assistance under a research grant.

Many thanks and appreciation are expressed to the following: Mr. Ike Warkentin for his continuous interest and input in this thesis, Terry Armstrong for his advice in using ANSYS, and to S. Jaganathan for his support and encouragement while this thesis was being written.

Special thanks goes to the technicians of the University of Manitoba for their help in equipment handling.

The author would like to finally express his gratitude to his mother and sister in Mauritius for their sincere encouragement and advice.

ABSTRACT

The development of low energy homes has made computer analysis of home heating requirement an important field of study. As low energy homes become more efficient, the basement heat loss becomes a larger percentage of the total heating requirement. This results in the need for an accurate method of predicting basement heat loss so that home designers may optimize basement insulation placement. Finite element analysis have been used in the determination of the below grade basement heat loss, and compared to two years of experimental ground temperature data. However, this thesis emphasizes the application of the ANSYS computer program to determine basement heat losses.

This study is based on a passive solar energy efficient home with 45% of the south wall comprised of triple pane low emissivity glass. Several sky models are compared in order to establish their effect on solar gains. The performance of a heat recovery ventilator under in situ conditions is also experimentally verified. An energy audit is performed to consolidate the use of the HOT-2000 program, which is an energy analysis program for the design of residences.

TABLE OF CONTENTS

LIST OF TABLES

LIST OF FIGURES

NOMENCLATURE

N = 4, the number of segments of the interior surface area
A_n = area of segment n
$q_n(t)$ = average heat flux through the segment area, A_n, at time t.
$q_{a,n}$ = annual mean value of $q_n(t)$,
$q_{v,n}$ = amplitude of the first harmonic of the heat flux variation,
ω = angular velocity of the first harmonic,
t = time.
S_n = the shape factor for the steady state heat loss component,
Θ_B = basement air temperature,
Θ_G = ground surface temperature averaged over both time and area
V_n = shape factor for periodic heat loss,
σ_n = amplitude attenuation factor,
Θ_v = amplitude of the first harmonic of ground surface temperature,
Δt_n = time lag of the heat flux harmonic relative to the surface variation.
$S_n(R)$, $V_n(R)$ = steady state and periodic shape factors for insulation with thermal resistance, R.
a_n, b_n, c_n, d_n = constants of a specific basement and insulation placement.
[K] = matrix relating [d] to [A] often called the stiffness matrix or coefficient matrix;
[d] = degree of freedom vector;
[A] = action vector.
[K] = thermal conductivity matrix;
[T] = temperature vector;
[Q] = heat flow rate vector.
[C] = specific heat matrix;
[T] = time-derivative of [T];
I_{th} = hourly global radiation on a horizontal surface (RF1),
I_d = hourly diffuse radiation on a horizontal surface (RF2),
I_b = hourly beam radiation on a horizontal surface,
I_o = hourly extraterrestrial radiation on a horizontal surface,
I_{tt} = total radiation on a tilted (slope) surface.
H = monthly average daily radiation on a horizontal surface,
H_o = monthly average daily extraterrestrial radiation on a horizontal surface,
m = depth of the atmosphere with respect to the vertical path at the equator (ie. m=1 at the equator).
R_b = Beam radiation on tilted surface/ beam radiation on horiz surface,
= $\cos\theta/\cos\theta_z$;
$\cos\theta$ = $\cos(L-\beta)\cos\delta\cos\omega + \sin(L-\beta)\sin\delta$;
$\cos\theta_z$ = $\cos L\cos\delta\cos\omega + \sin(L-\beta)\sin\delta$;
R_d = diffuse radiation on tilted surface/ diffuse on a horiz surface;
= $(1+\cos\beta)/2$;

R_r = $\rho(1-\cos(\beta))/2$;
θ = angle of incidence of beam radiation, measured between the beam and normal for the surface;
θ_z = zenith angle, the angle between the beam and the vertical to the earth's surface;
L = latitude angle;
β = angle between the plane surface and the horizontal, tilt or slope of the surface;
δ = angle of declination;
ρ = reflectance;
ρ = monthly average ground reflectance;
ρ_a = the cloudless sky reflectance- 0.25;
ρ_c = the cloud reflectance- 0.6;
n = number of hours of bright sunshine;
N = theoretical day length.
m = mass flow rate;
c_p = specific heat capacity;
ΔT_{max} = maximum temperature difference between hot and cold fluid.
H = Total space heating required (w);
L_t = Total heat losses above grade by transmission through exterior walls, ceilings, windows, doors (w);
L_a = Total heat losses due to indoor-outdoor air exchange (natural infiltration+mechanical);
L_b = Total Basement Heat Losses by Transmission below-grade;
η_i = Utilization factor for the internal gains from appliances and lighting, hot water heater and from occupants (%);
G_i = Total heat gain from internal sources (w);
η_s = Utilization factor for solar gains through glazing (%);
G_s = Total solar heat gains through glazing (w).
$t\infty$ = Ambient temperature;
$t\infty m$ = Ambient mean temperature;
ω = $2\pi f$, where f is the frequency;
k = constant, thermal conductivity of ground;
x = depth;
h = constant, convection coefficient;
τ = time lag = $x/(\sqrt{(2\alpha\omega)})$;
λ = $\sqrt{(\omega/2\alpha)}$;
α = thermal diffusivity.
%moist = % moisture content in soil;
ρ = density of soil.

1. INTRODUCTION

1.1 Background

The emphasis of the analysis is placed on the experimental evaluation of basement heat losses for an energy efficient residence, meticulously designed and now occupied by Prof. John Welch, Faculty of Architecture, University of Manitoba. The residence is located at 1 Stormont Drive (south of the perimeter highway) Winnipeg, Manitoba. Approximately 65 thermocouples were selectively located adjacent to the residence as shown in Fig.1 at various depths (Fig.2-Fig.3) to provide experimental data to verify the finite difference computer model that was developed at the University of Manitoba and to evaluate the basement heat losses predicted by the HOT-2000 computer program. This program was developed by the National Research Council and used by Energy, Mines & Resources to evaluate the energy consumption of the houses built under the R-2000 Program. Many published reports claim that existing computer models have been verified by field experimentation, but the predicted annual energy losses for basements vary by a factor of two [1]. Thus there is a need for additional experimental work on basement heat losses.

The project started as an experimental basement heat loss analysis in an attempt to reduce some of the uncertainties that lead to the discrepancy in losses predicted by some existing computer programs. However to verify the results it was necessary to perform an energy audit on the residence. It is a passive solar house (45% of the south wall is tripled glazed) equipped with several energy conserving features such as a heat recovery ventilator (HRV). Thus the project became a house energy analysis.

Continuous record of the ground temperatures and utilities were kept from September 1988 until August 1990, on a weekly basis. Hourly solar insolation data on a south facing vertical surface were maintained for the 1989/90 heating season to evaluate acceptable sky models. Monitoring of the HRV was also performed for the month of February 1990 and from mid-January to March 31/91 at two hour intervals in order to obtain the seasonal performance. Hourly internal and external environment conditions and weekly snow depth for the 1989/1990 heating season were also recorded. A blower door infiltration test was also performed by UNIES LTD, to determine the air tightness of the building envelope which is a pertinent factor in an overall energy balance of a residence.

1.2 Review of Previous Related Research Work on Basement Heat Losses

The HOTCAN computer model was developed by the Prairie Regional Office of Division of Building Research, National Research Council and was tested on unoccupied huts at the Alberta Home Heating Research Facility [2,3]. There is some evidence at that the computer program does not accurately predict losses from uninsulated basement walls. There was also other evidence that the Mitalas's heat loss method yields conservative results [1] and leads to high losses at depths of two metres or greater.

The University of Manitoba undertook a computer study related to basement heat losses during the summer of 1985 using a finite difference method; this was reported upon in 1986 [4]. The study identified a phenomenon that was not previously observed; namely that, the placement of horizontal insulation immediately above the weeping tile, which is intended to protect the tile from freezing, actually increased the heat losses from

the basement by 3 to 6% depending on its projection and the R value of the insulation. Another study of basement heat losses performed at the University of Saskatchewan indicated that radiation played a significant role in the calculations [5]. There is a lack of experimental data for the determination of basement heat losses and these were the reasons for initiating the present experimental studies in the summer of 1987. The two-dimensional finite difference calculations performed at the University of Manitoba were used as a guide in positioning the thermocouples at appropriate depths around the test house and thus establish the actual temperature contours. Previous authors have reported that computer models have been verified by field instrumentation but predicted annual energy losses vary by a factor of two [1].

Thermal contours based on the experimental data were compared to the University of Manitoba finite difference program which was developed by Timothy Kostyniuk. The results show that the actual measured frost line is above that predicted by the computer program; the computer model of the basement is extremely sensitive to snow cover. A more recent development, the ANSYS finite element computer program which would allow a theoretical two-dimensional transient analysis to be performed was considered adaptable to the basement heat losses and thus was included in the study.

1.3 Review of Solar Heat Gain

There is some indication that the direct fraction of monthly average total radiation used in the HOT-2000 program overestimated the solar heat gains, since most models of the sky radiation are empirical and inappropriate models may have been used. The over

estimation of the mean monthly solar fraction was as much as 40%. The total solar heat gain, estimated by the HOT-2000 program to be 36% of the annual space gain, is the most significant source of heat next to the furnace. Therefore this study includes the validity of the solar model used in the HOT-2000 program.

1.4 Necessity for an Energy Balance

The ability to determine the heat loss from residential buildings became an important topic in Canada with the advent of energy efficient homes brought about by rising energy costs. The increased interest in low energy homes such as the R-2000 has created a new field of research in heat loss prediction and analysis. Features such as leak-proof vapour barriers, double-wall construction, and air-to-air heat exchangers in new homes necessitated new methods of analysis. This home has the added passive solar feature. However to add credibility to this study it was necessary to perform a complete energy balance.

One of the major areas of research when analyzing the heat loss of a building is the losses throughout the basement walls and floor which are responsible for up to 25% of the total heat loss from a house [6]. Since the basement heat loss is a major component of the total house heating requirement, there is a need for an accurate method to predict basement heat loss [7]. An accurate means of predicting the basement heating load would allow home designers to select, through simulation checks, particular basement designs and to study the impact of the insulation placement on the heating requirements.

2. BACKGROUND AND THEORY

The basis for basement heat loss calculations is an application of the basic heat transfer equations. Its use have become extremely advanced using finite element modelling. The primary mode of heat transfer from basement walls and floor is conduction, which is the diffusion of heat from a higher to a lower temperature region due to the direct contact between molecules of the medium [8]. To establish the conduction through the walls and floor of the basement, the temperature field in the medium (i.e., the soil) is required. Most of the current research trends incorporate some form of finite element modelling to determine the temperature regime. The exception to this is the work completed by G.P. Mitalas of the National Research Council [7]. His method of calculation utilizes analytical and experimental data to develop a set of factors which are then used in the calculation of the basement heat loss [7]. It is this method of calculation which is used in the energy analysis software HOTCAN 3.0

The previous research [9] performed at the University of Manitoba was to compare computer simulated basement heat loss, developed by Tim Kostyniuk as an undergraduate thesis, with actual measured data. A finite difference computer program was used to determine the thermal regime at the centre line of the basement wall and the effects of insulation placement on basement heat loss. It is from the predicted thermal regimes that the basement heat loss is then calculated. This program is a modification of the program written by D. Whitmore and M. Zahn to predict the thermal regimes beneath roads and buildings where permafrost degradation is a problem [10].

2.1 Mitalas Basement Heat Loss Calculations in HOTCAN 3.0

As indicated previously, the research by G.P. Mitalas of the National Research Council (NRC) is the basis of heat loss calculation used in the HOTCAN 3.0 home energy analysis program. This computer program has been updated to version 5.06 and now is known as the HOT-2000 program since it was initially used for the analysis of R-2000 homes. Although there have been many improvements in the later versions of this program, there have been no changes made in the basement calculations. The program continues to use the Mitalas formulation. The main changes include the window solar heat gain and infiltration calculations.

2.1.1 Mitalas Description of the Basement Model

The Mitalas basement model takes into account five elements;

(a) the basement wall above grade;
(b) the basement wall and floor below grade;
(c) the ground surface adjacent to the basement;
(d) a lower thermal boundary at a constant temperature equal to the mean ground temperature;
(e) the conducting mass between the basement, the ground surface and the lower thermal boundary.

The model assumes that sufficient ground water flow occurs to maintain a constant temperature at some depth below the basement floor [7]. The cross section and plan view of the Mitalas basement model are shown in Fig. 4 and Fig. 5 respectively.

2.1.2 The Heat Loss Theory and Formulation

The above grade portion of the basement heat loss is treated similar to the walls in the remainder of the home (Fig. 4, A_1) and for this reason it is not relevant to this topic. The below grade instantaneous heat loss is calculated by:

$$Q(t) = \sum_{2}^{N} A_n \cdot q_n(t), \quad (1)$$

where: N = 4, the number of segments of the interior surface area,
A_n = area of segment n,
$q_n(t)$ = average heat flux through the segment area, A_n, at time t.

The heat flux at time, t, is given by

$$q_n(t) = q_{a,n} + q_{v,n} \sin(\omega t), \quad (2)$$

where: $q_{a,n}$ = annual mean value of $q_n(t)$,
$q_{v,n}$ = amplitude of the first harmonic of the heat flux variation,
ω = angular velocity of the first harmonic,
t = time.

The amplitude values of the first and second harmonics of the ground surface temperature for several locations in Canada are listed in Table I [7]. The first harmonic is used as the approximation of the annual ground surface temperature because the second and higher harmonics are attenuated considerably and they are relatively small. The soil surface temperature follows a sinusoidal curve as a function of soil composition, depth, air temperature, conductivity and time of year. The two components of the average heat flux throughout the area segment in equation (2) are given by,

$$q_{a,n} = S_n(\theta_B - \theta_G), \quad (3)$$

where: S_n = the shape factor for the steady state heat loss component,
Θ_B = basement air temperature,
Θ_G = ground surface temperature averaged over both time and area

$$q_{v,n}(t) = V_n \sigma_n \theta_v \sin\omega(t+\Delta t_n), \qquad (4)$$

where:
- V_n = shape factor for periodic heat loss,
- σ_n = amplitude attenuation factor,
- Θ_v = amplitude of the first harmonic of ground surface temperature,
- Δt_n = time lag of the heat flux harmonic relative to the surface variation.

The shape factor for the steady state heat loss component, S_n, given in equation (3) is the overall conductance between the basement interior surface and the two boundaries, that is the ground surface adjacent to the basement and the lower boundary at the mean ground temperature, as illustrated in Fig 4. This shape factor also takes into account the surface heat transfer coefficient of the basement interior wall.

The shape factor, V_n, in equation (4) represents the total conductance between the wall segment and the ground surface. This means that the steady state heat loss has two components while the periodic heat loss has only one component [7].

2.1.3 Determining the Mitalas Basement Heat Loss Factors

All of the factors employed in the Mitalas basement heat loss calculations, and given by equations (1) to (4), were determined by using the cross-sectional model shown in Fig.4. The model employs two-dimensional heat conduction along the basement walls and three dimensional heat conduction at the corners of the basement. This modelling neglects the following:

(1) time variations of ground water level and temperature,
(2) the flow of melt water and rain around the basement,
(3) the change in thermal properties of the soil due to backfilling and the effect of the freezing plane,

(4) ground temperature variation due to solar effects, adjacent buildings, and snow cover.

The thermal conductivity of the soil can be divided into two separate values, above and below the basement floor respectively. However, soil conductivities greater than 1.5 W/m K are beyond the scope of this method.

The shape factors, S_n and V_n, for any basement insulation arrangement are calculated using a temperature for each adjacent ground and basement temperature. From this the heat flux was determined through each area segment of the basement. The heat flux through the interior surface of the basement was determined by using the commercially known finite element package ANSYS for steady state computations and was compared to the periodic calculations using TWO-DEPEP. The two-dimensional finite element model used approximately 500 elements and the three dimensional sections at the corners used about 5000 elements.

The shape factor for the specific insulation placement is related to the insulation thermal resistance, R (for 1<R<5), by:

$$S_n(R) = \frac{1}{(a_n + b_n R)}, \tag{5}$$

$$V_n(R) = \frac{1}{(c_n + d_n R)}, \tag{6}$$

where: $S_n(R)$ and $V_n(R)$ = steady state and periodic shape factors for insulation with thermal resistance, R.

a_n, b_n, c_n, d_n = constants of a specific basement and insulation placement.

The expressions for S_n and V_n for different basement insulation placements at a given soil thermal conductivity are given in Table II. More tables are listed for a variety of insulation placements and soil thermal conductivities are in the Mitalas reference. The attenuation and time lag factors from equation (4) were determined by calculating the periodic heat flux using a sine wave for ground surface temperature. From these calculations, a set of attenuation and time lag factors were determined and are included in Table II.

The three dimensional effects at the corners of the basement are taken into account by the use of a corner allowance factor, L_n listed in Table II. This factor was determined by comparing the heat loss for the basement wall and floor segments with the estimated heat loss for the corners by the ANSYS program. A set of calculations using Mitalas formula is given in Appendix A.

2.2 Basement Heat Loss Determination: University of Manitoba

A finite difference program was developed by Tim Kostyniuk at the University of Manitoba [11]. The conditions employed for executing the program and the corresponding grid set up under the basement are illustrated in Fig.6. This computer program assumes a symmetrical basement with no variation in depth. Thermal contours obtained from the weekly experimental ground temperature record were compared with the results generated from the finite difference program, the results of his program predicted the frost to be deeper than the actual frost depth, based upon experimental data acquired. However, some of the differences in the results may be due to the snow depth.

Since the actual basement is bi-level and unsymmetrical, the assumption made in the

simulation is not applicable. Therefore there is invariably a need for modification of the program to adjust to the actual basement configuration. The modification could be accomplished by a similar analysis for the other half of the structure. However, a full two-dimensional analysis of the basement model should yield more accurate results. Therefore ANSYS has been applied to a two-dimensional thermal analysis and is considered the most desirable approach to solve this complex problem. The validity of this analysis is verified by comparing weekly experimental ground temperature results with calculated results.

2.2.1 Introduction to ANSYS and Solving Method

ANSYS was developed in 1970 by Swanson Analysis Systems Inc., and all further developments and updates have been maintained by the company. To date, this finite element program has been used in over 1600 applications, which includes 500 universities [40]. The program capabilities are listed as follows: static and dynamic structural analysis, fluid dynamics and acoustic analysis, kinematic analysis, and magnetic and piezoelectric analysis.

The ANSYS program allows for variable geometries and properties. The program was developed for stress analysis but is equally applicable to fluid flow and thermal conduction fields. In addition it can also handle transient problem and provides acceptable results. The ANSYS program in this study deals only with the below-grade losses of the residence.

The use of ANSYS involves three stages; first Preprocessing, which requires the user to define the analysis type, material and geometric properties, model geometry and

loading conditions. The second stage is termed the Solution phase where the program assembles, solves the simultaneous equations, and calculates the results. The third phase is known as the Postprocessing stage, where the user evaluates the results by creating graphic displays such as thermal contours and heat flux directions, tabular listings, x-y plots, etc. All three phases are further described below.

2.2.2 The Preprocessing Stage

In this stage the four different categories considered are as follows:

1. Analysis type: For this study, a thermal analysis with transient behaviour was chosen.
2. Material and Geometric properties: Each material used in the model was represented in terms of thermal conductivity, density, and specific heat. There were 12 materials that describe this model and they are listed as: concrete floor, void form, compacted gravel, concrete wall, unfrozen soil, Baseclad, wall insulation, drywall, concrete pile, styrofoam insulation, snow, soil.
3. Model Geometry: The model geometries can be defined in any of the three common co-ordinate systems. An element library consisting of 75 different element types shown in Appendix B can be used to properly distinguish the geometry, but choice of elements is dependent upon geometry and analysis type. Keypoints describing the geometry are specified and lines are then connected to the keypoints to define the areas bounded by these lines. Appropriate material property is then assigned to each of the defined areas followed by meshing of the area. A schematic model of the area, and the meshed model is presented in Fig.7 and Fig.8, respectively.
4. Loading Conditions: This is achieved by changing the boundary conditions over time;

for instance, the temperature and convection coefficients can be changed as required in order to represent the varying weather conditions.

2.2.3 The Solution Stage

In heat transfer applications the heat flow rate is termed the action and the temperature is the degree of freedom (DOF). The action and the DOF are related by a set of basic equations. The purpose of the finite element method is to determine the solution to these equations across the engineering system being analyzed (model). The simplest form of such an equation is as follows:

$$[K]\ [d] = [A]\ , \tag{7}$$

where: [K] = matrix relating [d] to [A] often called the stiffness matrix or coefficient matrix;

[d] = degree of freedom vector;

[A] = action vector.

In general, [K] and [A] are known, and [d] is initially unknown. For a steady state thermal analysis, the equation is:

$$[K]\ [T] = [Q]\ , \tag{8}$$

where: [K] = thermal conductivity matrix;

[T] = temperature vector;

[Q] = heat flow rate vector.

For this study a transient thermal analysis for the below grade portion of the basement

was required. Its purpose was to determine the temperature distribution as a function of time and/or the rates of heat transfer and heat storage within a structure subjected to time-varying thermal loads. The main difference between a steady state and a transient thermal analysis in ANSYS is that in a transient analysis the applied loads (temperatures and convection coefficients) are time-dependent therefore the solution is time dependent. However all other considerations, such as types of thermal loads, the modes of heat transfer are similar to a steady state analysis. A transient analysis can be described as

$$[C]\,[\dot{T}] + [K]\,[T] = [Q]\,, \tag{9}$$

where: [C] = specific heat matrix;

$[\dot{T}]$ = time-derivative of [T];

[K] = thermal conductivity matrix;

[T] = nodal temperature vector;

[Q] = heat flow rate vector.

The only difference between equations (8) and (9) is the term involving the specific heat matrix that accounts for the heat stored in the model.

In order to solve the basic equation (7) across the entire system, the system must be represented by discrete, interconnected pieces (elements). Once the thermal conductivity matrices are determined for each element, all of the individual [K] matrices are assembled to form the set of simultaneous equations [K][d]=[A]. The solution of the simultaneous equations gives response values at every degree of freedom across the entire system. Equation (9) is solved similarly as equation (8), but the specific heat matrix and

time derivative of [T] are included in the solving process.

The element type best suited for this study is STIFF55 (see Appendix B for detail), with four nodes for a two-dimensional space and temperature being the DOF (the unknown). For the solution of the simultaneous equation with large systems, the program uses the wave-front direct solution method. It involves assembling and solving the overall stiffness matrix for the structure. Upon calculation of this matrix, the program begins solving for the individual DOF, and removing them from the original matrix by a Gaussian elimination. The final DOF set in the matrix is referred to as the "wave front'.

2.2.4 The Postprocessing Stage

In this section, a review of the results of the analysis is performed. Graphical displays of temperature, heat flux and thermal gradient are possible. The ANSYS program has two types of post processors: post 1, the general postprocessor, and post 26, the time-history post processor. Post 1 allows a review of the results of any load step and iteration for the entire model. For example, it is possible to display temperature distribution for load step 3 or at a specified time in a transient thermal analysis. Post 26, allows a review of the variation of a result, such as the time history of the temperature at a specific location in the model with respect to time.

2.2.5 Algorithm of the Model

The program is structured in such a way that the thermal analysis is performed over the period of May 1989 to August 1990. ANSYS performs a steady state solution for the first load step which corresponds to a solution for the first week of May 1989. From thereon, weekly solutions for each loadstep are carried out. There are seven

iterations per loadstep, with an iteration for each day of a week (the basement model program and load file is included in Appendix B.

Within each loadstep the following parameters are specified:

1. time corresponding to each week,
2. weekly ambient temperature and convection coefficients at the surface of the ground/or snow depending on time of year,
3. fixed convection coefficient and ambient temperature inside the basement,
4. fixed mean deep ground temperature of 6.1°C which is an isothermal boundary.

Since the properties of certain materials are not constant over the analysis period, ANSYS enables the user to stop the program and change the material properties. Thereafter the program restarts from the previous load step solution. This feature allows for the presence of snow in the winter time (depending on snow record) and its absence for the rest of the year.

The restart option allows for change in thermal conductivity, density and specific heat for the respective zones shown in Fig.9 and Fig.10 from unfrozen soil to frozen soil because the ground adjacent to the wall freezes to a certain depth. The sequence with snow cover and changes in properties of the different zones as well as the ground under the basement floor (denoted as rest of ground) is illustrated in Fig.9 and Fig.10.

2.3 Solar Modelling

ASHRAE methods are based on a "hypothetical " calculation of the atmospheric transmissivity at m=1 and an extinction coefficient for altitude angles other than 90 degrees. On the other hand, active solar researchers have been attempting to use the records of solar radiation data collected by the Canadian Atmospheric Environment Services (AES) over the years. The nomenclature used is as follows:

I_{th}- hourly global radiation on a horizontal surface (RF1),

I_d- hourly diffuse radiation on a horizontal surface (RF2),

I_b- hourly beam radiation on a horizontal surface,

I_o- hourly extraterrestrial radiation on a horizontal surface,

I_{tt}- total radiation on a tilted (sloped) surface.

RF1 and RF2 are the respective readings made for I_{th} and I_d by the AES weather stations.

H - monthly average daily radiation on a horizontal surface,

H_o - monthly average daily extraterrestrial radiation on a horizontal surface,

m - depth of the atmosphere with respect to the vertical path at the equator (ie. m=1 at the equator).

If the instantaneous values of the solar radiation and hourly values are not available or there is a need to reduce the number of calculations for a computer analysis, it may be convenient to use the monthly average daily values. There are well known relationships for calculating the total radiation on a tilted surface for isotropic sky conditions and are given by;

$$I_{th}=I_b+I_d, \tag{10}$$

$$I_{tt}=R_bI_b+R_dI_d+R_rI_{th}, \tag{11}$$

where: R_b = Beam radiation on tilted surface/ beam radiation on horiz surface,

$= \cos\theta/\cos\theta_z$;

$\cos\theta = \cos(L-\beta)\cos\delta\cos\omega + \sin(L-\beta)\sin\delta$;

$\cos\theta_z = \cos L\cos\delta\cos\omega + \sin(L-\beta)\sin\delta$;

R_d= diffuse radiation on tilted surface/ diffuse on a horiz surface;

= $(1+\cos\beta)/2$;

R_r= $\rho(1-\cos(\beta))/2$;

and θ = angle of incidence of beam radiation, measured between the beam and normal for the surface;

θ_z = zenith angle, the angle between the beam and the vertical to the earth's surface;

L = latitude angle;

β = angle between the plane surface and the horizontal, tilt or slope of the surface;

δ = angle of declination; ρ = reflectance;

For the physical significance of angles see Fig.11.

The above relationships assumes the isotropic sky and is based on the concept of clearness index first introduced by Liu and Jordan [12]. The clearness index, K_t, is the ratio of the measured total horizontal solar intensity on the earth surface to the extraterrestrial horizontal insolation and is an apparent transmissivity. By 1975, Canada had built up twenty years of diffuse radiation measurements for only four weather stations which were analyzed at the University of Manitoba [13].

Orgill and Hollands [14] equations (12),(13) and (14), are based on original data evaluated at the University of Manitoba and there is good agreement between each other. The University of Wisconsin work includes Erbs et al [15] equations (15), (16) and (17) and more recently (1990) Reindl et al [16] developed equation (19), (20) and (21) and all

are compared in Fig. 12.

ORGILL and HOLLANDS CORRELATION:

For $K_t<0.35$ then:

$$K=1.0-0.249K_t, \tag{12}$$

For $0.35\leq K_t\leq 0.75$ then:

$$K=1.557-1.84K_t, \tag{13}$$

For $K_t>0.75$ then:

$$K=0.177, \tag{14}$$

ERBS and KLEIN CORRELATION:

For $K_t\leq 0.22$ then:

$$K=1.0-0.09K_t, \tag{15}$$

For $0.22<K_t\leq 0.80$ then:

$$K=1.0-0.09K_t+4.388K^2{}_t-16.638K^3{}_t+12.336K^4{}_t, \tag{16}$$

For $K_t>0.80$ then:

$$K=0.165, \tag{17}$$

An anisotropic model was developed by Professor J. Hay of the University of British

Columbia, a climatologist with extensive experimental experience. He developed an anisotropic sky model in 1979 and he pointed out the difficulty with the simple empirical models was that the coefficients showed substantial hourly, as well as spatial variations. The relationships between the fractional time of bright sunshine and the apparent atmospheric transmissivity could not be correlated for different locations and for different times. Also isotropic assumption leads to root mean square errors of between +/- 7 and +/- 18% for Vancouver and Toronto respectively.

Hay's anisotropic correlation for a monthly average clearness index by given in the following equation:

$$\frac{H}{H_o} = \frac{[0.1572+0.5566(n/N)]}{[1-\rho[\rho_a(n/N)+\rho c(1-n/N)]]}, \qquad (18)$$

where: ρ = monthly average ground reflectance;

ρ_a = the cloudless sky reflectance- 0.25;

ρ_c = the cloud reflectance- 0.6;

n = number of hours of bright sunshine;

N = theoretical day length.

The reflectance from the ground, the clear sky and cloud cover are introduced in equation (18). A polynomial relationship for the ratio of the diffuse to the horizontal is then developed in terms of monthly clearness index [17]. By the application of a correction for the ratio of the daily bright sunshine to the total daylight hours and reflection transmissivity, correlation was extended to daily rather than hourly values. The correlation was verified within the accuracy of the instrumentation for Vancouver and

Whitehorse at 30, 60, 90 degrees tilt angles facing south. The method is extremely complex and restricted to mid-latitude and continental climate.

Professor J.K. Page, University of Sheffield, developed a correlation [18] which was thorough and verified by solar data collected from 10 wide-spread sites from latitude 40^0North to 40^0South. It gives excellent results for high latitudes, Bergen, Italy, Norway (Lat.60N), as well as Canadian cities. The method is simple and easy to use. The RMS error is between 0.18 and 0.756 for nine sites checked in Europe and Canada.

Version 5.06 of HOT-2000 program started out with the Erbs et al [15] model (equations 15,16,17) to obtain the direct and diffuse components and then converted these into monthly apparent values using the technique developed by Hay to create an anisotropic model. Hay used variables such as, fraction of bright sun, cloudless sky reflectance and a cloud reflectance to correlate the data. HOT-2000 modified the polynomial relationship developed by Hay by expressing the clearness index in terms of the fraction of bright sunshine.

The Hay model has not been accepted widely by the engineering community. It depends on human judgemental variables such as the cloud and clear sky reflectance which weakens his approach. The correlation is shown in Fig.12 and tends to yield considerably lower values of radiation on the tilted surfaces as shown by the AES plot in Fig.13. Whereas later developments at the University of Wisconsin used variables provided by the actual weather data. The more recent work by Reindl et al (University of Wisconsin) 1990 was finally selected as the best model currently available. The reason being that an anisotropic model depends upon unmeasurable variables such as cloud and

sky reflectance whereas Reindl et al use measurable variables such as the clearness index (K_t), altitude angle (α), ambient temperature (T_a) and relative humidity (ϕ) (see equations 19, 20, 21). The Erbs et al model was not selected because it is an isotropic model and provides higher radiation on a vertical surface (Fig.13).

Interval: $0 \leq K_t \leq 0.3$; Constraint: $I_d/I \leq 1.0$.

$$\frac{I_d}{I} = 1.000 - 0.233 K_t + 0.0239 \sin(\alpha) - 0.000682 T_a + 0.0195 \phi \quad (19)$$

Interval: $0.3 \leq K_t \leq 0.78$; Constraint: $0.1 \leq I_d/I \leq 0.97$.

$$\frac{I_d}{I} = 1.329 - 1.1716 K_t + 0.267 Sin(\alpha) - 0.00357 T_a + 0.106 \phi, \quad (20)$$

Interval: $0.78 \leq K_t$; Constraint: $I_d/I \geq 0.1$.

$$\frac{I_d}{I} = 0.426 K_t - 0.256 Sin(\alpha) + 0.00349 T_a + 0.0734 \phi, \quad (21)$$

Their correlation reduce the residual sum of the squares by 14% over the use of the clearness index only [16]. The data has been verified experimentally in Gainsville, Fa, New York, Copenhagen, Hamburg, Oslo and Valentia (Ireland) and agrees with Erbs et al model which is verified by 20 world sites [15].

2.4 Heat Recovery Ventilator Analysis

The purpose of a heat recovery ventilator (HRV) is to maintain ventilation in a space sealed by a continuous vapour barrier and recover some of the heat from the

exhaust air to preheat the fresh incoming air. During the winter months the cold fluid is fresh outdoor air and the hot fluid is the indoor air. The two fluids are forced to cross through the HRV core as illustrated in Figs. 15 and 16. The core consists of a series of flow passages; the hot and cold fluid flow through adjacent passages without interacting with each other, which is achieved by placing a heat transfer surface between them. This heat exchange configuration is known as a cross flow because the fluid streams flow perpendicular to each other. By using the HRV the house is able to receive the required airchanges per hour (ACH) while reclaiming some of the energy from the air exiting from the house.

2.4.1 Theory

Residential heat recovery ventilators use a cross flow heat exchange flow pattern illustrated in Fig.16. Performance is analyzed by the determination of effectiveness and temperature efficiency. Effectiveness is defined as the ratio of the actual heat transfer to the maximum possible heat transfer rate. The maximum heat transfer rate is a function of the mass flow rate, specific heat capacity and maximum temperature difference between the two fluids and is given by:

$$Q_{max} = (mc_p)_{min} (\Delta T_{max}) , \qquad (22)$$

where: m = mass flow rate;

c_p = specific heat capacity;

ΔT_{max} = maximum temperature difference between hot and cold fluid.

The term $(mc_p)_{min}$ denotes the minimum heat capacity of the fluid. Therefore the

effectiveness for heating the cold fluid is given by :

$$\varepsilon = \frac{m_c C_{pc} (T_{co} - T_{ci})}{(mC_p)_{min} (T_{hi} - T_{ci})}, \qquad (23)$$

The temperature efficiency for a balanced system and the same fluid is then given by:

$$\eta = \frac{(T_{co} - T_{ci})}{(T_{hi} - T_{ci})}, \qquad (24)$$

It is equal to the effectiveness when the heat capacity of the cold fluid is equal to the minimum heat capacity, that is balanced flows, which should be closely approximated for residential application.

2.5 Infiltration Test Description

To determine the air tightness of the residence the fan depressurization method was used which is in accordance with the Canadian General Standards Board. Before the test was conducted, certain preparatory steps were necessary. The openings such as the fireplace, furnace combustion air intake, ventilation air intake, exhaust fans and dryer vents were sealed. Also the windows and doors were latched.

A fan was used to exhaust air from the building at rates required to maintain the specified pressure difference of 50 Pa across the building envelope. The air flows and pressure differences were measured. The purpose was to subject the complete envelope to a simultaneous air pressure difference [19]. The relationship between the flow and the pressure difference is used to calculate the equivalent leakage area of the building envelope. For a more detailed theory and calculation method, see Appendix C.

2.6 Above Grade Heat Losses

The rate of heat loss, through building elements such as the ceiling, doors or windows, and main walls were obtained from the HOT-2000 program results. For further details refer to [17].

2.7 House Energy Balance

The calculation procedure for the house energy balance is similar to the HOT-2000 program. The different types of heat gains and heat losses are shown in Fig.17 [31]. The basic equation for the heat balance is given by:

$$H = L_t + L_a + L_b - \eta_i G_i - \eta_s G_s, \qquad (25)$$

where: H = Total space heating required (w);

L_t = Total heat losses above grade by transmission through exterior walls, ceilings, windows, doors (w);

L_a = Total heat losses due to indoor-outdoor air exchange (natural infiltration+mechanical);

L_b = Total Basement Heat Losses by Transmission below-grade;

η_i = Utilization factor for the internal gains from appliances and lighting, hot water heater and from occupants (%);

G_i = Total heat gain from internal sources (w);

η_s = Utilization factor for solar gains through glazing (%);

G_s = Total solar heat gains through glazing (w).

3. EXPERIMENTAL PROCEDURE

The test home used in this study is located at 1 Stormont Drive and is the permanent residence of Prof. J.D. Welch, of the Faculty of Architecture, University of Manitoba. The R-2000 building guide was used in the design and construction of the test home. Some features of the test home include: an air-to-air heat exchanger, double thickness insulation in the walls and ceiling, and a leak proof vapour barrier.

3.1 Thermocouple Placements for Ground Temperature Measurement

During construction of the residence, thermocouples were placed at 27 stations to measure the soil temperatures at the locations as shown on Fig.1. The thermocouples are located two meters from the centre plane of the basement walls and at three levels A, B, C. These levels are located approximately 0.5 meter, 1.5 meters and 2.5 meters below grade respectively. Other thermocouples, located one meter from the centre plane of the basement wall, have two levels, A and B. A profile of each station is shown in Fig.2 and Fig.3.

The thermocouples used in this study are copper-constantan. All thermocouple sets, once installed, were fed into one of three rotary dial switching boxes which facilitate recording the soil temperatures from each thermocouple. Switching boxes were located at the north-east and south-west corner of the building respectively. In total, 65 thermocouples were installed during the fall of 1987; 57 thermocouples remained operational during the period from September 1988- August 1990.

The wiring for the thermocouples was installed using three different methods. The

first method consisted of placing conduit under the foundation and the floor during construction. The second method consisted of thermocouples placed inside PVC tubing encased in urethane foam, and protected from environmental damage by the use of silicone cement. The third method consisted of inserting thermocouples into grooved dowels. For the last two methods, the locations were augered to the appropriate depths before the site was landscaped.

The thermocouples were read using a digital voltmeter and a reference temperature simulating zero degree Celsius. Measurements were recorded on a weekly basis during the heating season and on a two week basis for the rest of the year. Readings began on September 26th 1988 and ended August 31st 1990.

3.2 Solar Radiation Measurement

An Eppley Black and White Pyranometer was used for measuring total radiation on a vertical surface. The experimental period was from Feb-Mar 1989 and for the full heating season of 1989/90.

The pyranometer produces a voltage from thermopile detectors that is a function of the incident radiation. A potentiometer/analogue recorder was used to detect and record the output. Radiation data must be integrated over the period of time, such as an hour or a day for the test period.

3.3 Heat Recovery Performance Monitoring

The heat recovery ventilator used in this residence is the Lifebreath model 195 DCS. This particular HRV is a dual core unit, to increase the heat transfer area without an excessively large case. A schematic of the flow of stale air and fresh air is represented

in Fig.18.

The heat transfer coefficient of two fluids and amount of heat transfer area determines the amount of heat transferred. In order to maximize the heat transfer coefficient, it is desirable that both fluids have turbulent flow. This is achieved by mounting the plates, close together in the core as shown in Fig.15. The maximum number of plates in the core is constrained by the allowable pressure drop across the core and space. Also shown in Fig.15, is the flow of the hot and the cold fluids through the core which are isolated by the plates.

3.3.1 Equipment used to Monitor HRV

The temperatures at the inlet and outlet of the cold and hot air were measured as well as the pressure differences in the ducts using a Hewlett Packard 3056L data logger system.

Temperature Measurement: Three copper- constantan thermocouples were placed in each duct (#1,2,3,4) as shown in Fig.18. The thermocouples were evenly spaced to obtain an average temperature profile in the duct. During the test period the reference junction is provided by the Hewlett Packard data logger. The accuracy of the thermocouple and data logger combination was tested against a mercury thermometer in two situations. The first was at room temperature, while the second was in an ice bath. In both cases the difference between the two measurements was 0.5 ^{0}C.

Pressure Measurement: This was required in order to determine the air flow in the ducts. The flow rate was obtained through the use of flow collars illustrated in Fig.19 connected to pressure transducers. The flow collars were located in the fresh air intake and stale

exhaust ducts. In order to obtain the flow rate from the data logger, voltage output calibration curves for both the pressure transducer and flow meter had to be considered.

The transducer calibration curve was obtained by placing a pressure differential across the transducer as well as a micromanometer. The transducer output was monitored with a voltmeter. The calibration curve along with the flowmeter calibration, obtained from the manufacturer, is included in Appendix D.

3.4 Thermohygrograph

The relative humidity (RH) inside the residence is an important factor for human comfort. Since temperature is linked to changes in RH, both temperature and RH were monitored using a thermohygrograph manufactured by Casella London LTD, model T9240. The measurements were carried out at three locations: basement bathroom and laundry room and kitchen on the main floor.

The humidity measurement is performed by a humidity element which is sensitive to changes in RH. This element has the capability of shortening as RH decreases and conversely lengthening as the RH increases. Changes in length is transmitted via a linkage to a pen arm carrying a pen which marks the scaled (0-100%)graph paper.

The temperature measurement is performed using a bimetallic strip sensitive to temperature changes. The movements of the strip are transmitted via a linkage to a pen arm and pen which marks the scale graph paper (-15-40°c) [20].

4. RESULTS AND DISCUSSION

4.1 Results of Mitalas Research

Determination of basement heat losses depend on numerous factors including several which have a large impact on the heat loss rate. As an example, a one degree change in the basement temperature can change basement heat loss by 5 to 10 percent [7]. Other important factors include the thermal conductivity of the soil, the mean ground temperature, the effect of snow cover, the ground water temperature and level.

The accuracy of the Mitalas method was tested by comparing the calculated values with NRC test facilities in Ottawa, Saskatoon and Charlottetown. These facilities were equipped with calorimeters on the basement walls and floor. A comparison of each of these basements, which had different insulation placements, with the Mitalas computer simulated results is given in Table III. Tables IV and V illustrate the results for the HUDAC Mark XI Houses and the test homes in Gatineau, Quebec, respectively and compares them with the Mitalas results [7].

A comparison of the results demonstrated that the calculation procedure for basement heat loss is capable of accounting for all the weather parameters and basement shapes. The only significant shortcoming of the program was the factors used in the calculation of floor-surface heat loss which were under-estimated. This indicates that the conductance between the basement and the lower thermal boundary layer is larger than what the formula indicates. This was corrected by increasing the floor shape factor by 50 %. The corrected values are the values listed in Table VI.

The other minor change which was made in the heat loss factors was the

amplitude attenuation which was increased to account for the underestimation of the variation in the floor surface heat flux. The corrected values are listed in Table VI for a small cross section of basement insulation placements at the given soil thermal conductivity.

4.1.1 Conclusions and Recommendations based on Mitalas Research

There are many conclusions made from the comparison of measured and calculated basement heat losses, some of these include:

(1) The variation of ground surface temperature can be estimated accurately by a periodic heat flow calculation approach,

(2) Simple rectangular basements can be treated well using the straight wall calculations and shape factors along with the corner allowance factors,

(3) Total heat loss and sectional heat loss of a basement can be determined within +/- 10 percent provided there is some form of insulation present,

(4) Allowance for high ground water may be incorporated by assuming a 30% to 70% decrease in ground thermal resistance depending on the assumed severity of the ground water effect,

(5) The basement heat loss prediction does not take into account the variation of ground surface temperature caused by solar gain, snow cover, and adjacent structures.

The Mitalas method of calculating basement heat loss is correctly used in HOTCAN 3.0. For instance, the results illustrated in Fig.20 and Fig.21 which indicate the heat loss versus the time history were in good agreement with that of the Earth

Sheltered Housing Design [EHSD] and Interzone Temperature Profile Estimation [ITPE] computer programs.

4.2 Results of University of Manitoba Research

4.2.1 Experimental Ground Temperature Behaviour

Two years of underground temperature records at No 1. Stormont Drive have been completed. The thermocouples were strategically placed in the ground during the construction of the house as shown in Fig.1, to determine the behaviour of the ground temperatures at specific locations under the premises and in its proximity.

Station 8, shown in Fig.1, is located several meters from the house and is used as a reference point. It has thermocouples A,B and C which are at depths of 0.5m,1.5m and 2.5m respectively. The temperature obtained for two years at these locations were graphed and examples are shown in Fig.22. The ambient temperature is also shown to point out the relationship between the ground temperature and the ambient temperature. The interesting features are the sinusoidal shape of all curves and that the ground temperatures lags the ambient temperature by approximately eight to ten weeks. Penrod and Steward (1966) measured soil temperatures to a depth of 3.4 m for ten successive years and showed conclusively that the annual variation in daily mean soil temperatures is harmonic. As anticipated, the winter underground temperature increases with depth.

It will be noted that no freezing occurred at station 8. There was also evidence of considerable natural snow drifting at this location, which demonstrates the insulating effects of snow. To confirm the obtained results, ground temperature records from Atmospheric Environment Service (AES) located at the Winnipeg International Airport

were plotted against experimental data at corresponding depths and illustrated in Figs.23, 24 and 25. Fig.25 shows no freezing occurring at 2.5m. At 0.5m,1.5m and 2.5m the curves are similar in shape, but in the case of 0.5m and 1.5m the AES curves intersects the experimental curves which indicates the ground at the AES station is warming faster due to less snow cover depth and/or different soil conditions. AES later decided their site was not suitable and it has been relocated, additional data are not available. Research conducted on soil temperatures indicates that a time lag exists between seasonal mean air temperature and seasonal mean soil temperature. Soil temperatures at depths more than two meters remain relatively constant in spite of variation with location, type of soil, depth, time of year, etc.

Station 8 is not subjected to any effects from the house, but it is interesting to compare the effects of the residence on Stations 1,9 and 14 (relative to Station 8), as shown in Fig.26, 27 and 28. The thermocouples A,B and C, of Station 1,9 and 14 are at the same depths as at Station 8. The temperature trends at Station 1,9 and 14 were observed; there is indication of freezing at 14A which is at the 0.5m depth. Station 1,9 and 14 should be warmer due to the heat loss from the basement in comparison with Station 8. During the winter months there tends to be limited snow cover around the perimeter of the house because most of it is wind-swept, depending on the direction of the wind, thereby decreasing the insulating effect of the snow. The turbulence caused by the wind around the house also gives rise to a higher convective heat transfer coefficient. With the decreasing thermal resistance due to snow removal and the high convective heat transfer the increased heat loss from the ground results in lower temperatures at Stations

1,9 and 14 compared with Station 8 for the same depth.

An analysis of the ground temperature was performed on thermocouples 14B,15 and 16 and on 1B,2 and 3 (all 2m apart,and all at a depth of 1.5m) as shown in Figs.29 and 30 respectively. Thermocouples 3 and 16 are beneath the concrete basement floor, thermocouples 2 and 15 are under the basement wall and 1B and 14B are 2m from the wall. It was observed that thermocouples 3 and 16, which are under the floor, were at the warmest temperatures. Thermocouples 2 and 15 were intermediate temperatures due to basement heat loss. At thermocouples 1B and 14B, lowest temperatures were observed because of the lack of snow cover and the influence of the wind. But these temperatures must be affected by the basement heat loss since there is no lagging of the temperature profile at these positions.

In order to find the ground temperature, analytically, it can be modelled as conduction in a semi-infinite solid and either the surface temperature of the ground or the ambient temperature has to be known. The problem is mathematically modelled in such a way that the ambient temperature is periodic with time and given by:

$$t_\infty = t_{\infty m} \cos(\omega t), \tag{26}$$

and the boundary condition is:

$$-k\left(\frac{\partial t}{\partial x}\right)_{x=0} = h\left(t_{x=0} - t_\infty\right), \tag{27}$$

The solution to the governing equation (26) with boundary conditions (27) is given by;

$$t(x) = \frac{t_{\infty m} e^{-\lambda x}}{[1 + \frac{2\lambda k}{h} + 2(\frac{\lambda k}{h})^2]^{1/2}} COS(\omega\tau - \lambda x - \tan^{-1}[\frac{1}{1 + \frac{h}{\lambda k}}]), \quad (28)$$

where: t_∞ = Ambient temperature;

$t_{\infty m}$ = Ambient mean temperature;

ω = $2\pi f$, where f is the frequency;

k = constant, thermal conductivity of ground;

x = depth;

h = constant, convection coefficient;

τ = time lag = $x/(\sqrt{(2\alpha\omega)})$;

λ = $\sqrt{(\omega/2\alpha)}$;

α = thermal diffusivity.

From equation (28) [21] the higher the frequency (ω) the less the penetration (depth) and there is additional attenuation due to convection. Also the greater the thermal diffusivity (α), the deeper the penetration. From equation (28) the phase lag depends on the convection coefficient, and thermal conductivity. As the convection coefficient (h) goes to infinity, the phase lag with the $\tan^{-1}$ term goes to zero, therefore suggesting a decrease in phase lag, which ties in with Figs. 29 and 30 which shows no relative lag of temperatures at thermocouples 1B,2,3 and similarly with temperatures at 14B, 15 and 16.

A comparison of the ground temperatures under the basement floor was made. The ground temperatures were measured by thermocouples 3, 11, 16, 21 and 24 and the results are shown in Fig.31. The south thermocouple temperature (11) was found to be consistently higher than the other thermocouples. This could be due to the effect of solar

radiation on the basement floor and good snow cover that existed over thermocouple 9. The east floor thermocouple temperature (16) is lower than the rest of the under floor temperatures. One reason is the lack of snow cover on that side of the house as a result of easterly winds. The west under floor thermocouple temperature (3) is the next warmest, which suggests that side of the residence is sheltered from frequent westerly winds, hence a higher temperature compared to the temperature of thermocouple 16. The north (24) thermocouple is however colder than south (11), this is due to sheltering from solar radiation. The north corner (21) is the second overall coldest temperature measurement, as a result of lack of exposure of the ground from solar radiation. Another factor that could affect the temperature of thermocouple 21 is the easterly wind which decreases the ground temperature on that side of the house and thermocouple 21 is closer to the east wall than thermocouple 24.

A comparison of the temperatures under the basement wall as measured by thermocouples 2, 10, 15, 20 corresponding to the west, south, east and north walls respectively shows (Fig.32) that the highest temperature occurred at the south wall which is a result of solar exposure on that side of the residence.

4.2.2 Basement Heat Loss Results

The basement model below-grade used in ANSYS program consisted of 1045 (Fig.8) elements with varying thermal properties over time. The calculations performed by ANSYS were the temperature distribution, thermal flux, and the temperature gradient all on a weekly basis for the period of September 1989 to August 1990. The basement heat loss was also determined from the thermal heat flux.

4.2.3 Accuracy of ANSYS Computer Model

The experimental results for Stations 1 and 14 were compared with ANSYS results and are shown in Fig.33 and Fig.34 respectively. For the case of thermocouple 1A the maximum temperature difference between ANSYS and the experimental data was 3°C, for the case of 1B was 1°C and for 1C was 2°C. Similarly the maximum temperature differences were 5°C, 2°C and 2°C for thermocouples 14A, 14B and 14C respectively.

The trends of both experimental and ANSYS temperature profile are similar to each other which indicates that the proper combination of freezing and thawing of adjacent ground and snow cover was used. However the differences in temperatures is a direct result of the choice of thermal property values for the soil. The ANSYS temperature curve could match the experimental data curve by adjusting the thermal conductivity of the soil. However it was considered that the resulting temperatures were accurate enough to proceed with the basement heat loss calculation, since the basement model program takes nine hours to run for each trial of different soil thermal conductivity.

4.2.4 Thermal properties

The thermal properties consisted of the thermal conductivity, density and specific heat capacity. Most of these properties for the building materials were obtained from the ASHRAE handbook. However, difficulty was encountered when selecting the property of soil, specifically the thermal conductivity. There are substantial amounts of data scattered throughout the literature on thermal properties of soils with wide difference in

texture. Gravel, sand, sandy loam, silt loam and clay and even rocks and peats have been thermally described.

Kersten (1948) [22] did many experiments to determine the properties of soil. Nineteen different soils were monitored at various conditions of moisture content and density. It was also found that the thermal conductivity differs according to phase of moisture in the soil. At a constant moisture content, an increase in density results in an increase in conductivity. An increase in moisture content at a constant density also results in an increase in conductivity.

For unfrozen silt and clay soil :

$$K=0.1442\,[0.9\log(\%moist)-0.2]\,10^{0.0006243\rho}, \qquad (29)$$

For frozen silt and clay soil :

$$K=0.1442\,[0.01(10^{0.0013197\rho})+0.025(10^{0.00087\rho})\,\%moist], \qquad (30)$$

where: %moist = % moisture content in soil;

ρ = density of soil.

Equations (29) and (30) apply to soil moisture content greater than 7% and the predicted values of thermal conductivity should be within 25% [22]. A graph was generated using equations (29) and (30) (Fig.35) to show the effect of moisture content on thermal conductivity and also indicates the regions of dry, wet and permafrost soil which was defined in the Mitalas study, and applied to the University of Manitoba basement model presented in this study.

The specific heat capacity of the soil was assumed to be constant over the study

period because it varied only by 9% over the temperature range from -15°C to 20°C based on Kersten's work. The specific heat of twelve different mineral soils and soil materials were measured by Kersten(1948) [22]. He found that the specific heat of mineral soils varied linearly from 0.67 J/cm^3 °C at -18 °C to 0.8 J/cm^3 °C at 60°C.

The density of the soil was also assumed constant based on a Carter study [23]. Carter (1951) measured both the specific heat and thermal diffusivity of various soil samples. It was reported that in most cases the variation in thermal diffusivity with moisture is small over the range of 10 to 25% moisture content [23].

4.2.5 Boundary Conditions

Fig.7 shows the basement model which has four boundary conditions as follows: (a) a fixed mean ground temperature of 6.1 °C at a depth of 15 m which was obtained from the HOT-2000 weather data file corresponding to Winnipeg, (b) an inside basement temperature and a convection coefficient of 18.3 °C and 10 W/m^2 °C, (c) mean weekly temperature and a convection coefficient for 52 weeks, obtained from Atmospheric Environment Services, (d) adiabatic surface since the heat flow is only in the y-direction.

4.2.6 Basement Heat loss Results

The basement heat loss calculation was performed in the post1 postprocessor. The results obtained were for the walls and floor below grade. The calculation was as follows:

(1) Specify the path by node selection, to define the outline of the area which requires the heat loss calculation.

(2) The heat flux is then loaded from the results file, and an integration is performed over the path, therefore the solution will be in heat loss per unit

length.

(3) The overall heat loss is then calculated by multiplying by the width of the basement.

An example of the calculation steps and explanation is given in Appendix B [24].

4.2.7 Results

The basement heat loss below grade was found to be 15835 MJ/year based on weekly calculations. This includes the wall and the floor below grade. Fig.36 illustrates the heat loss characteristics together with the ambient temperature from September 1989 to August 1990.

Throughout the period of September 89 to August 90, basement floor heat loss was observed and varied from 90 W to 200 W (week1 corresponds to first week of September 1989 and week 52 corresponding to last week of August 1990). There is also a lag in the floor heat loss, since the effect of the cold weather starts to appear 18 to 20 weeks from the coldest week which is week 22 (corresponding to -33°C ambient temperature), whereas the peak heat loss occurs in week 40 to 42. The thermal contours below grade were also generated from ANSYS for the month of March of 1990 and are illustrated for each week in March 1990 in Figs.37-40. The different thermal contours showed warmest temperatures below the basement floor. The change in level of the basement floor increases the floor heat losses at that location. The soil adjacent to the wall and under the weeping tile styrofoam insulation shows no sign of freezing throughout the study period. According to the sequences of the thermal contours around the basement model for each week from March to mid-April 1990 (Figs. 37-42) the

pattern of the thermal regimes for week 3 in March is similar to week 2 in April. The heat loss from the basement floor is still affected from the summer of the previous year which is shown in Fig.36 from week 25 to 29. In April the heat loss below the floor increases due to the lagging effect from the winter conditions. Therefore, there is a good reason to insulate the basement floor or use the ground as a storage medium for the application such as a heat pump or another heat recovery method.

The basement wall heat losses were influenced most by the ambient temperature. There was very little lag shown by the weekly calculations and modelling of the adjacent ground when it freezes or thaws. The peaks observed are the results of phase changes (Fig.36) occurring in the soil adjacent to the wall and it is clear that these peaks are present when the ambient temperature is below 0° C. Three peaks are noticeable between weeks 12 to 22 which corresponds to the change in the thermal properties of the soil from the ANSYS program. The heat below 0 W indicates that there is heat gain from the soil which is apparent from week 35 and onwards and is occurring only at the walls. The sudden sharp behaviour change in the week 43 to 45 indicates a phase change from frozen to unfrozen soil.

The right (east) wall curve heat loss is not identical to the left (west)wall. It is evident that the left wall heat loss is consistently higher than that of the right due to the change in the depth of the basement (bi-level) and perhaps variation of snow cover.

4.2.8 Comparison of Mitalas Method(HOT-2000) with ANSYS

The Hot-2000 program predicted a basement heat loss of 17110 MJ/year. This study indicated that the actual heat loss for the same house to be 15836 MJ/year. The

Mitalas method is higher by about 7.5% compared to this study. There is evidence that the Mitalas method uniformly predicts higher heat losses. For example Yard, Profile and ASHRAE results are shown in Fig.43 together with Mitalas method [25]. A portion of the difference in the basement heat loss may be explained by the fact that the values of the floor shape factor in the Mitalas method were arbitrarily increased by 50% above those predicted by the numerical model so as to agree with observed results from a series of monitored basements [25].

The wall heat losses below grade was higher using ANSYS. For basement walls below grade, the temperature difference for winter conditions is greater than for the floor. Also the option of changing the thermal properties over time as well as snow cover may have a direct effect of this behaviour.

4.3 Solar Energy Results

The original total solar heat gain was estimated by the HOT-2000 program to be 36% of the annual space heating, therefore it is a significant source of heat.

The calculation of the passive solar heat gains for a residence is complex and involves the following three distinct steps:

1. From the available sources of weather data which are measured on a horizontal surface, the total or global readings (RF1) must be broken down into direct and diffuse, unless the diffuse is measured directly (RF2). Then the straight forward geometric relationships (section 2.3) are used to calculate the respective components on vertical surfaces at any desired orientation. Several methods have been developed for this purpose but there is no general agreement as to which technique will yield better results

for a specific purpose. Methods now in general use assume an isotropic sky although it is anything but isotropic. This step is then to establish a method to calculate the diffuse and direct components which will yield results on the vertical surface that compares best with the available experimental data.

2. The second step involves the selection of a source of solar resource database that predicts the solar heat gains for a residence providing confidence for use at other sites. All Canadian data has been collected by the Atmospheric Environment Service (AES) and a few researchers. However AES and some of the researchers have little knowledge about the needs for engineering design requirements. Therefore, the use of some of the available databases is questionable.

3. Calculation of the usable solar heat gains on the vertical surfaces, such as walls and windows due to the absorptivity of the walls, glazing transmissivity of windows and overhangs. In Winnipeg, most of the surfaces with southern exposure are oriented so that a normal to the surface is 18^0 east of south which is the case with this residence.

The experimental data were measured for Feb/Mar 1989 and for the full season of 1989/90. Unfortunately, a data logger was not available and the readings were obtained by an analogue recorder. The time required to convert the readings to digital format and massage the data was considered excessive and its value is limited since a general solution is being sought. However, the experimental data are valuable for identifying the most suitable data source and for checking questionable heat balances.

The intent then was to establish the most acceptable source of solar data. The following three sources of solar data were available:

1. The University of Manitoba (U of Man) experimental,
2. Typical Meteorological Yearly (TMY),
3. Solar Radiation Data for Canada 1967-1976 published by AES, Environment Canada(AES).

The TMY concept was initiated in Canada by the Solar Energy Centre of Excellence, University of Waterloo for use with WATSUN solar simulation program. The WATSUN is an internationally accepted program used for the design of solar facilities such as hot water systems, swimming pool systems, etc. The program performs an hourly analysis and thus typical data are required for the transients since the effects of peaks and valleys are lost by using averaged data.

The TMY records are made up of typical months that have been statistically determined to be the most representative of that particular month. For instance weather data for the months of January and February are excerpted from records for 1965 and the year 1975 is isolated as providing the most representative data for March. AES provides TMY data on diskettes available for use in personal computers and the data available from the WATSUN computer program.

The AES data, referred to in item 3 above, are available in hard copy format [26]. Average hourly monthly radiation values are provided for the total horizontal(global) as well as diffuse and direct. They are listed as long term averages for years 1965 to 1976. The long term averages are acceptable for this study since it is to perform average weekly audits. However, the AES lists the global and diffuse (RF1 & RF2) readings respectively which implies these readings were taken in Winnipeg. RF2 readings were not in

Winnipeg during the 1965 to 1976 period [26]. Upon investigation, the 1985 AES publication [26] is based on Hay's [27] 1979 anisotropic model which was verified by limited site studies compared to many of the University of Wisconsin and other models.

The HOT-2000 author refers to Erbs et. al as well and appears to have developed his own approach which has not been published. The details of the models used to calculate the diffuse and direct solar radiation components from the global radiation on a horizontal surface are provided but need experimental verification.

Fig.12 was generated by using the normal geometric techniques used for the isotropic models. The discrepancies between the different methods are minimal. Bradley (HOT-2000) did not use the normal geometric methods in transferring the data from the horizontal to a vertical surface but rather used a more recent development (1981) [28] by the New Zealand Meteorological Service. At this stage the only rational approach is to proceed with reliable well proven methods. The Erbs et al model was originally selected even though it is not the simplest but it is well proven and provides a method of coping with dawn conditions. Diffuse radiation is available before sunrise and after sunset which is not important as far as energy is concerned but few models acknowledge the existence of these conditions.

As indicated previously, three sources of solar data were available. The experimental data were used to evaluate the other available sources which essentially consist of the TMY data versus the AES long-term (1967 to 1976) averaged data. The sample of the experimental data selected for this evaluation was recorded from Feb. 18th to Mar.17th 1989, the eighth to the eleventh week of the year, but experimental

verification is limited.

A graph has been prepared for each week which shows a plot of the average hourly radiation (W/m^2) on a vertical surface (90^0 tilt) versus solar time for the average weekly day. Fig.13 indicates the results for a typical week (Feb 18th-25th). The AES data for February, recall that the AES represents the average hourly data for the month and thus theoretically should represent Feb.15th. The values are significantly lower than the TMY data using the Erbs et.al and University of Wisconsin (Reindl et.al) models to calculate the radiation on a vertical surface.

In this case the experimental data are higher but there are some noteworthy differences in other characteristics. The peak occurs at 1:00PM which in part is due to the fact that Winnipeg streets run 18^0 east of north (see Fig. 1) and thus the vertical surface for the measurements was not mounted perpendicular to the N-S plane. This orientation also accounts for the higher AM readings and the lower PM readings over the other plotted data in Fig.14. However, it will be noted the TMY data also peak at 1 PM. Since Winnipeg's longitude is 97^0 14min this causes a delay of 29 min since the sun has certain perturbations in its orbit. Another 13 to 14 min delay exists in February and solar noon occurs at approximately 12:42 in mid-February. This means the TMY data is corrected to central standard time whereas the AES data is not since it peaks at solar noon.

Again in Fig.13, the AES average March data has been included and it is lower than the TMY data used with the University of Wisconsin and Erbs et.al sky model. Because of the anomalies encountered in the AES data, the radiation on the vertical

surface was calculated in the same manner as it was for the TMY, namely from the horizontal global radiation. The AES also includes the average monthly daily energy on a vertical surface with their data. A comparison of the sources of data for the four week average is shown in Table VII. The average daily energy for each source for the period shows reasonable agreement.

The difference in using the TMY data instead of the experimental data is 9% based on this limited analysis. However, the results can only be universally acceptable by using a national data base. Experimental solar data was used to check the results in an attempt to consolidate the energy balance.

4.4 Heat Recovery Ventilator Results

The HRV was tested by the Energy and Mines and Resources Canada, and Ontario Research foundation at 0°C and -25°C; with varying flow conditions. The effectiveness, temperature efficiency and mass flow at 0°C were 91%, 80%, and 117 cfm (60 L/s) whereas in the case of the -25°C condition, were 91%, 77% and 117 cfm.

The testing of the HRV at 1 Stormont Drive was conducted from mid-January to the end of March 1991. The daily results (efficiency, effectiveness and mass ratio) were obtained when the unit was operating. Then the results are superimposed on one graph for each month (Jan, Feb, March) and are shown in Figs. 44-46. The average temperature efficiency, effectiveness and mass ratio for the month is shown in Table VIII as well as the monthly efficiency used in the HOT-2000 program.

The mass flow is dependent upon the average velocity, density of fluid and temperature, from Table VIII, Fig. 44,45 and 46 it is evident that the HRV flow is

balanced since the mass ratio is near unity.

Balancing importance: Balanced air flow is very important for proper operation of an HRV. If the supply air from outside is greater than exhaust air from the house, the imbalance may induce frosting of the HRV and the freezing of leakage points such as doors and locks. If the exhaust air from the house is greater than the supply air from outside, combustion appliance backdrafting may bring exhaust fumes into the house. A balanced condition ensures optimum performance [29].

A result of balanced mass flow rates under insitu conditions indicate that the equations (23) and (24) are equal, which suggest that effectiveness and temperature efficiency are equal.

Three plots of HRV efficiency against outdoor temperature (Figs.47-49) for each month shows that the actual HRV efficiency is 76% at 0°C and 74% at -25°C. The efficiency used in the HOT-2000 program was higher in comparison with experimental results. The reason is due to the use of a typical weather data for Winnipeg, whereas the experimental results were for the actual temperature conditions. The scatter of the efficiency for the month of January 1991 is a direct effect of an unusually warm month (Fig. 47).

4.5 Infiltration Test Results

The test performed by UNIES Ltd., revealed major leakages in the exterior door weather stripping, in the living room area and patio doors, around the fire place unit, electrical wires through the wall in the office, window latches in the basement, electrical panel, beam penetrations and plumbing in the basement and the vent through the floor

in the basement laundry room and specifically through the cantilevered floor joist in the living area. Some minor leakages were observed in the office, doors and switches along the bottom of the house and the garage interface and finally plumbing through the wall in the basement laundry room.

The test results indicated an air change of 3.02 ACH at 50 Pa depressurization of the residence which is twice the value of an airtight house according to Table IX. The results fall in the category of 1961-1980 airtightness test. Therefore a great deal of heat loss is attributed to the infiltration losses. The HOT-2000 program indicates losses of the order of 24% of the input energy.

4.6 House Energy Balance Analysis

An original HOT-2000 house analysis for 1 Stormont Drive was available at the beginning of this study [Appendix E]. However, there were a few discrepancies in the input. The original basement was modelled as a combination of shallow and a full depth basement with exterior insulation and both having one side attached. From the original drawings of the residence it shows that the basement was insulated on the inside and only on one side, the shallow side was attached to the garage, and the full basement was not attached. A summary of the energy analyses are shown in Table X which were carried out and discussed in the following steps:

Case 1. Original HOT-2000 house analysis (Sept 1989)

Case 2. Modified version to accommodate for correct interior insulation and actual infiltration from the blower door tests (3.02 ACH at test pressure of 50 Pa. (Aug 5/91)

Case 3. Same as Case 2 but with new solar data from an improved sky model included and the revised basement heat losses obtained by ANSYS program shown separately for comparative purposes.

Copies of the computer analysis are contained in Appendix E. The following points may be noted from summary table:

i) Case 1 the heat loss from the shallow basement walls below grade was double the same item for the other Cases. This suggests it is beneficial to insulate the basement on its interior. However, the heat losses in the centre area of the floor of the shallow basement increase substantially for Cases 2 and 3. An explanation for this behaviour is the increase in the overall resistance of the wall when insulated from the interior and certainly higher than the uninsulated basement floor which is another major area for the heat transfer by a parallel path with a lower resistance.

ii) In Case 2, although the basement insulation placement was corrected, the purpose of this case was to show the effect of increased infiltration which was determined by standard test procedure. According to the R-2000 homes building code, a residence with 1.5 ACH at 50 Pa is considered airtight and for this residence the infiltration was 3.02 ACHs at 50 Pa.

The ventilation and infiltration ACHs increased to 0.79 from the standard of 0.5 ACH required for ventilation purposes of which 0.45 ACH was provided by the HRV. The associated heat loss increased from 10398 MJ/year to more than 26000 MJ/year. The seasonal efficiencies of the HRV were adjusted by the results obtained from the field tests. The laboratory results used in the program are 80% at 0°C and 77% at -25°C and

these were changed to 76% and 74% respectively.

iii) Case 3 demonstrates the effect of changing the method of determining the solar heat gains. The changes are not significant (+4%) but the program does not allow for orientation of the vertical surfaces from south except to provide inputs for south-east (azimuth angle=-45°) and south-west (azimuth angle=45°) surfaces. Most buildings in Winnipeg with pseudo south facing surfaces have an azimuth angle of -18°. The values of the solar radiation on the vertical surface oriented at 18° for the Winnipeg latitude were from 3 to 5 % lower than on a vertical surface facing south. The variance depends upon the time of the year. Although the total energy difference is not significant, the solar gains are higher in the mornings and lower in the afternoon as can be observed on Fig.14.

It will also be noted that the solar heat gains tend to increase with an increase in infiltration. Without more detailed knowledge of the HOT-2000 program it is not possible to provide an explanation. One cause may be due to the fact that the heat capacity of the walls, plumbing fixtures, electrical fixtures etc, around which the infiltration occurs, is at lower temperature and thus provides more potential for a heat sink.

The basement heat losses were also adjusted for this case by subtracting the total below grade heat losses as calculated by the program using the Mitalas method and adding the heat losses determined by a two-dimensional analysis using ANSYS program The ANSYS, as previously explained, is a complex finite element program. The experimental data recorded over the two year period was used to compare the ANSYS temperature profile. The basement heat loss results were lower than those predicted by

the Mitalas method by 7.5%.

Typical Meteorological Yearly (TMY) data were used throughout the analysis since it is well established database for Canada and the United States. All the data are available on an hourly basis and the analysis was performed on a weekly basis using average hourly values for the week. It was anticipated that additional accuracy would result.

Based on the natural gas consumption for the calendar year 1990. The predicted losses were at least 5% higher than the annual furnace load using the manufacturer listed seasonal efficiency for a condensing furnace of 90%. Discussion with personnel of UNIES Ltd. Winnipeg, who have monitored numerous R-2000 homes indicate that this is a considerable variation in the results obtained. However, unless the furnace is oversize there is no justification for assuming that the seasonal efficiency of the condensing furnace is below 85%. In this case the design heat loss at -33°C is 12.6 KW and the furnace output capacity is listed as 17.6 Kw.

5.0 CONCLUSIONS AND RECOMMENDATIONS

Conclusion

1. The major energy losses of the residence were as follows:

	HOT-2000	HOT-2000 (revised)
Windows	37%	33%
Infiltration	10%	24%
Envelope	28%	27%
Basement (below grade)	22%	14%
Unaccounted for	29%	6%-8%

2. Basement floor losses for this home totalled approximately 10000 MJ/year, more than half of the total basement heat losses, thus basement floor insulation should be considered.
3. Soil temperatures adjacent to the house (within 1 meter) do not normally decrease below 0°C thus there is no necessity for thermally protecting the weeping tile.
4. The basement heat loss calculation using ANSYS indicates good agreement with the Mitalas Calculation (7.5% discrepancy) for the same residence site specific).

Recommendations

1. Develop a three-dimensional use of ANSYS for the prediction of heat transfer in soils.
2 Investigate the effects of differences in exterior and interior insulation on below-grade basement walls.
3. Adjust the thermal conductivity of the soil so that the ANSYS basement model temperature profile exactly fits the available experimental data and repeat the energy analysis.

4. Necessity for research on the thermal conductivity of soil versus moisture content.

REFERENCES

1. MacDonald G.R, Claridge D.E, and Oatman P.A, " *A Comparison of Seven Basement Heat Loss Calculation Methods Suitable for Variable Degree-Day Calculations*", ASHRAE Transactions, V.91 Pt.1, 1985.

2. Dumont, R.S., Lux,M.E., and Orr, H.W, " *HOTCAN: A Computer Program for Estimating The Space Heating Requirement of Residences*", NRC, Division of Building Research, Ottawa, 1982.

3. Dumont, R.S, and Orr, H.W and Lux, M.E, "*Comparison of Energy Consumption Using HOTCAN with Measured Values From Unoccupied Test Units*", Proceedings of the Solar Energy Society of Canada Incorporated, 9th Annual Conference Windsor, Ontario, 1983.

4. Kostyniuk, T.M. and Trupp, A.C, "*Effect of Exterior Insulation Placement on Basement Heat Losses*", Proceedings of the Solar Energy of Canada Incorporated, Renewable Energy Conference, Winnipeg, Manitoba, 1986.

5. Richmond, W.R. and Besant, R.W, "*A Study of Basement Heat Loss* ", Proceedings of the Solar Energy Society of Canada, Renewable Energy Conference, Winnipeg, Manitoba, 1986.

6. Tilley, G.L., "*Outside basement Insulation using styrofoam Sm*", Bulletin No.64, Dow Chemical Canada, Limited, Sarnia, Ontario, 1978, Pp. 2.

7. Mitalas, G.P., " *Calculation of Basement Heat Loss*", Division of Building Research, National Research Council of Canada, Paper No. 1198, Ottawa, Ontario, 1983.

8. Incropera, F.P., and Dewitt, D.P., " *Fundamentals of Heat and Mass Transfer*", 2nd edition, John Wiley and sons, New York, 1985, Pp. 3.

9. Peters, P., and Paulic, L., " *Basement Heat Loss Determination*", B.Sc Thesis, University of Manitoba, 1989, pp 9-10.

10. Whitmore, D.W. and Zahn, M.J., " *Application of the Finite Difference Method to Thermal Problems in Perma Frost Engineering*". B.Sc. Thesis, University of Manitoba, Winnipeg, Manitoba, 1983, Chapter 5.

11. Kostyniuk, T.M., " *Analysis of Exterior Basement Insulation Using Finite Difference Method*", B.Sc Thesis, University of Manitoba, 1986.

12. Liu, .B.Y.H. and Jordan, R.C, "*The Interrelationship and Characteristic Distribution*

of Direct, Diffuse and Total Radiation", Solar Energy, 4, 1960, pp3.

13. Ruth,D.W. and Chant, R.E., "*The Relationship of Diffuse Radiation to Total Radiation in Canada*", Solar Energy, 1976, pp153.

14. Orgill, J.F., and Hollands, G.T, " *Correlation Equation for Hourly Diffuse Radiation on a Horizontal Surface*", Solar Energy, Vol.19, 1977, pp357-359.

15. Erbs, D.G, Klein, S.A, and Duffie, J.A., " *Estimation of the Diffuse Radiation Fraction For Hourly, Daily and Monthly-Average Global Radiation*", Solar Energy, Vol.28, No.4, 1982,pp293-302

16. Reindl, D.T., Beckman, W.A, and Duffie, J.A., " *Diffuse Fraction Correlation*", Solar Energy, Vol.45, No.1,1990, pp 1-7

17. Bradley, B., " *HOT-2000 Technical Manual V5.06*", 1989.

18. Page, J.K., "*Estimation of Monthly Mean Values of Daily Total Short Wave Radiation on Vertical and Inclined Surfaces from Sunshine Records for Latitudes 40^0N-40^0S*", Proceedings of the UN Conference on New Sources of Energy, 1964, pp378.

19. Canadian General Standard Board, " *Determination of the Air Tightness of Building Envelopes by the Fan Depressurization Method*", Ottawa, 1986.

20. Casella London LTD, " *Instruction Leaflet 972/83, Thermohydograph T9246*", pg1

21. Trupp, A.C., " *Conduction Heat Transfer Course Notes*", University of Manitoba, 1990, pp145.

22. Kersten, M.S, "*The thermal Conductivity of Soils*", High-way Research board, Proceedings, Twenty-eighth Annual Meeting, 1948, pp391-409.

23. Carter, C.L., "*Soil Temperature, Moisture Content and Thermal Properties*", Engineering experiment Station Bulletin NO.15, University of Tenessee, Knoxville, 1951.

24. Swanson Analysis System, " *ANSYS Heat Transfer Seminar*", Houston, Texas, 1990, pp4_20-4_30.

25. Parker, D.S., " *F-Factor correlations for determining Earth contact Heat loads.*" ASHRAE TRANSACTIONS VOL 3 Pt. 1. Publication ASHRAE, Atlanta, G.A., 1988, Pg. 7884-7890.

26. Mc.Kay and Morris, R.J, "*Solar Radiation Data Analyses for Canada 1967-1976*", Vol.4, The Prairie Provinces, 1985.

27. Hay, J.E., and Wardle, D.I., " *An assessment of the Uncertainty in measurements of Solar Radiation*", Solar Energy, Vol.29, No.4, 1982, pp271-278.

28. Revfiem, K.J.A., " *Simplified Relationships for estimating Solar Radiation on any Flat Surface*", Solar Energy, Vol.28, No.6, 1982, pp509-517.

29. Howell Mayhew Engineering Inc., " *Assessment of Heat Recovery Ventilator Operation and Performance in Alberta*", July 1990, pg F4.

30. Walton, G.N.N., " *Estimating 3-D heat loss from Rectangular Basements and stabs using 2-D calculations.*" ASHRAE Transactions V g 3 Pt. 1. Publication by ASHRAE, Atlanta, G.A., U.S.A., 1987, Pp. 791-797.

31. Wardrop, C.A.,"*Insitu Performance Of A Residential Heat Recovery Ventilator*", B.Sc Thesis, University of Manitoba, 1990, pp 5-18.

32. Duffie, J.A., and Beckman, W.A, " *Solar Engineering Of Thermal Processes*", John Wiley and Sons, 1980.

33. Bradley,B., " *HOT-2000 Users Manual V5.06*", 1989.

34. Lei, Q., " *Computer Aided Design For Sol-Air Heat Exchangers*", University of Manitoba, M.Sc Thesis, 1985, pp 15-17.

35. Swanson Analysis System, " *ANSYS Primer for Thermal Analysis*", Houston, Texas, 1989.

36. Barakat, S.A., " *Comparison of Models for Calculating Solar Radiation on Tilted Surface*", Proceedings of the Fourth International Symposium on the use of Computers for Environmental Engineering Related to Buildings, Tokyo, Japan, 1983.

37. Klein, S.A., " *Review Paper, Calculation of Monthly Average Insolation on Tilted Surfaces*", Solar Energy, Vol.19, 1976, pp325-329

38. Ackerman, M., and Dale, J.D., " *Measurement And Prediction Of Insulated Basement wall Heat Losses in a Heating Climate*", ASHRAE Transactions, V.93, Pt.1, 1987.

39. Bahnfleth, W.P., and Pedersen C.O, " *A Three Dimensional Numerical Study of Slab-on-Grade Heat Transfer*", ASHRAE Transactions, V.96, Pt.2, 1990, Pp61-81.

40. Subbarao, K. and et.al, " *Short Term Energy Monitoring: Summary of Results from Four Houses*", ASHRAE Transactions, V.96, Pt.1, 1990, Pp1459-1457.

41. Jones, J.R., and Boonyatikarn, S, " *Factors Influencing Overall Building Efficiency*", ASHRAE Transactions, V.96, Pt.1, 1990, Pp1449-1457.

42. Ternes, M.P., " *Energy Savings and Performance of Improved Energy Efficiency Measure Selection Technique*", ASHRAE Transactions, 1990.

43. Robinson, D.A and et. al., " *Cold Climate Foundation Insulation Retrofit Performance*", ASHRAE Transactions, 1990.

44. Wong, S.P.W., and Wang, S.K.," *Fundamentals Of Simultaneous Heat and Moisture Transfer Between the Building Envelope and the Conditioned Space Air*", ASHRAE Transactions, 1990.

45. Yoshino, H. and et. al., "*Effects of Thermal Insulation Located in the Earth Around a Semi-Underground Room: A Two Year Measurement in a twin type Test House Without Auxiliary heating*",ASHRAE Transactions, V.96, Pt2, 1990, Pp53-60.

46. Yoshino, H. and et. al., " *Effects of Thermal Insulation Located In The Earth Around a Semi Underground Room: Computer Analysis By Finite Element Method*", ASHRAE Transactions, V.96, Pt.1, 1990, Pp103-111.

47. Yuill, G.K., and Wray, C.P., " *Verification of the Below Grade Elements of HOTCAN 3.0*" G.K. Yuill and Associates, Winnipeg, Manitoba, 1986, Pg.8

48. Shipp, P.H., " *Basement, Crawl Space on grade. Thermal performances,*". Proceedings from the conference on the Thermal Performance of the exterior Envelopes of Building II, Las Vegas, NV, 1983.

Location	Annual Mean Ground Temp. Θ_G, °C	Amplitude of 1st Harmonic Θ_v, °C	Amplitude of 2nd Harmonic $\Theta_{v,2}$ °C
Goose Bay, Nfld.	4.9	10.3	2.9
St. John's West, Nfld.	6.7	8.5	1.5
Truro, N.S.	7.9	9.9	1.5
Kentville, N.S.	8.4	11.4	1.6
Charlottetown, P.E.I.	7.5	10.1	1.6
Fredericton, N.B.	7.7	11.9	1.5
La Pocatière, P.Q.	7.7	10.4	1.7
Normandin, P.Q.	5.7	8.9	2.7
Ste-Anne de Bellevue, P.Q.	6.9	12.1	2.3
St. Augustin, P.Q.	7.4	10.5	2.3
Val D'Or, P.Q.	6.5	10.6	2.5
Toronto, Ont.	11.1	12.1	1.3
Kapuskasing, Ont.	5.9	10.6	2.4
Vineland, Ont.	10.6	11.0	0.9
Ottawa, Ont.	8.9	11.4	1.8
Atikokan, Ont.	7.1	11.0	2.4
Winnipeg, Man.	6.1	12.4	1.2
Saskatoon, Sask.	5.9	14.6	1.2
Regina, Sask.	4.9	14.0	0.9
Swift Current, Sask.	5.7	11.4	1.2
Lacombe, Alta.	6.3	12.2	2.2
Edson, Alta.	5.2	8.9	1.7
Peace River, Alta.	5.3	12.0	1.5
Calgary, Alta.	6.3	12.2	0.9
Vegreville, Alta.	4.6	12.1	1.4
Summerland, B.C.	12.3	11.9	0.9
Vancouver, B.C.	11.3	8.5	0.9

In all cases, the minimum ground surface temperature occurs in January. If January is designated as $m = 1$, then the first harmonic can be expressed as $\Theta_v \cdot \sin(30 \cdot (m+8))$ where m is in months and sine angle is in degrees.

Table I : Ground Surface Temperatures for Selected Locations

In all cases for the range $1 \le R \le 5$:

$\tau_2 = 0.9$ $\quad \Delta t_2 = 0$

$\tau_3 = 0.7$ $\quad \Delta t_3 = -1$

$\tau_4 = 0.4$ $\quad \Delta t_4 = -2$

$\tau_5 = 0.3$ $\quad \Delta t_5 = -1$

Units:

S, $W/m^2 \cdot K$ $\quad$ R, $m^2 \cdot K/W$

V, $W/m^2 \cdot K$ $\quad$ τ, dimensionless

C, m^2 or dimensionless $\quad$ Δt, month

(Δt is the time delay of heat flux sine wave relative to the ground surface temperature sine wave.)

SECTION A: SOIL THERMAL CONDUCTIVITY: k upper = 0.8 W/(m.K); k lower = 0.9 W/(m.K)

Insulation System	S_n, V_n, and C_n Factors	Wall Segments		Floor Segments	
		Top strip just below grade, n = 2	Bottom strip, n = 3	1 m strip adjacent to wall, n = 4	Centre, n = 5
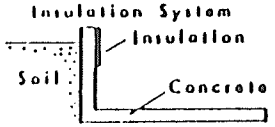	S=	$(0.53 + 1.42R)^{-1}$	$(1.06 - 0.013R)^{-1}$	0.36	0.14
	V=	$(0.53 + 1.43R)^{-1}$	$(1.15 - 0.016R)^{-1}$	0.25	0.05
	C=	0	1.0	2.6	0.5
	S=	$(0.58 + 1.10R)^{-1}$	$(1.23 + 1.45R)^{-1}$	$(2.05 - 0.066R)^{-1}$	0.15
	V=	$(0.58 + 1.12R)^{-1}$	$(1.31 + 1.55R)^{-1}$	$(2.[illegible] - 0.11R)^{-1}$	0.07
	C=	0	0.6	2.4	0.5
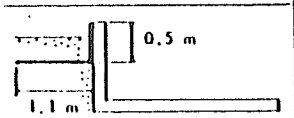	S=	$(1.21 + 0.60R)^{-1}$	$(1.78 + 0.081R)^{-1}$	0.33	0.13
	V=	$(1.22 + 0.65R)^{-1}$	$(2.07 + 0.12R)^{-1}$	0.22	0.05
	C=	0	1.0	2.6	0.5

SECTION B: SOIL THERMAL CONDUCTIVITY: k upper = 1.2 W/(m.K); k lower = 1.35 W/(m.K)

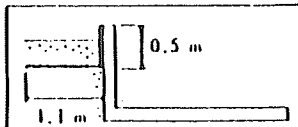	S=	$(1.19 + 0.47R)^{-1}$	$(1.43 + 0.58R)^{-1}$	0.36	0.13
	V=	$(1.18 + 0.51R)^{-1}$	$(1.60 + 0.07[illegible]R)^{-1}$	0.26	0.05
	C=	0	1.0	2.6	0.5

Table II : Example Shape, Attenuation, Time Lag and Corner Allowance Factors for Selected Insulation Placements

Location	Test Year	Test Area Location	Insulation and R value $m^2 \cdot K/W$	Basement Space Temp., °C	Winter Season Heat Loss, W/m^2	Steady-State Component	Variable Component	Total	Difference between measured and calculated values, W/m^2
Saskatoon, Basement A	78/79	N. Wall	R=1.6;0.6 m below gr.	13	14	6.2	6.7	13	1
		N. Wall	None	13	33	17	13	30	3
	79/80	N-W Corner	None	20	48	31	17	48	0
		N. Wall	None	20	44	26	13	39	5
		N. Wall	R=1.6;0.6 m below gr.	20	22	11	7	18	4
		Floor	None	20	3.4	3	1.3	4.8	-1.4
Saskatoon, Basement B	78/79	N. Wall	None	17.3	30	24	12	37	-7
		N. Wall	R=1.87;Full height	17.3	10	5.1	3.1	8.1	1.9
Saskatoon, Basement C	78/79	Floor	None	20	5	3	0.6	3.6	1.4
	79/80	N. Wall	R=1.32 above gr.	20	23	17	11	28	-5
		N. Wall	R=1.32 above gr. and 1.2 m on gr.	20	18	9	4.7	14	4
Ottawa, Basement E	79/80	N. Wall	None	20	20	13	10	23	-3
		Floor	None	20	3	2.9	0.6	3.5	-0.5
Charlottetown, Basement A	78/79	N. Wall	R=1.41 Full Hgt.	17	14	7	4	11	3
	79/80	N. Wall	R=3.52 Full Hgt.	20	6	2.5	1.3	2.8	3.2
		Floor	None	20	6	1.8	0.2	2	4
Ottawa, Basement D	80/81	N. Wall	R=1.76 Full Hgt.	23	8	4	3	7	1
		E. Wall	R=1.76 Full Hgt.	23	8	4	3	7	1
		Floor	None	23	5	3	4	3.4	1.6

*See References 16 and 17 for details of measurements

Table III : Measured and Calculated Basement Heat Losses of NRC Test Basements

Basement

G-1	Uninsulated
Measured**	2.3 to 2.7 kW
Calculated	Jan. 2.5 kW Feb. 2.6 kW March 2.4 kW
G-2	Insulation: 0.9 m strip on top section of wall. R = 1.32 m^2K/W
Measured**	1.6 to 1.8 kW
Calculated	Jan. 1.6 kW Feb. 1.6 kW March 1.5 kW
G-3	Insulation: Wall full height R = 1.58 m^2K/W
Measured**	1.2 to 1.5 kW
Calculated	Jan. 1.1 kW Feb. 1.1 kW March 1.0 kW

*See Reference 15 for details of experiment.

**The measured total basement heat loss was reduced by the estimated allowance for air infiltration loss. Depending on the assumed air infiltration rate, lower and higher loss values were obtained.

Table IV : Measured and Calculated Basement Heat Losses of the HUDAC Mark XI Test Houses

HOUSE	Heat Loss, W/m^2	
	Measured*	Calculated*
House 4 West Wall	5.7 + 4.8 sin 30 (m + 7)	5.7 + 4.4 sin 30 (m + 7)
House 4 North Wall	8.4 + 6.7 sin 30 (m + 7)	6.1 + 4.6 sin 30 (m + 7)
House 1** North Wall	11.0 + 8.5 sin 30 (m + 7)	10.1 + 6.6 sin 30 (m + 7)
House 4 Floor	5.2 + 0.3 sin 30 (m + ?)***	2.7 + 0.5 sin 30 (m + 4)

*January is denoted by m = 1, February by m = 2, etc.

**H1 with partial insulation on basement wall

***Time lag could not be determined from measured data.

Table V : Measured and Calculated Basement Heat Losses of Gatineau Test Homes

In all cases for the range $1 < R < 5$:

$\sigma_2 = 0.9$ $\quad \Delta t_2 = 0$

$\sigma_3 = 0.7$ $\quad \Delta t_3 = -1$

$\sigma_4 = 0.4$ $\quad \Delta t_4 = -2$

$\sigma_5 = 0.3$ $\quad \Delta t_5 = -4$

Units:

S, $W/(m^2 \cdot K)$ $\quad$ R, $m^2 \cdot K/W$

V, $W/(m^2 \cdot K)$ $\quad$ σ, dimensionless

C, m^2 or dimensionless $\quad$ Δt, month

(Δt is the time delay of heat flux sine wave relative to the ground surface temperature sine wave.)

SECTION A: SOIL THERMAL CONDUCTIVITY: k upper = 0.8 W/(m.K); k lower = 0.9 W/(m.K)

Insulation System (Soil, Insulation, Concrete)	S_n, V_n, and C_n Factors	Wall Segments: Top strip just below grade, n = 2	Wall Segments: Bottom strip, n = 3	Floor Segments: 1 m strip adjacent to wall, n = 4	Floor Segments: Centre n = 5
1	S_n	1.9	0.71	0.42	0.17
	V_n	1.9	0.65	0.24	0.05
	C_n	0	1.0	2.6	0.5
2	S_n	$(0.53 + 1.42 \cdot R)^{-1}$	$(1.06 - 0.013 \cdot R)^{-1}$	0.41	0.18
	V_n	$(0.53 + 1.43 \cdot R)^{-1}$	$(1.15 - 0.016 \cdot R)^{-1}$	0.25	0.05
	C_n	0	1.0	2.6	0.5
3	S_n	$(0.58 + 1.10 \cdot R)^{-1}$	$(1.23 + 1.45 \cdot R)^{-1}$	$(1.81 - 0.051 \cdot R)^{-1}$	0.19
	V_n	$(0.58 + 1.12 \cdot R)^{-1}$	$(1.31 + 1.55 \cdot R)^{-1}$	$(2.77 - 0.11 \cdot R)^{-1}$	0.07
	C_n	0	0.6	2.1	0.5

Table VI : Corrected Shape, Attenuation, Time Lag and Corner Allowance Factors for Basement Heat Loss Calculations

SOURCE	DAILY -W/M^2	STD.DEV
AES	4104	-
TMY	5017	1034
U OF MAN	5478	368

Table VII : Average Daily Available Radiation on Vertical Surface.

Month/1991	Efficiency	Effectiveness	Mass Ratio	HOT-2000 Efficiency
January	77.40%	78.40%	0.9994	77.8%
February	78.36%	77.45%	0.9926	78.6%
March	76.92%	77.02%	1.0025	79.4%

Table VIII: Heat Recovery Ventilator Performance Under Insitu Conditions.

	AC/hr at 50 Pa depressurization
Pre-1945	10.35
1946-1960	4.55
1961-1980	3.57
Special airtight house	1.49

Table IX : Values for Airtightness Test Over the Years.

SUMMARY OF HOT- 2000 STORMONT HOUSE ENERGY ANALYSES

ITEMS	SEPT 1990	AUG 5/91 REV'SED INFLT	AUG 5/91 REV'SED INFLT	
HEAT LOSSES	MIL BTU	MJ	MJ	SOLAR & BASEMENT DATA MJ
ABOVE GRADE				
Ceiling	8.588	9060	9060	9061
Main walls	16.588	17500	17500	17501
Doors	1.164	1228	1228	1228
Floor overhang	1.102	1163	1163	1163
Base walls above grd	3.72	3921	3921	3922
Total Envelope	27	32872	32872	32875
Percent of total losses		28%	27%	27%
Windows south	23.359	24644	24644	26972
" east	3.546	3741	3741	4095
" north	6.134	6471	6471	7080
" west	3.552	3747	3747	4102
Total window losses	37	38604	38604	42249
Percent of total losses		37%	33%	34%
Ventilation .5ACH	9.856	10398	28625	30062
		RSI = .70		RSI = .70
Percent of total losses		10%	24%	25%
SHALLOW BASE AREA				
Base walls below grd		9433	4152	3912
Perimeter area		2591	1860	1736
Centre area		5300	6260	7477
FULL BASE AREA				
Upper base walls		388	388	407
Lower base walls		2227	2227	1230
Perimeter area		1645	1645	1481
Centre area		753	753	867
Total basement heat losses		22336	17284	17110	15836
Percent of total heat losses		22%	15%	14%	13%
Total heat losses		103031	117385	122296	121170
GROSS HEATING LOAD	97.66	103031	117385	122444	121170
Usable heat gains	-14.22	-15002	-14983	-15003	-15003
Usable sol heat	-35.52	-37474	-39744	-41340	-41340
Vent equip elec	-1.544	-1629	-1629	-1604	-1604
Furnace annual load	46.38	48927	61029	64497	63223
@ 90% annual eff	51.52	54354	67810	71663	70248
Actual Gas Consumption					
76200 cu ft=76200*950=72.39		76371	76371	76371	76371
Unaccounted for		22017	8561	4708	6123
Or equivalent furnace		(29%)	(11%)	(6%)	(8%)
seasonal efficiency of		64%	90%	84%	83%

ANSYS BASEMENT HEAT LOSS

SEPT	268.15	702.59
OCT	331.16	867.69
NOV	394.17	1032.78
DEC	776.86	2035.49
JAN	651.86	1707.97
FEB	748.36	1960.82
MAR	622.55	1631.17
APR	603	1579.95
MAY	680.36	1782.65
JUN	563.7	1476.98
JUL	444.68	1165.13
AUG	-41.11	-107.71
TOT	6043.74	15835.55

TABLE X HOUSE ENERGY ANALYSIS

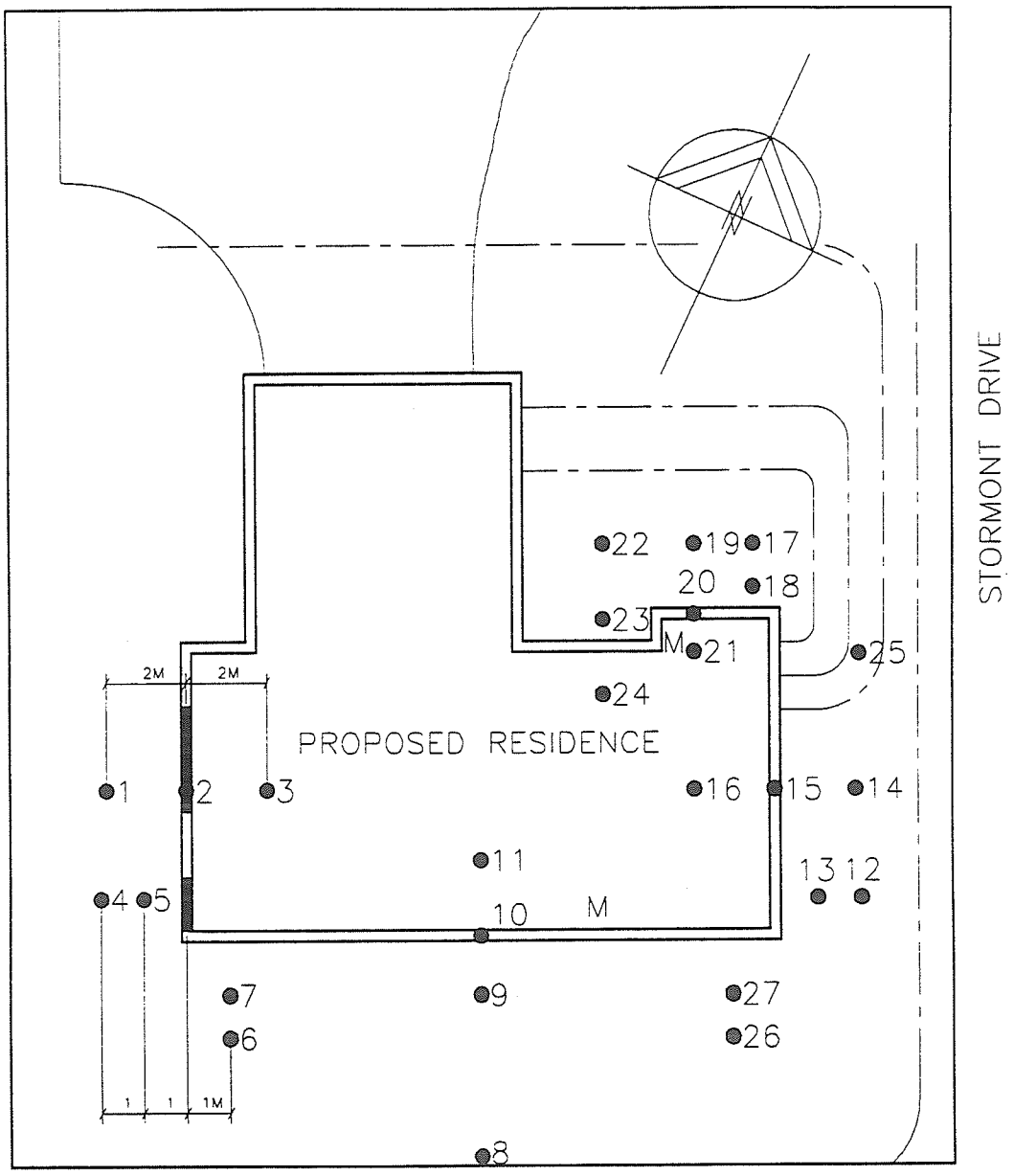

Fig.1 : Thermocouple Station Location at 1 Stormont Drive.

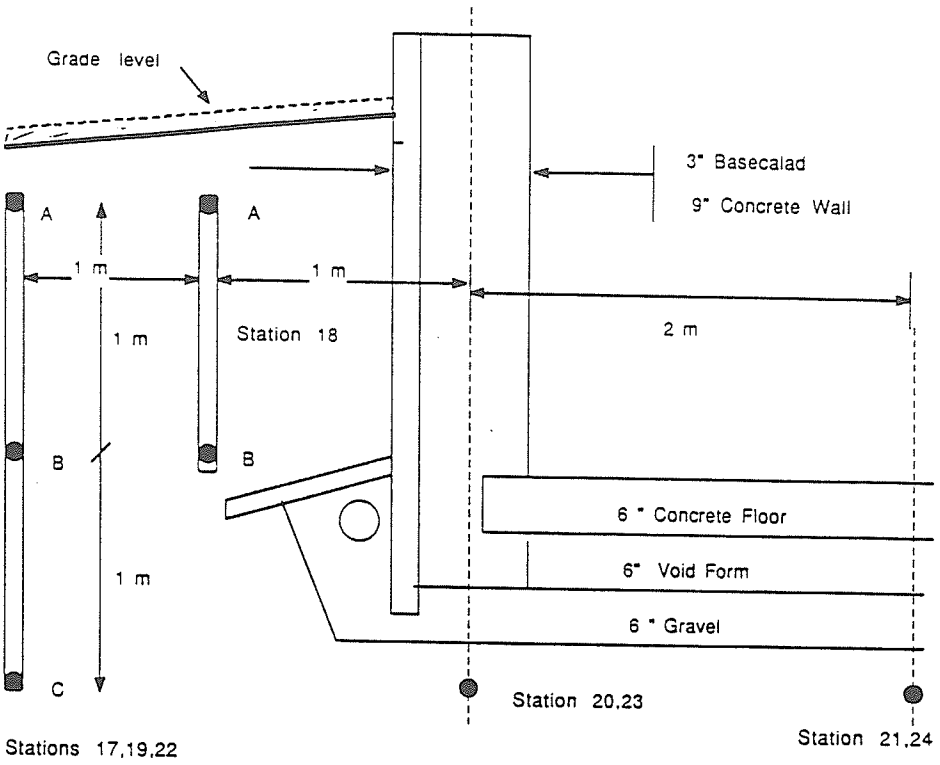

Fig.2 : Location of Stations and Thermocouples Placement on Full Depth Basement Side.

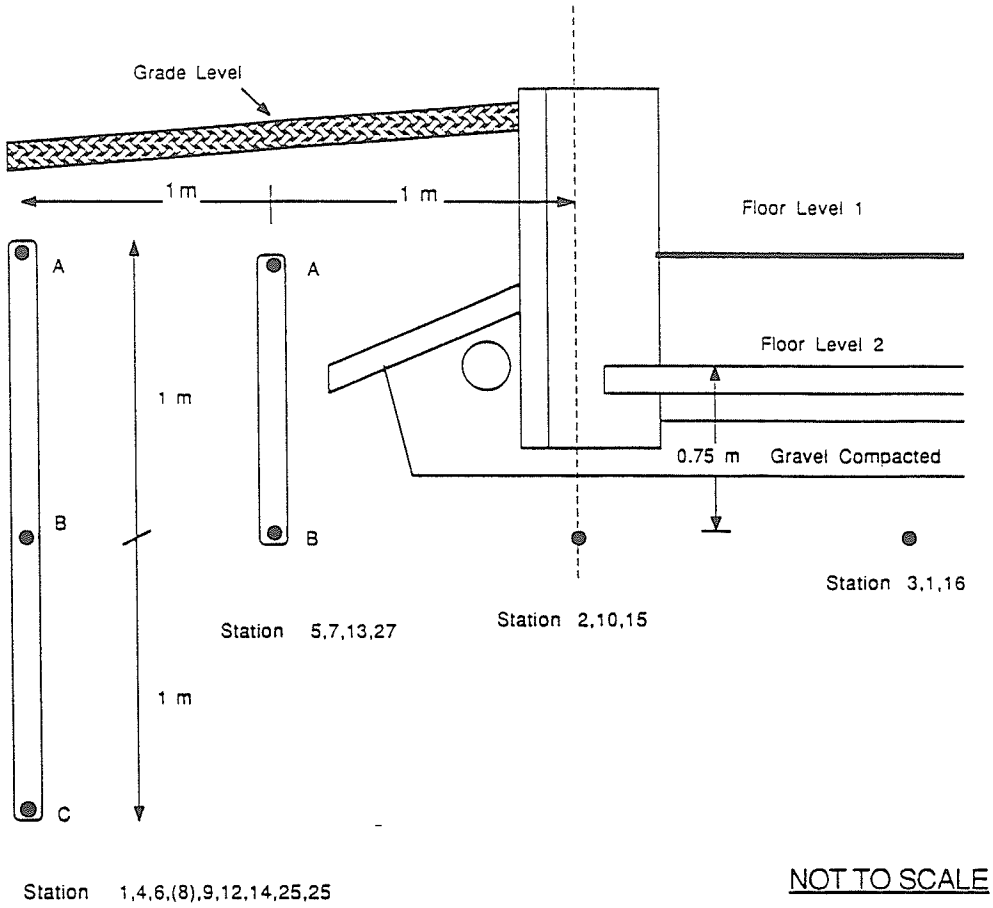

Fig. 3 : Location of Stations and Thermocouples Placement on Shallow Side.

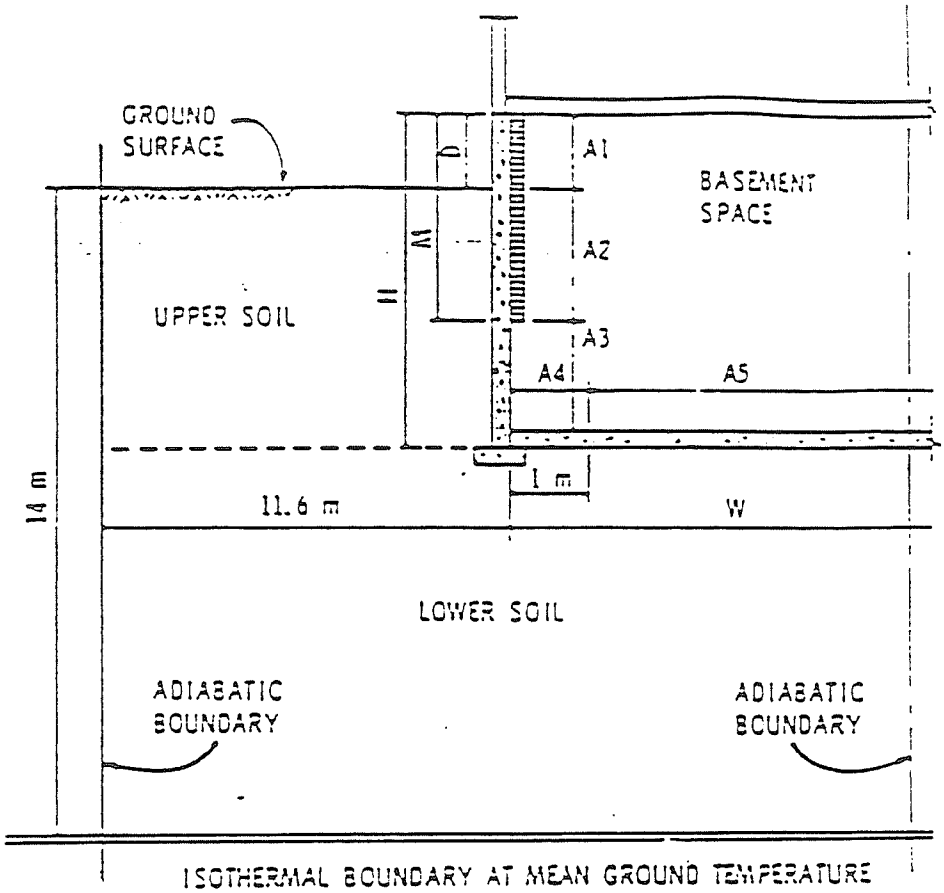

Fig.4: Mitalas Basement Model Profile [2].

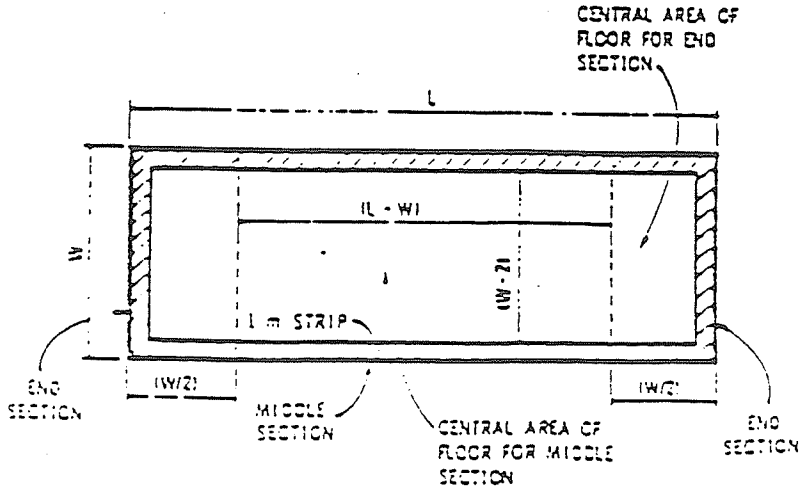

Fig.5: Floor Plan of Rectangular Basement [2].

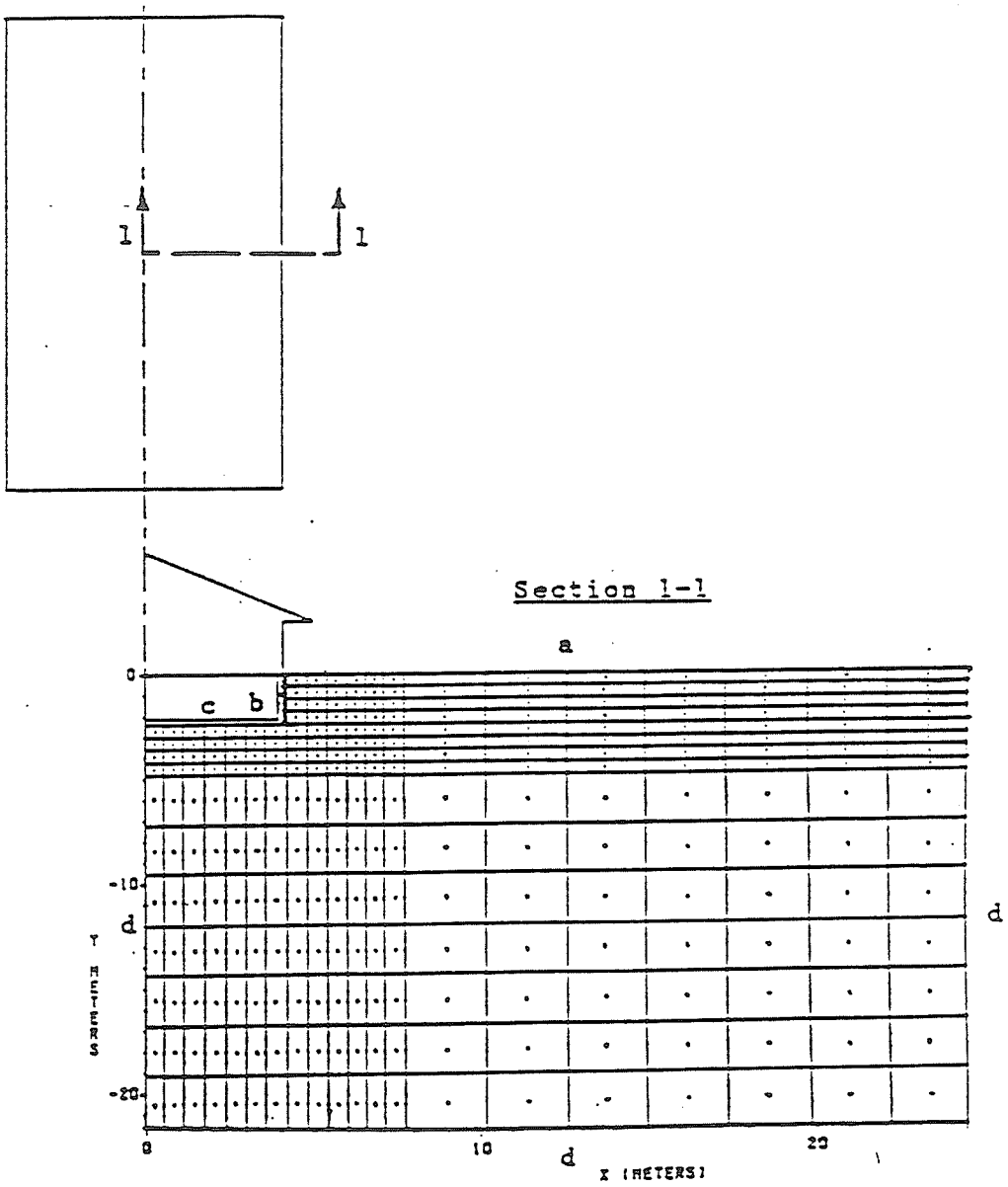

Boundary Conditions : a) Mean daily air temperature boundary

b) Heat loss through the basement wall

c) Heat loss through the basement floor

d) Adiabatic boundary

Fig.6: Finite-Difference Grid Pattern for Prediction of the Soil Temperatures. around a House Basement and its Boundary conditions [11].

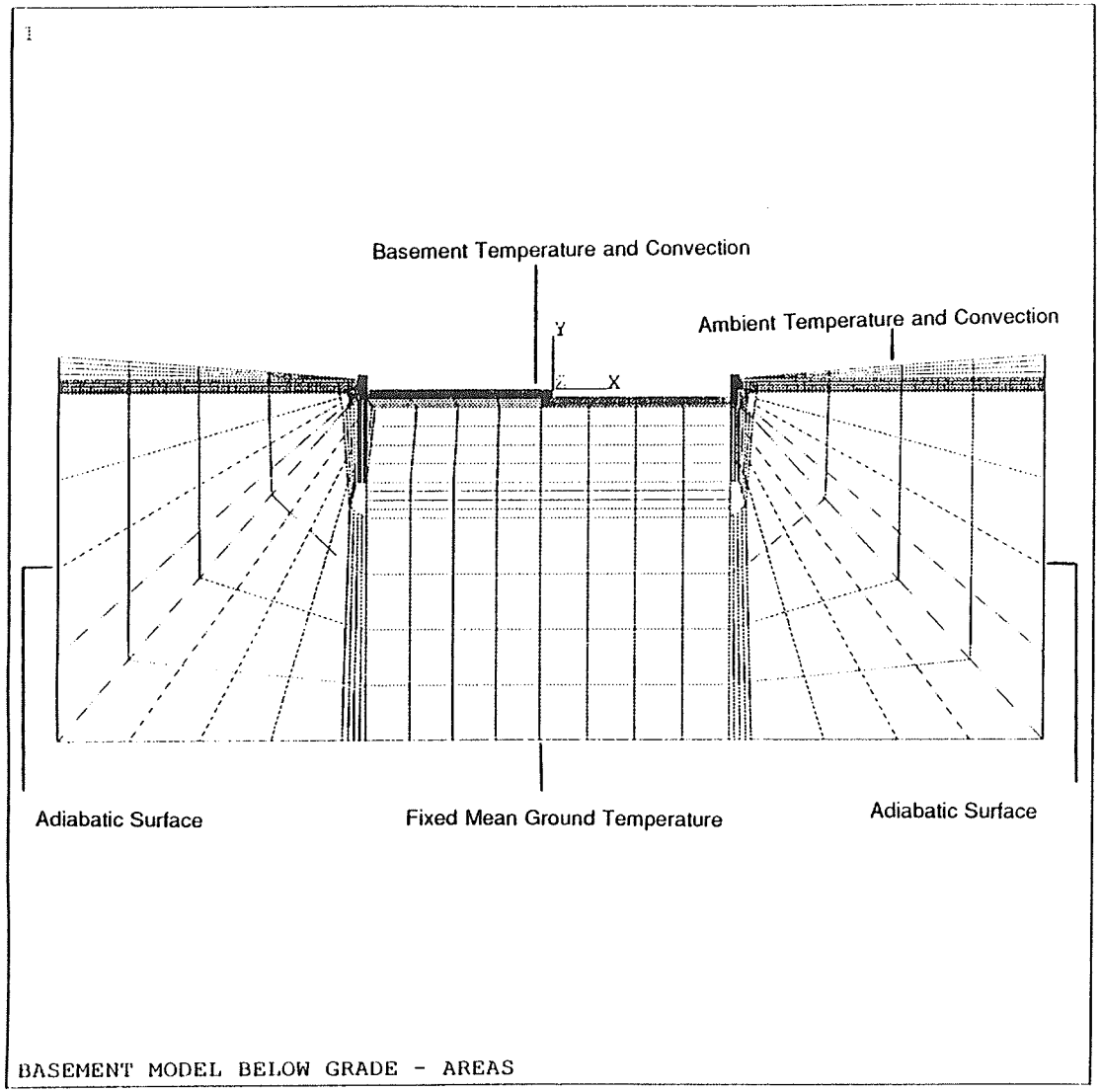

Fig.7: Areas to be Meshed of Basement Model Below-Grade.

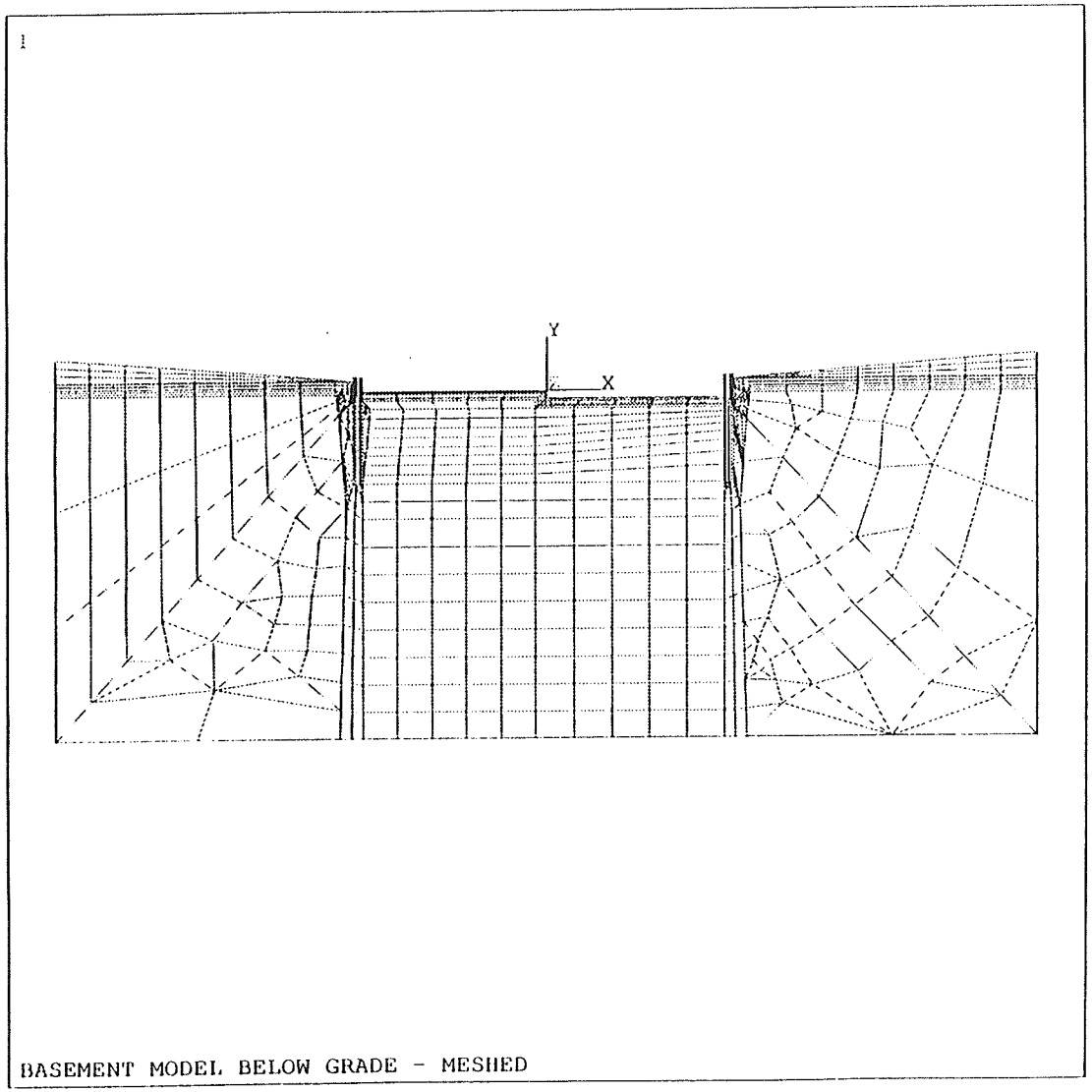

Big.8: Basement Model Below-Grade Meshed.

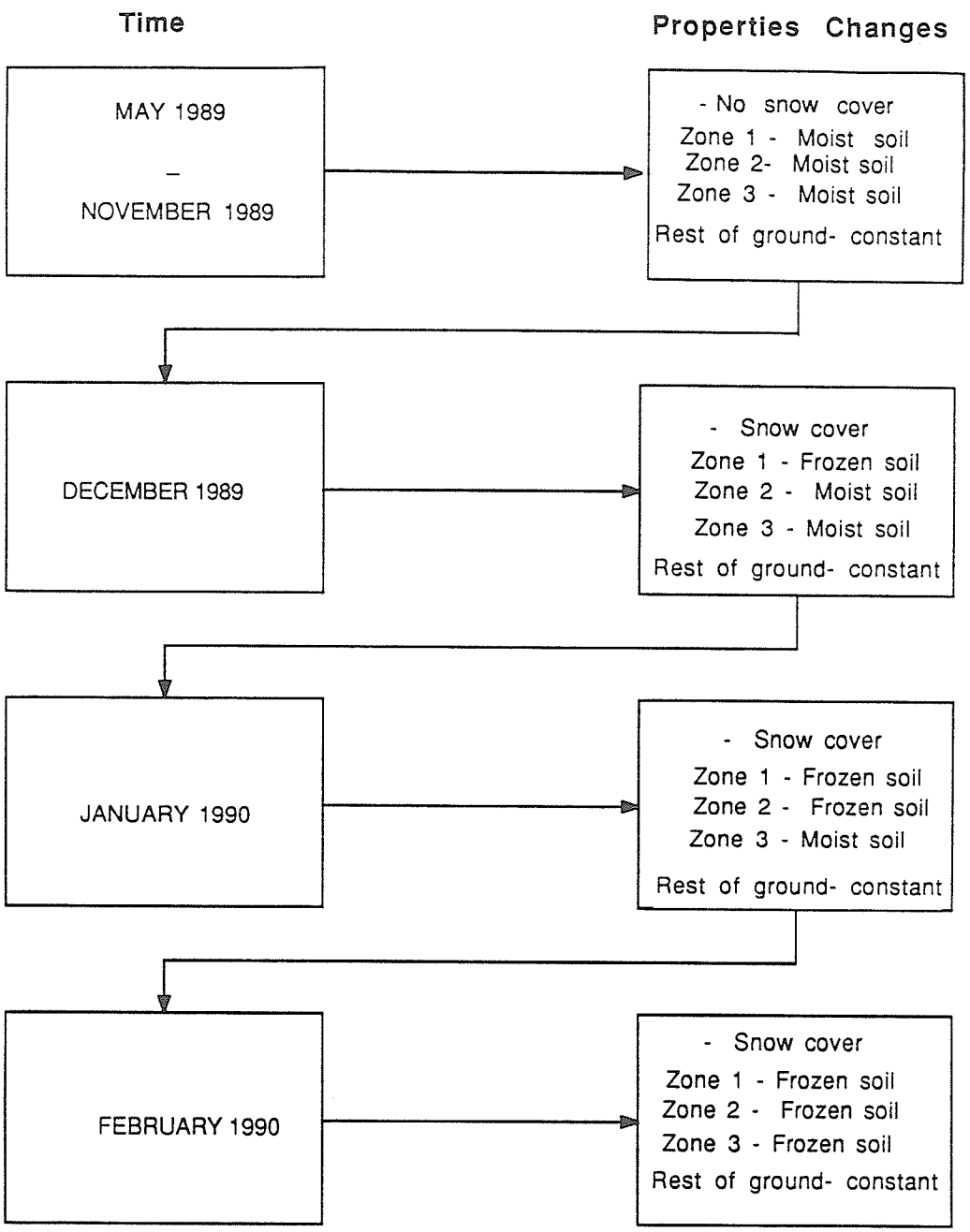

Fig.9: Time and Corresponding Property Change Sequence in Basement Model.

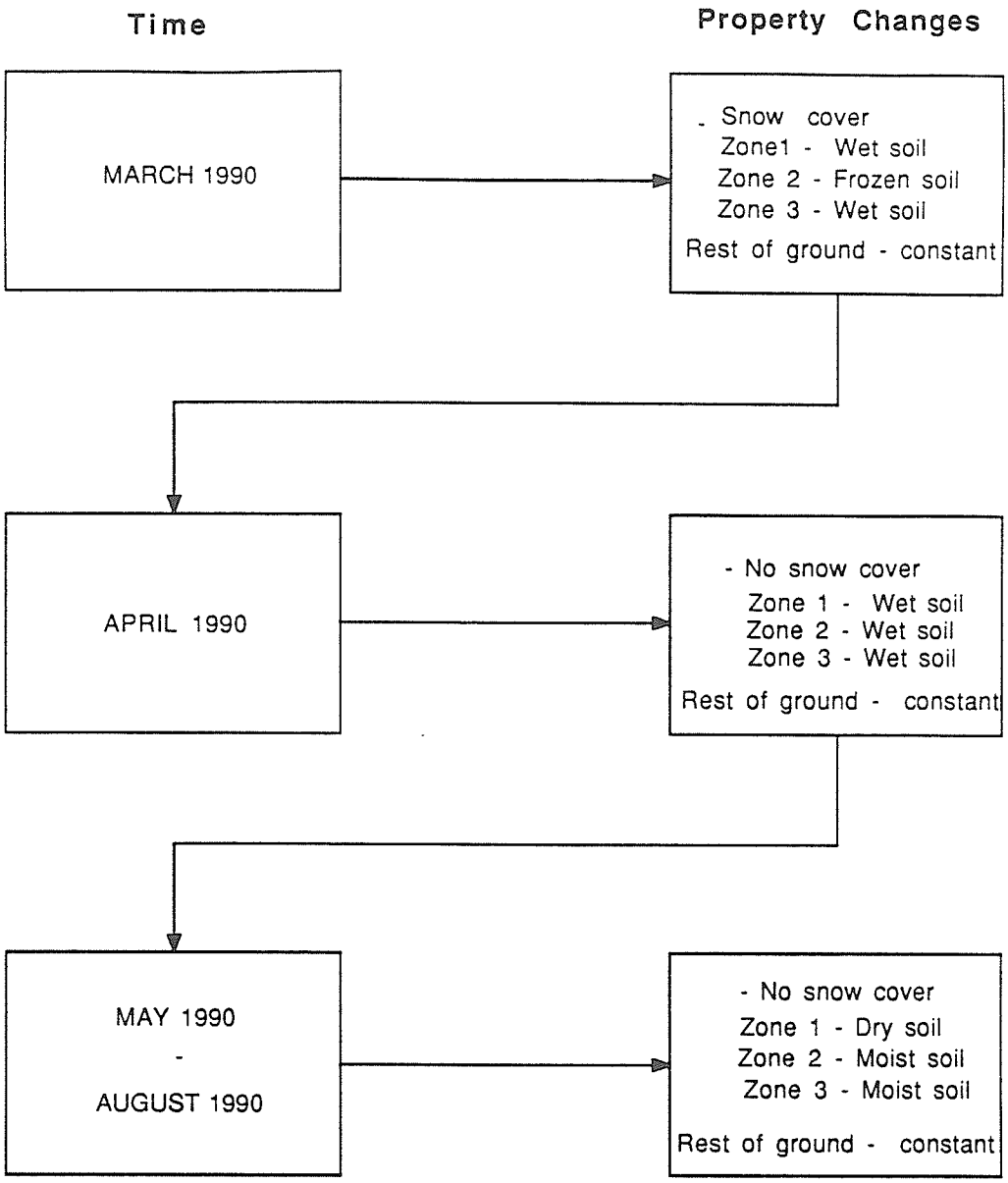

Fig.10: Time and Corresponding Property Change Sequence in Basement Model.

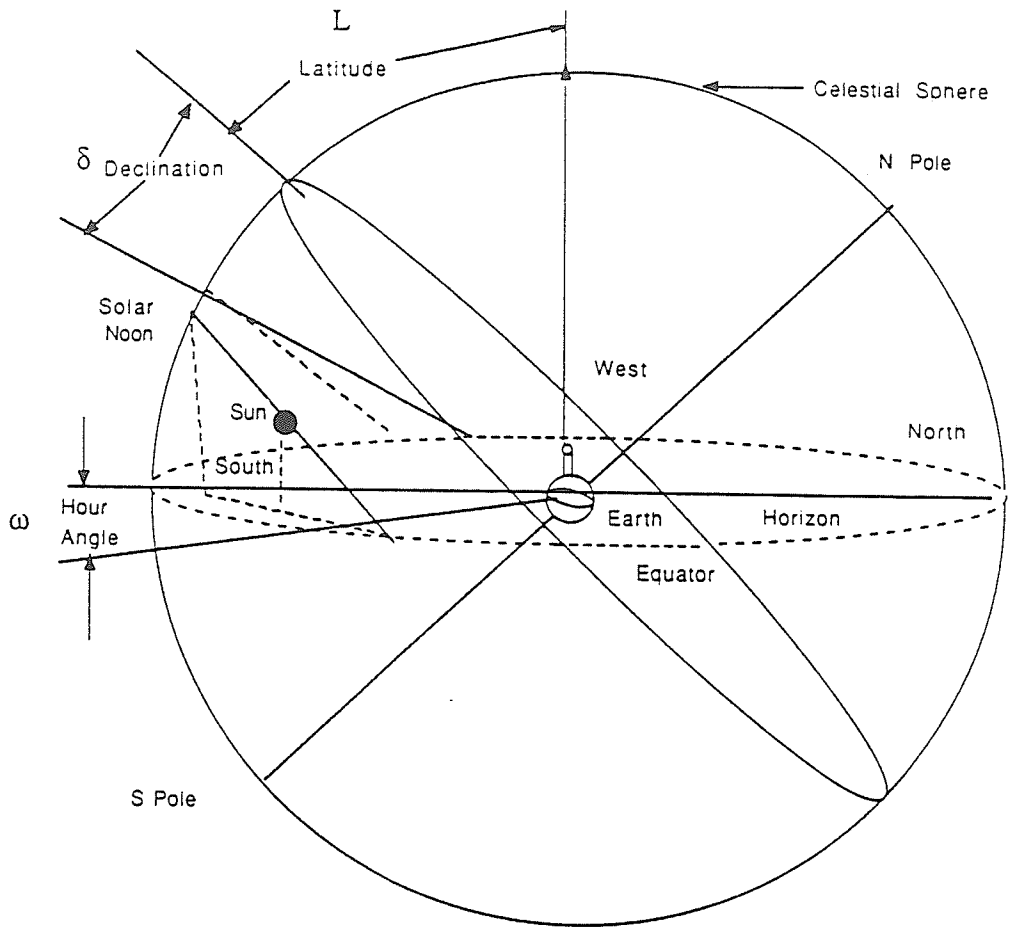

Ratio of Beam Radiation on Tilted Surface to that on Horizontal Surface

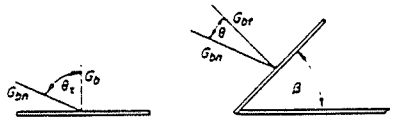

Beam radiation on horizontal and tilted surfaces.

Declination - Northern Hemisphere

L- Latitude (Winnipeg 49^{0}54');

$\delta = 23.45 [\sin 2\pi (284+n)/365]$;

δ- Declination;

n= day of the year;

ω- Hour Angle;

Fig.11: Solar Celestial System.

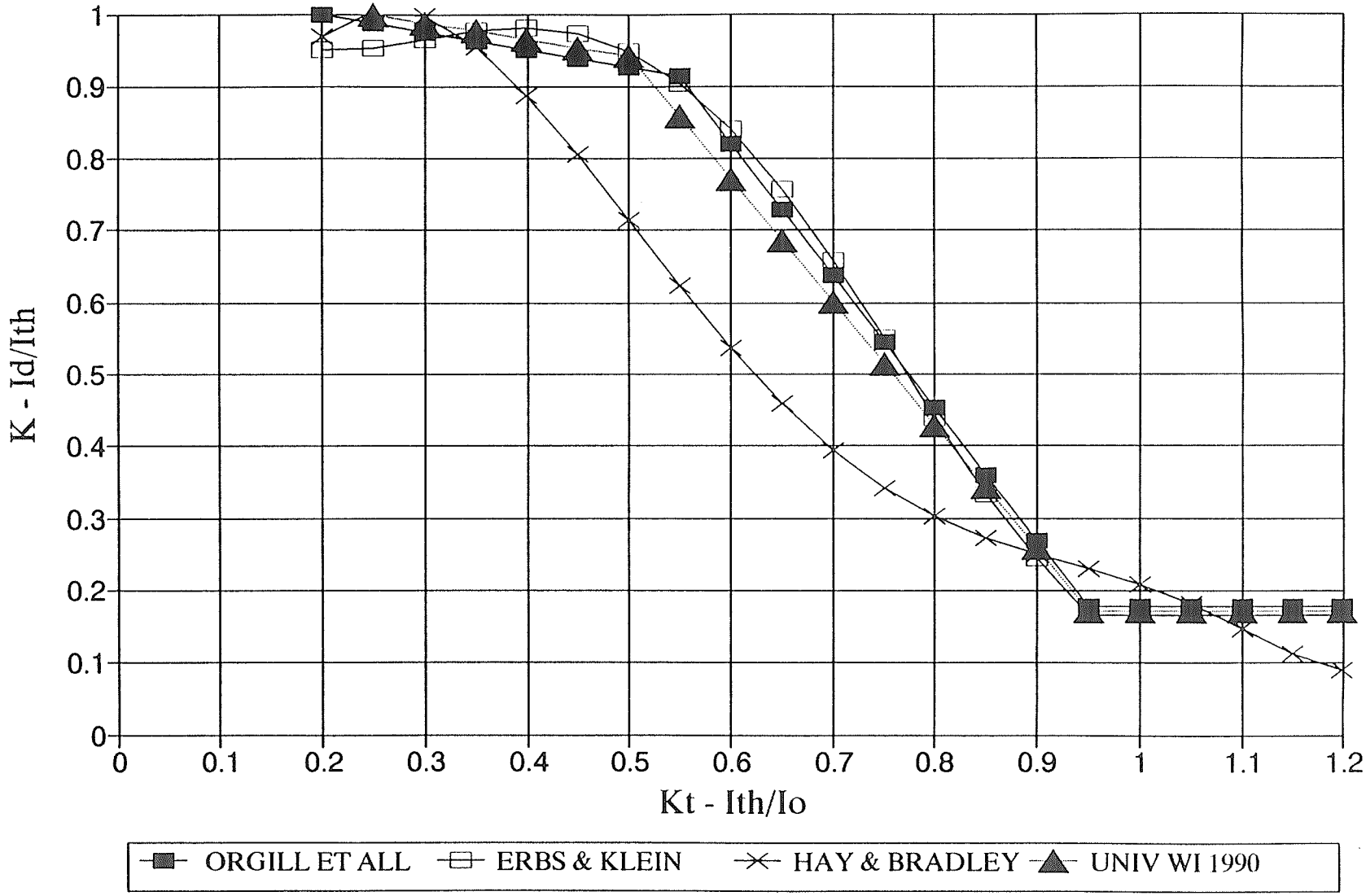

Fig.12: Ratio of Diffuse to Total Radiation Versus Clearness Index.

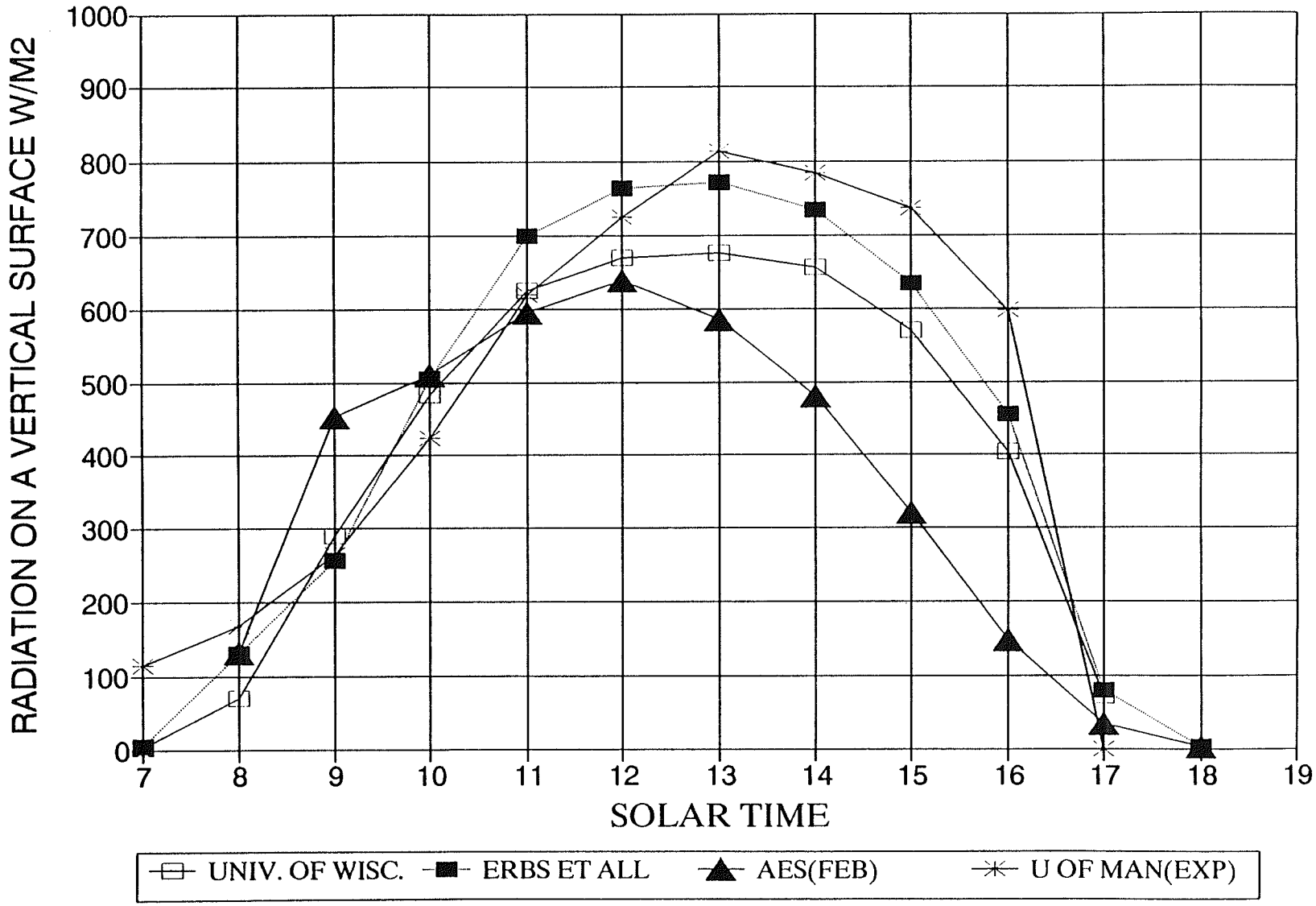

Fig.13: Comparison of Sources of Data for the Eighth Week-Feb 18th to 25th.

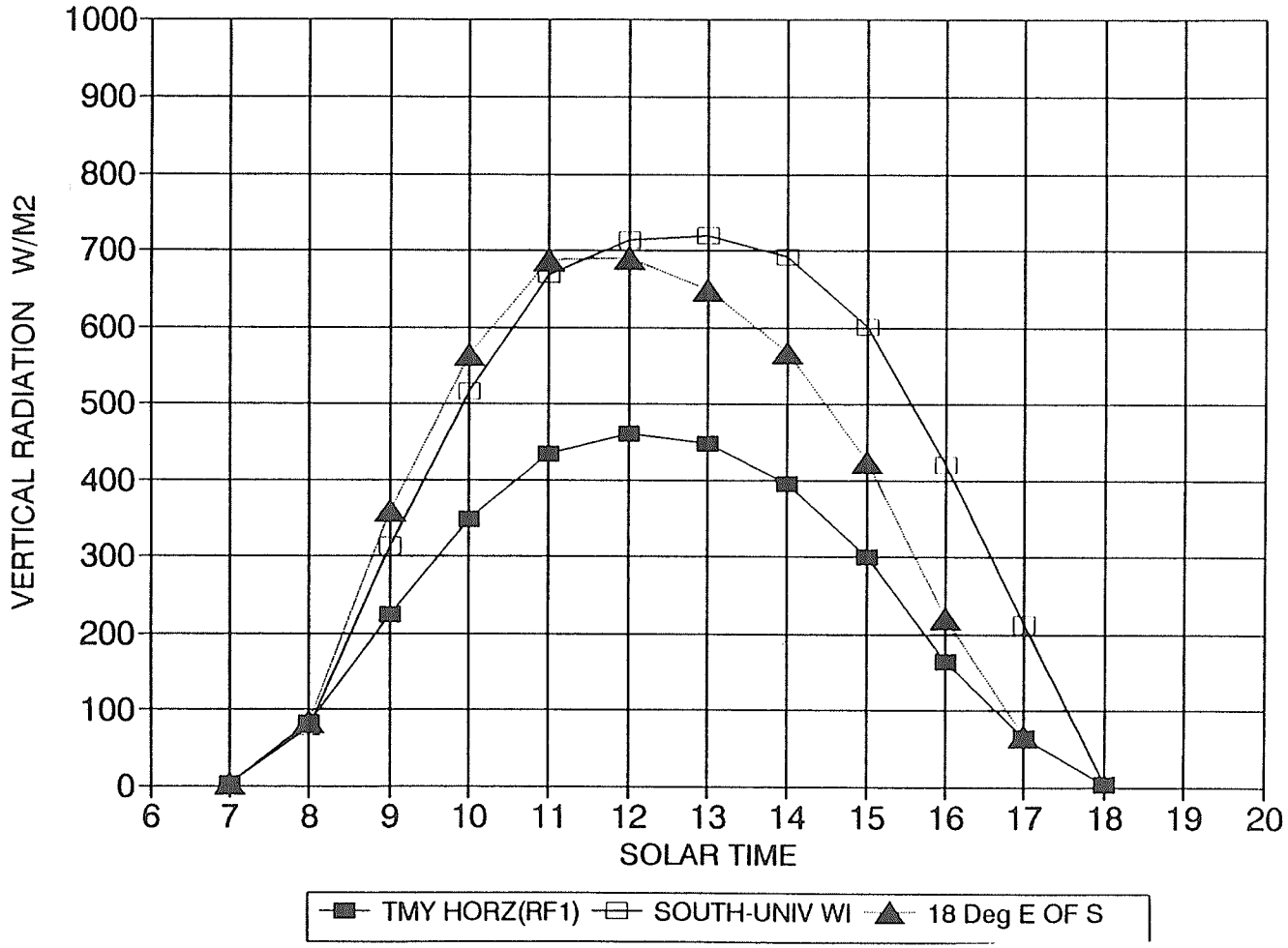

Fig.14: Effect of slope and Orientation on Radiation for Eighth Week-Feb 18th to 25th.

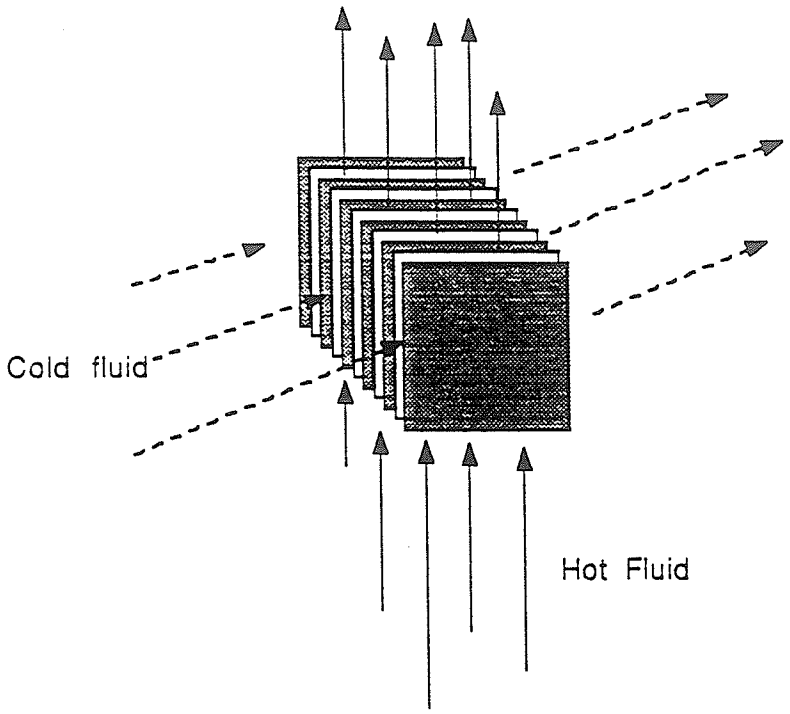

Fig.15: View of Core and Flow Pattern of Hot and Cold Fluid.

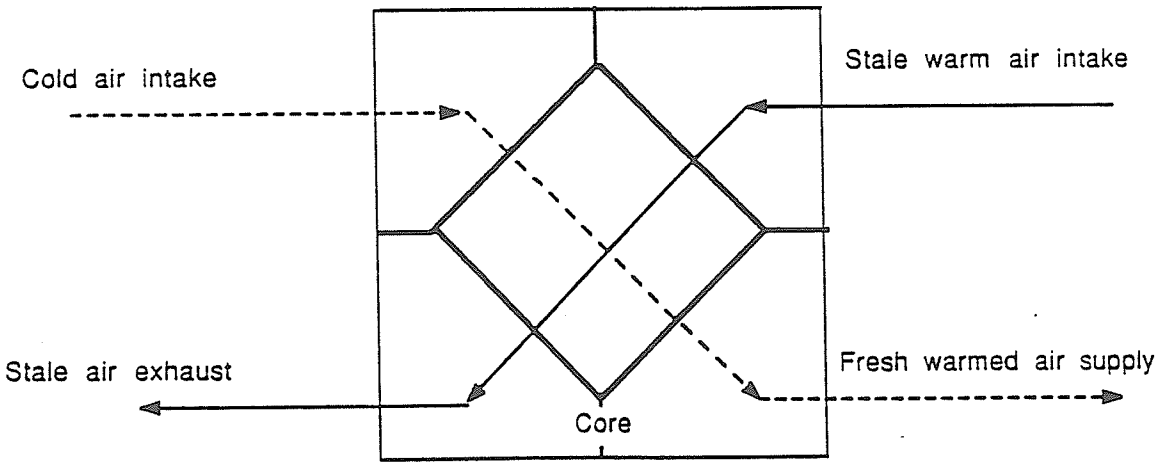

Fig.16: Residential Heat Recovery Flow Path.

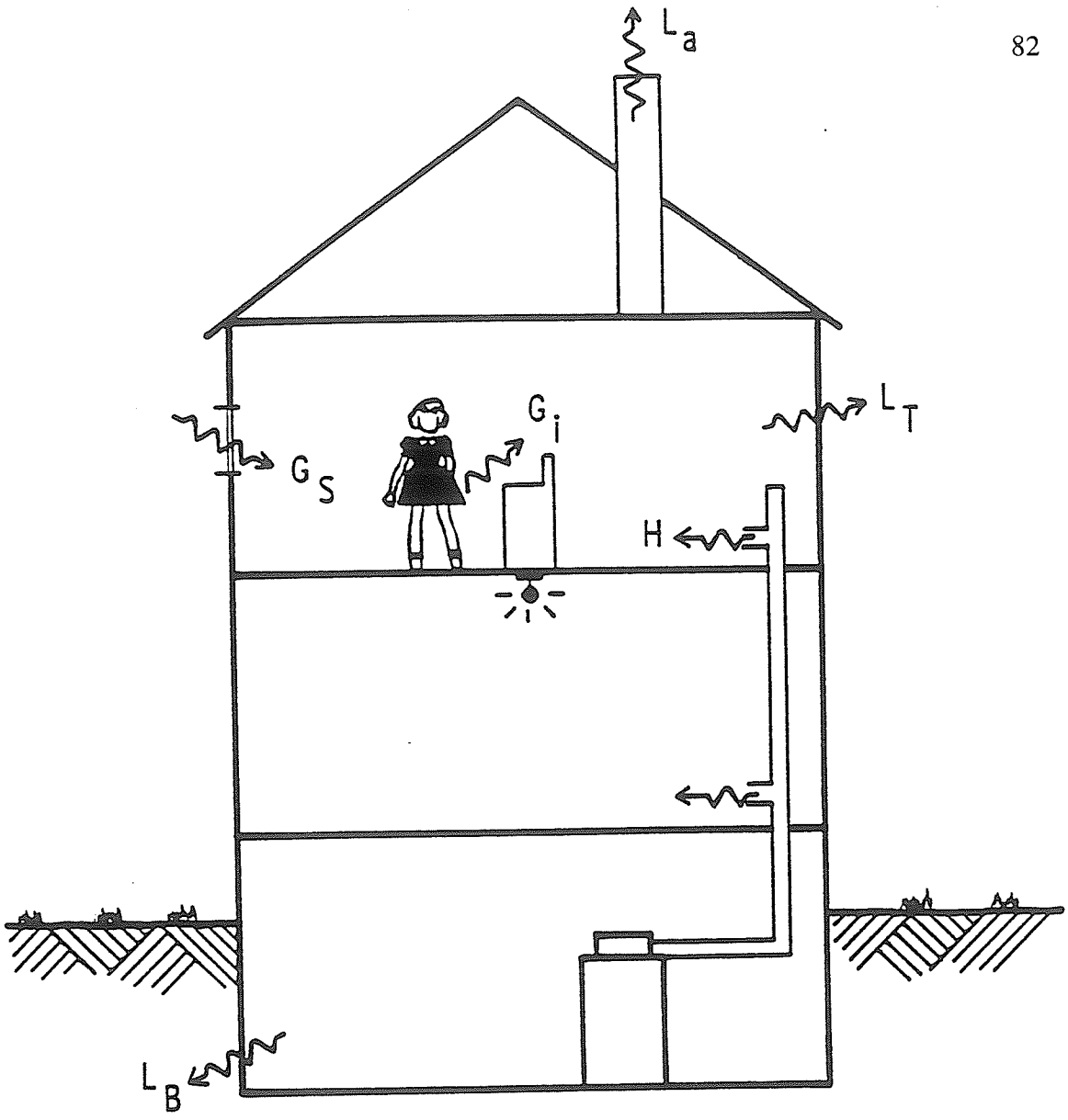

$$H = L_T + L_a + L_B - \eta_i G_i - \eta_s G_s$$

Fig.17: Schematic of Heat Losses Present in a Residence [2].

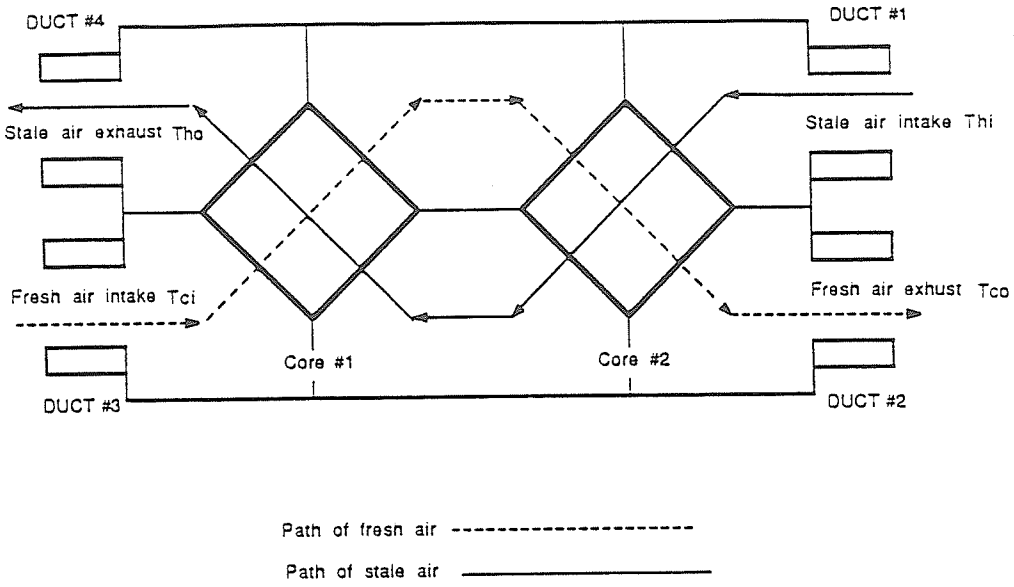

Fig.18: Schematic of Heat Recovery Ventilator on Site.

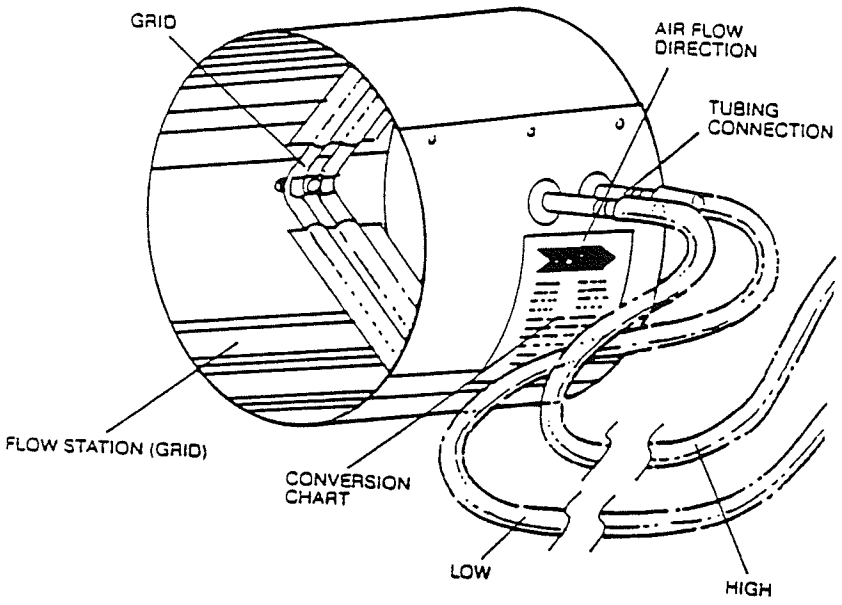

Fig.19: Schematic of Flow Collar Used in Heat Recovery Ventilator Duct [29].

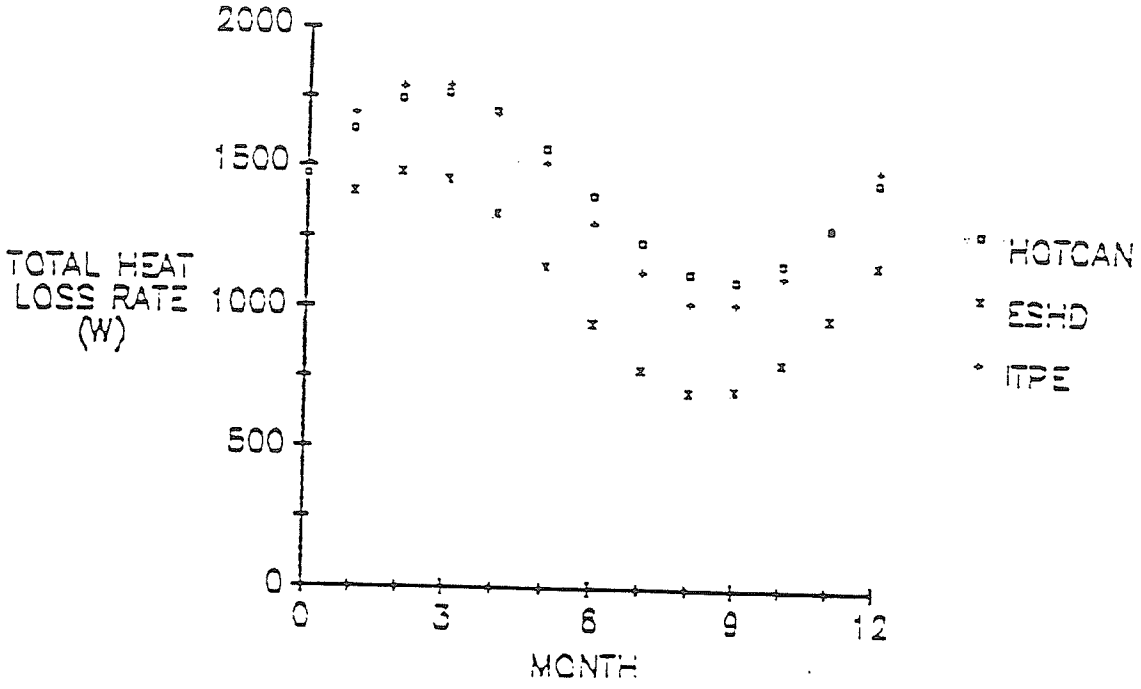

Fig.20: Comparison of HOTCAN 3.0 with EHSD and ITPE, for Monthly Average Heat Loss Rates for a Basement with Inside Wall Insulation.

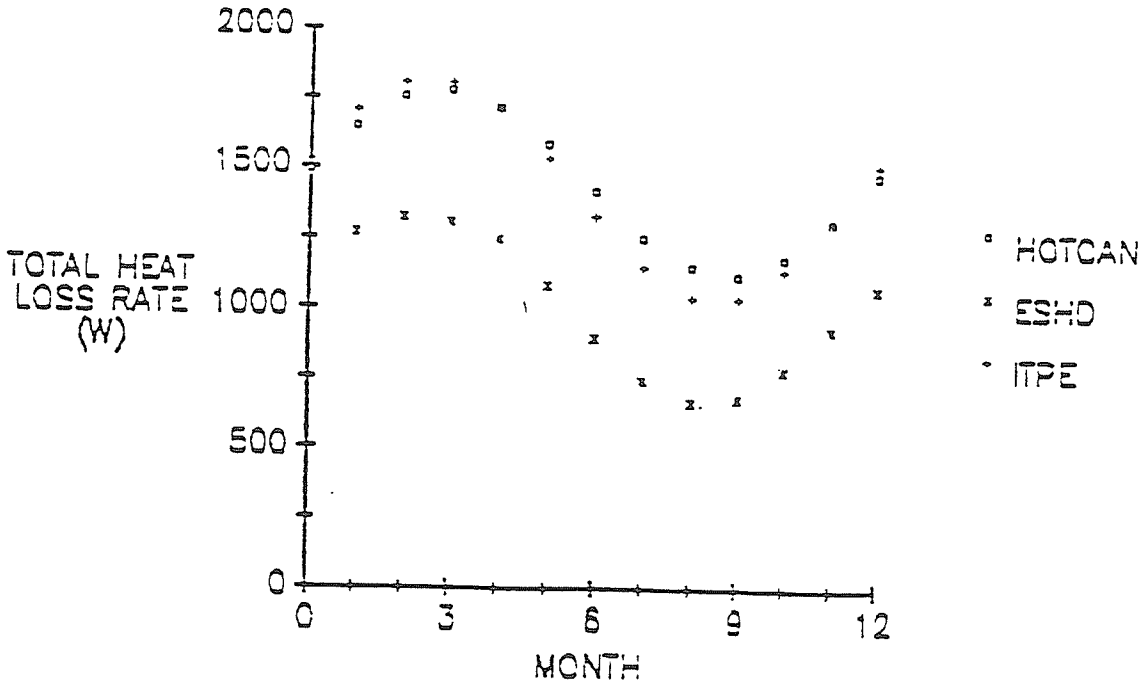

Fig.21: Comparison of HOTCAN 3.0 with EHSD and ITPE, for Monthly Average Heat Loss for a Basement with Exterior Wall Insulation.

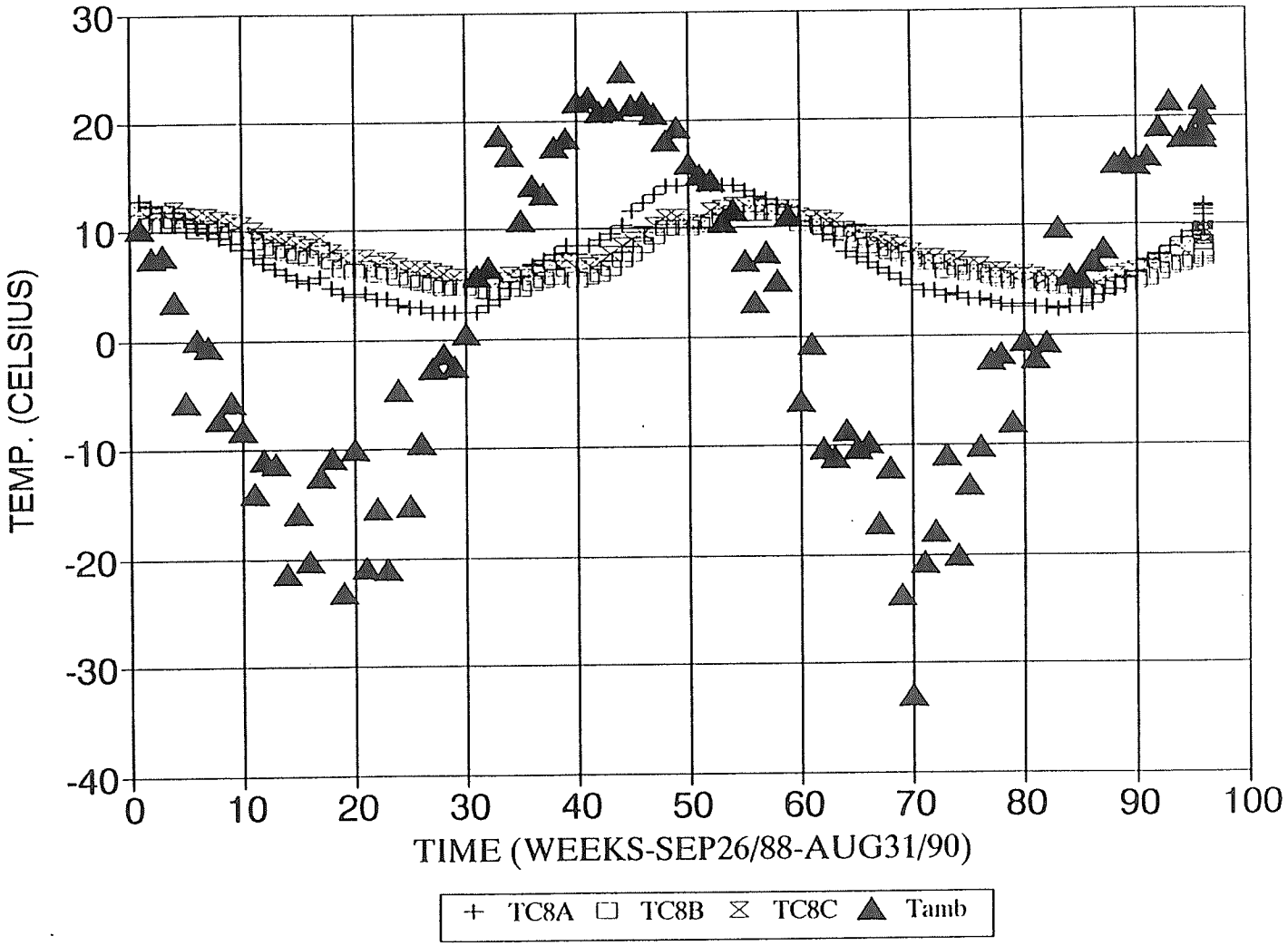

Fig.22 : Ambient and Ground Temperatures at Station 8.

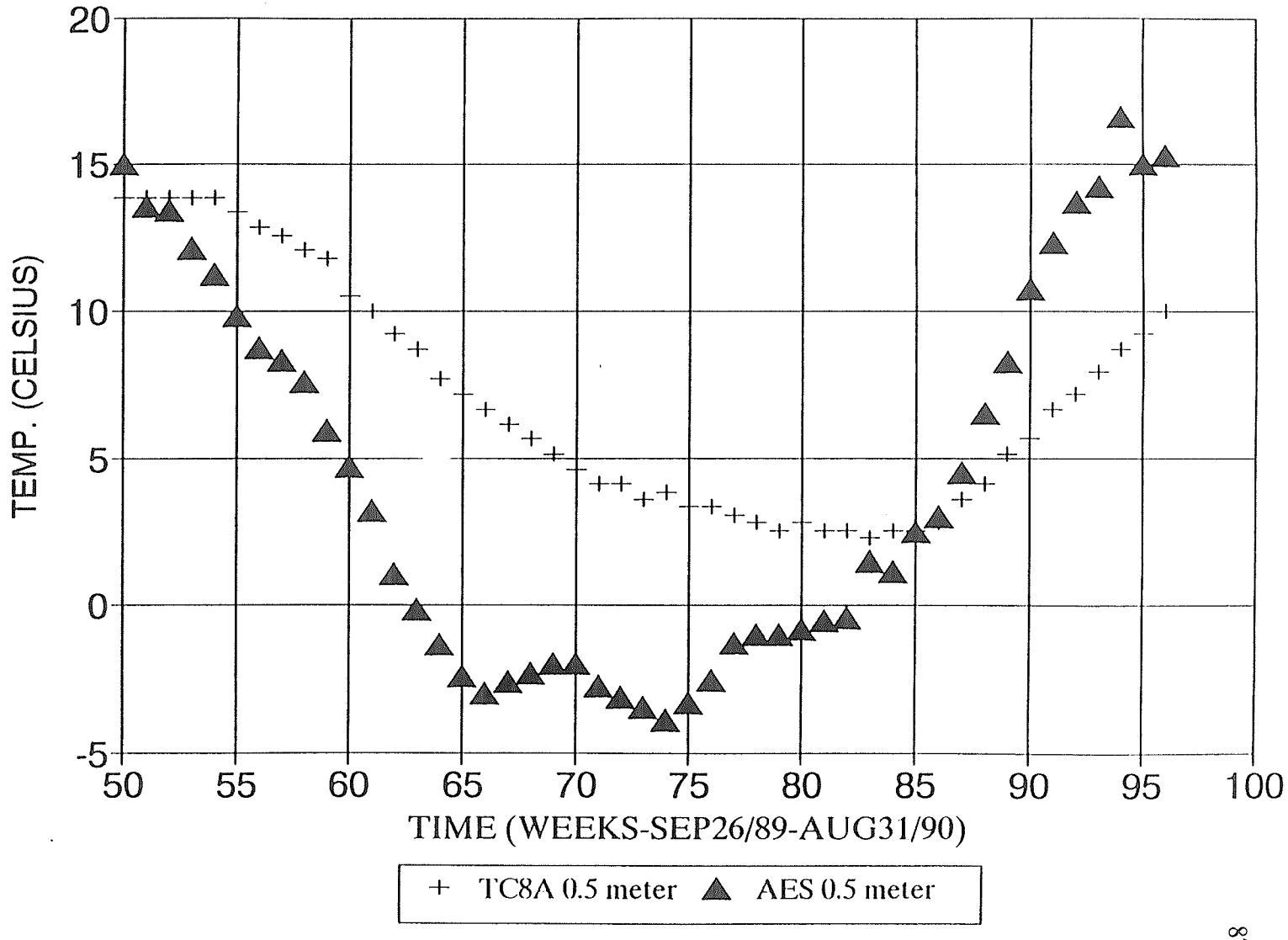

Fig.23: Ground Temperatures at Thermocouple 8A and AES Data.

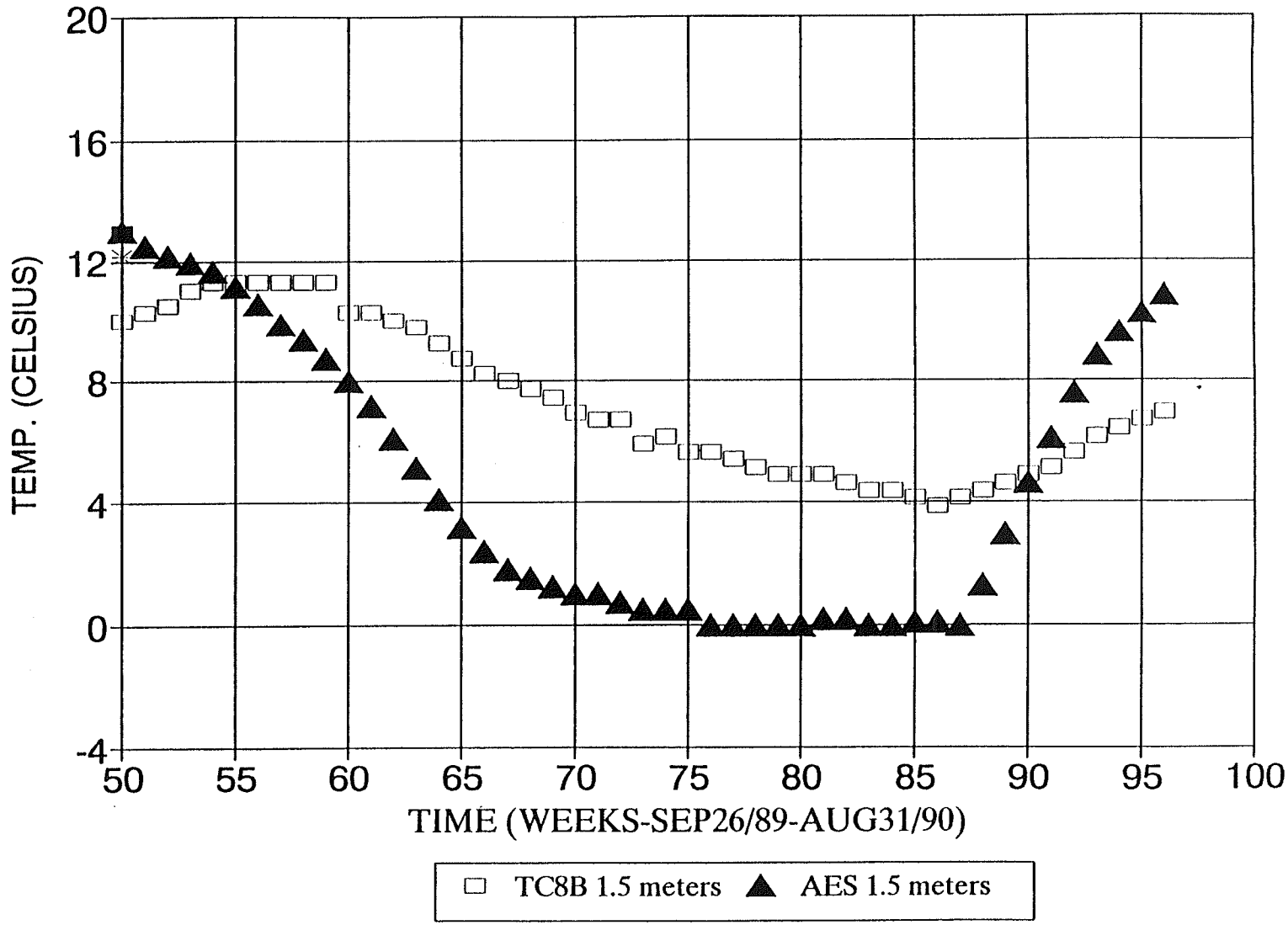

Fig.24: Ground Temperatures at Thermocouple 8B and AES Data.

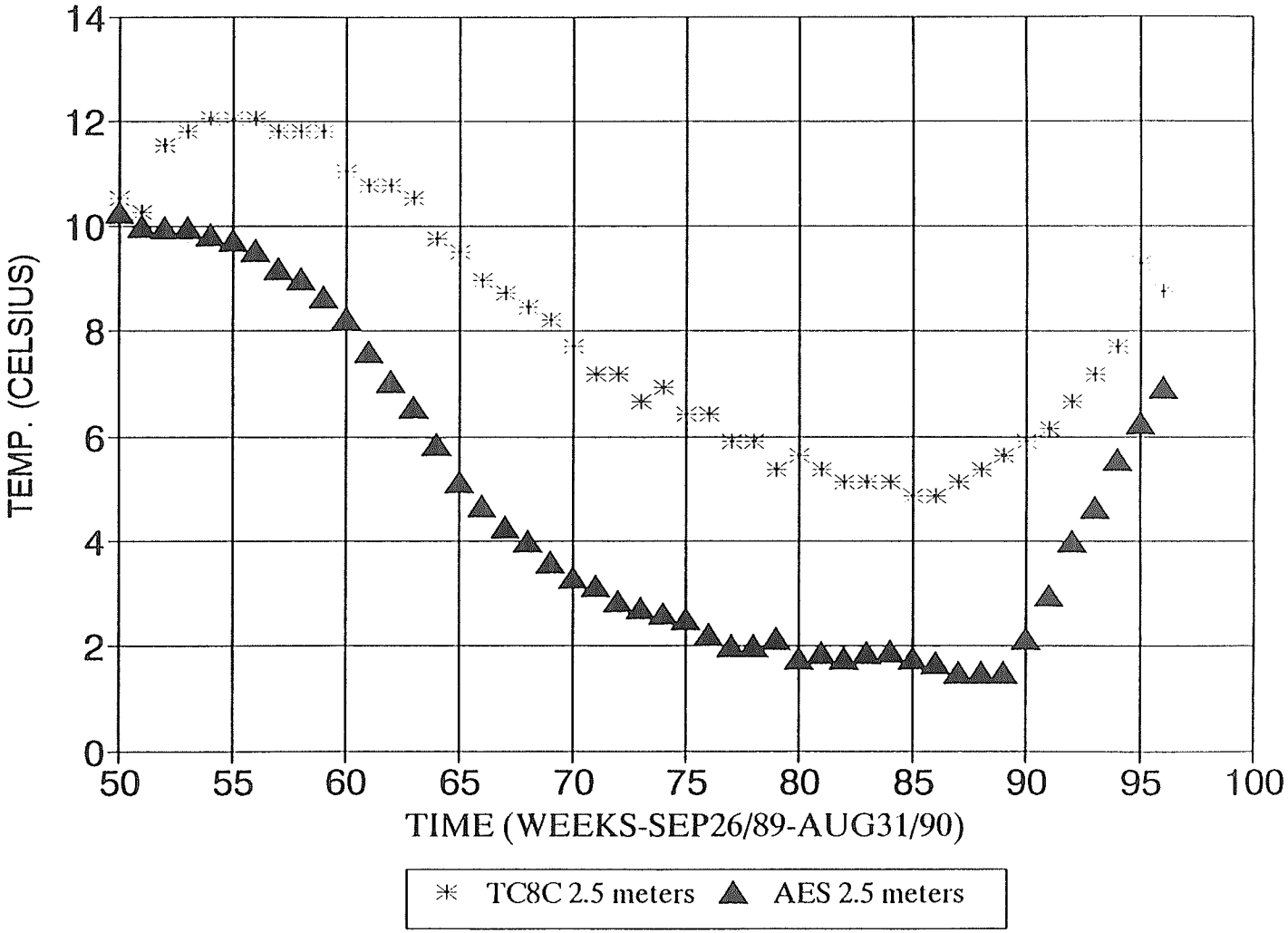

Fig.25: Ground Temperatures at Thermocouple 8C and AES Data.

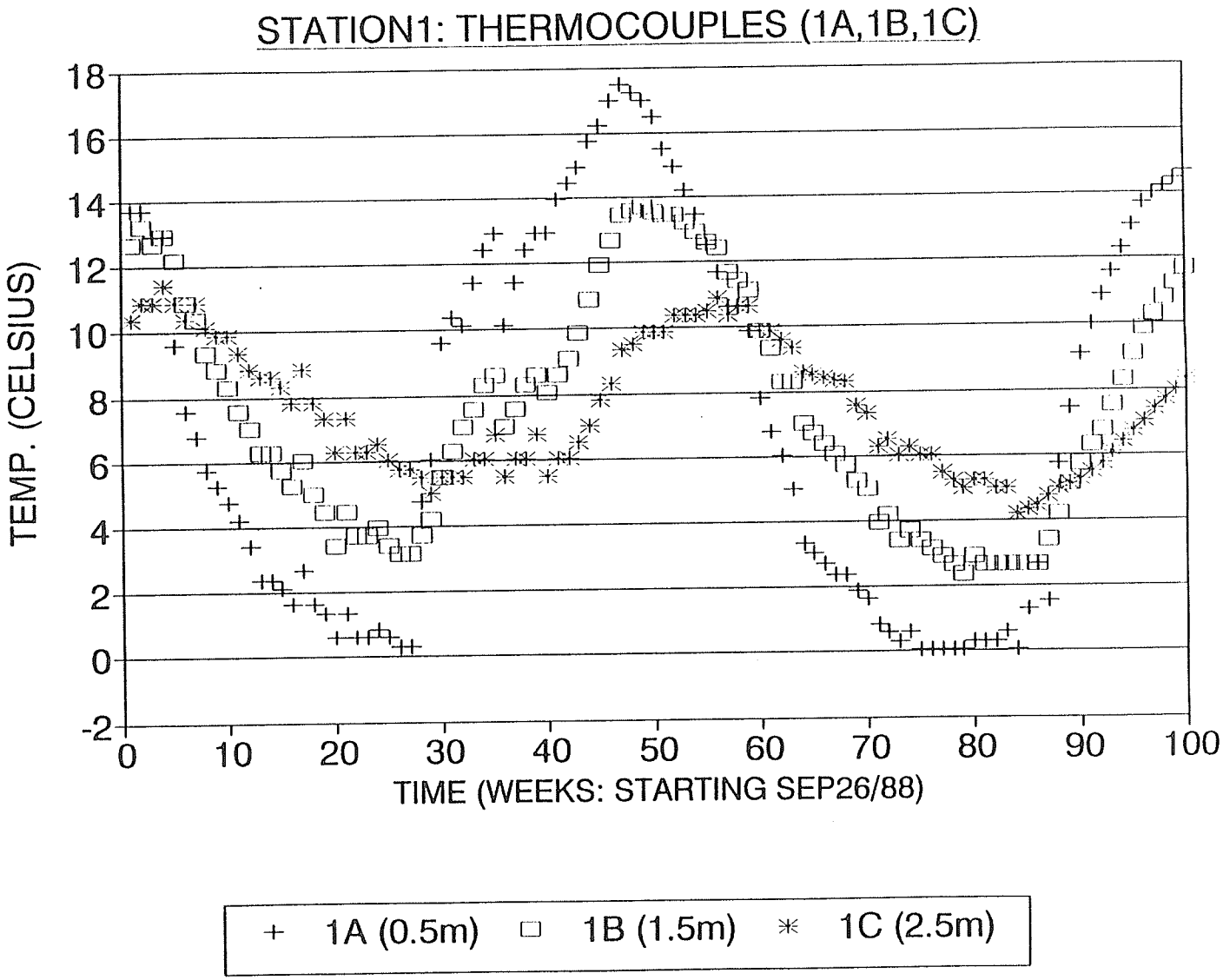

Fig.26 : Ground Temperatures at Thermocouples 1A, 1B, 1C.

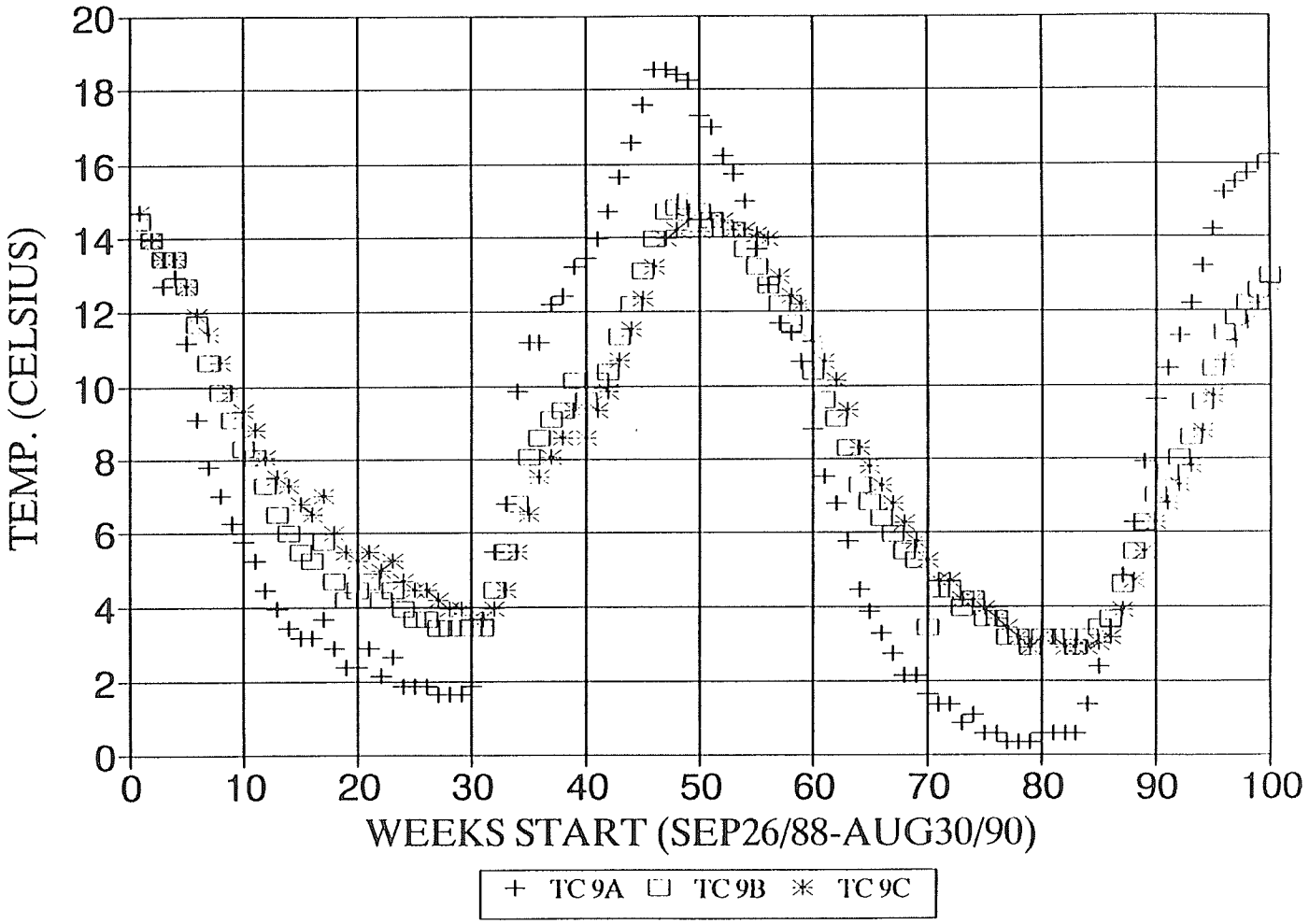

Fig.27: Ground Temperatures at Thermocouples 9A, 9B, 9C.

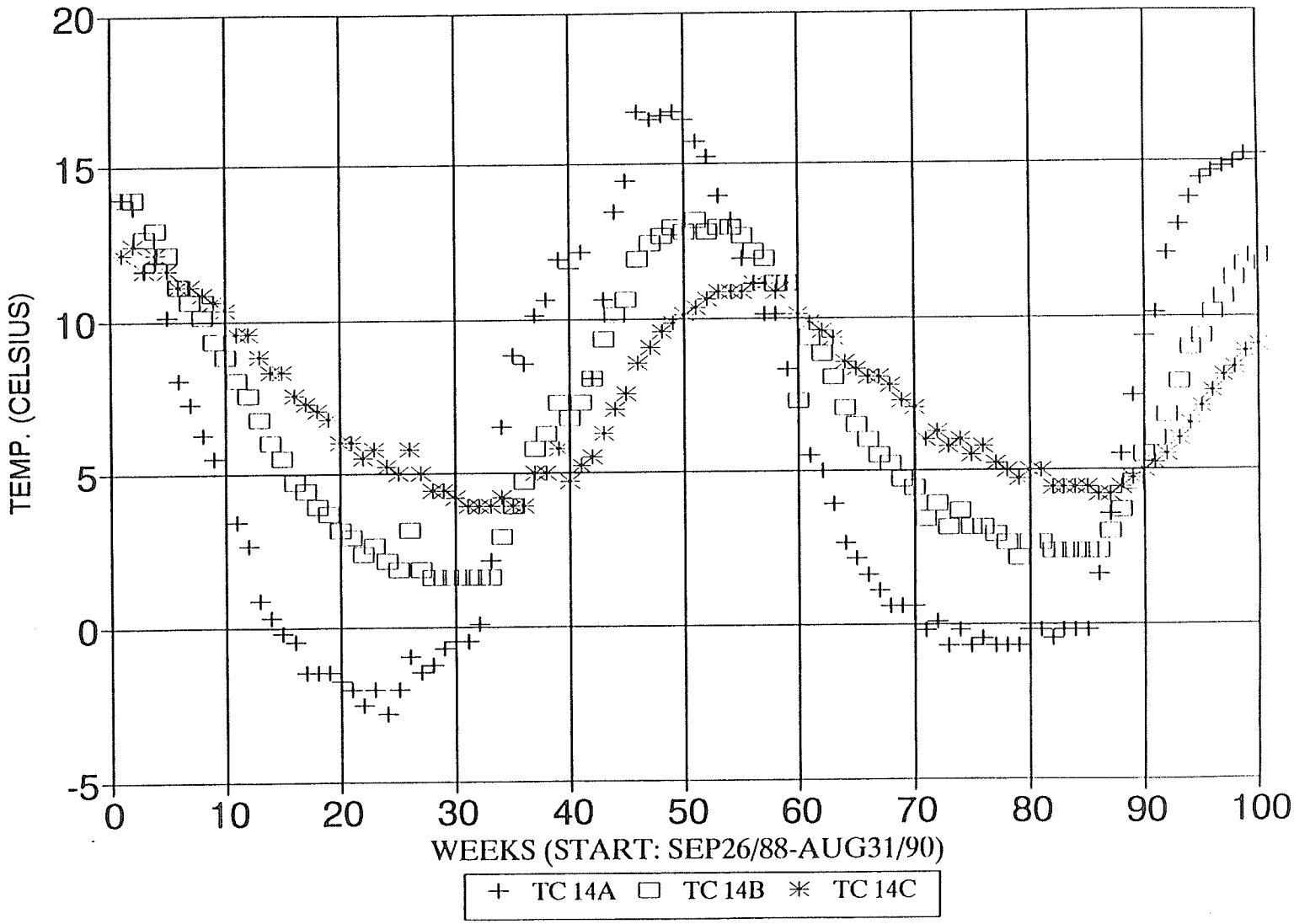

Fig.28: Ground Temperatures at Thermocouples 14A, 14B, 14C.

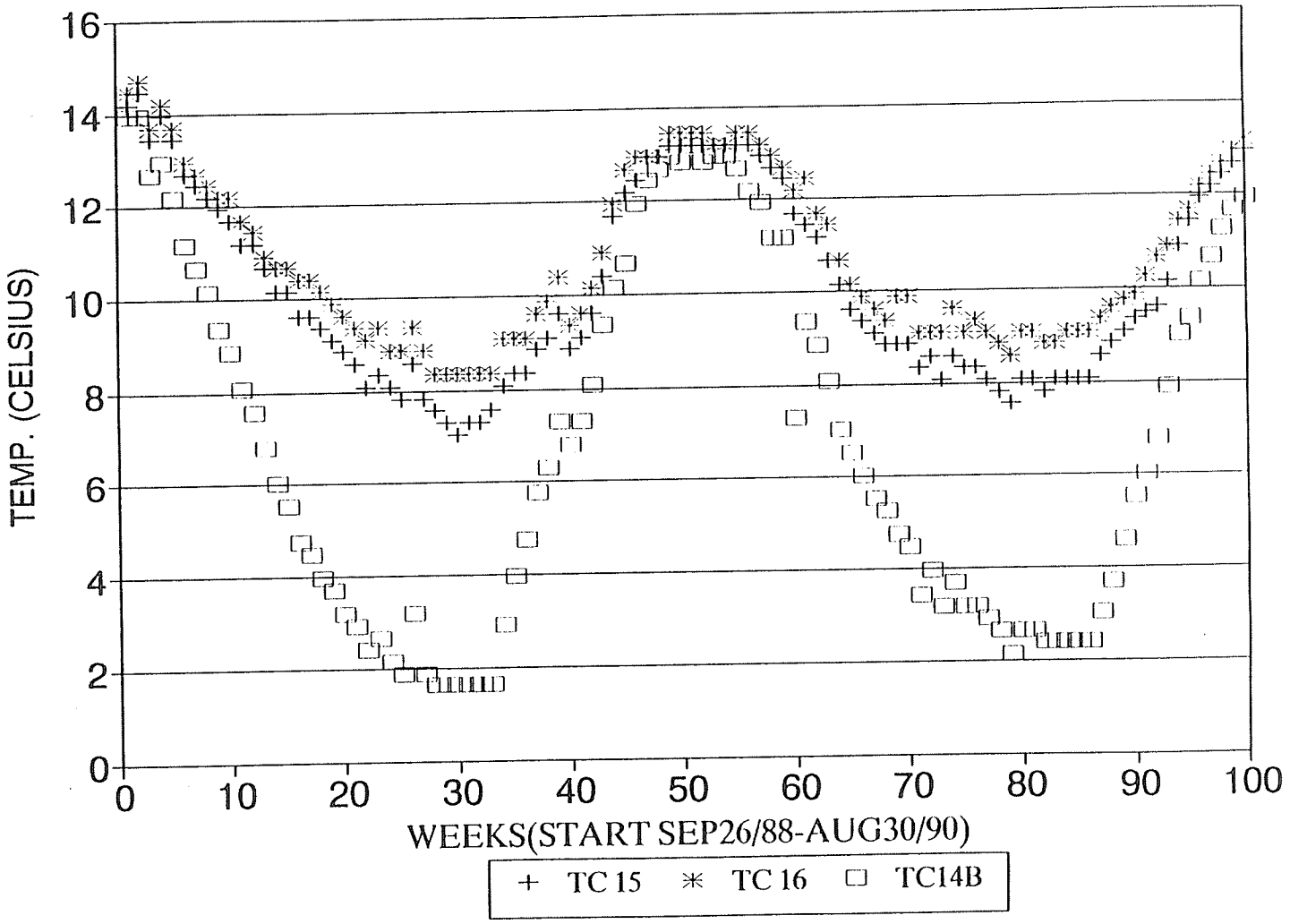

Fig.29 : Ground Temperatures at Thermocouples 15, 16, 14B.

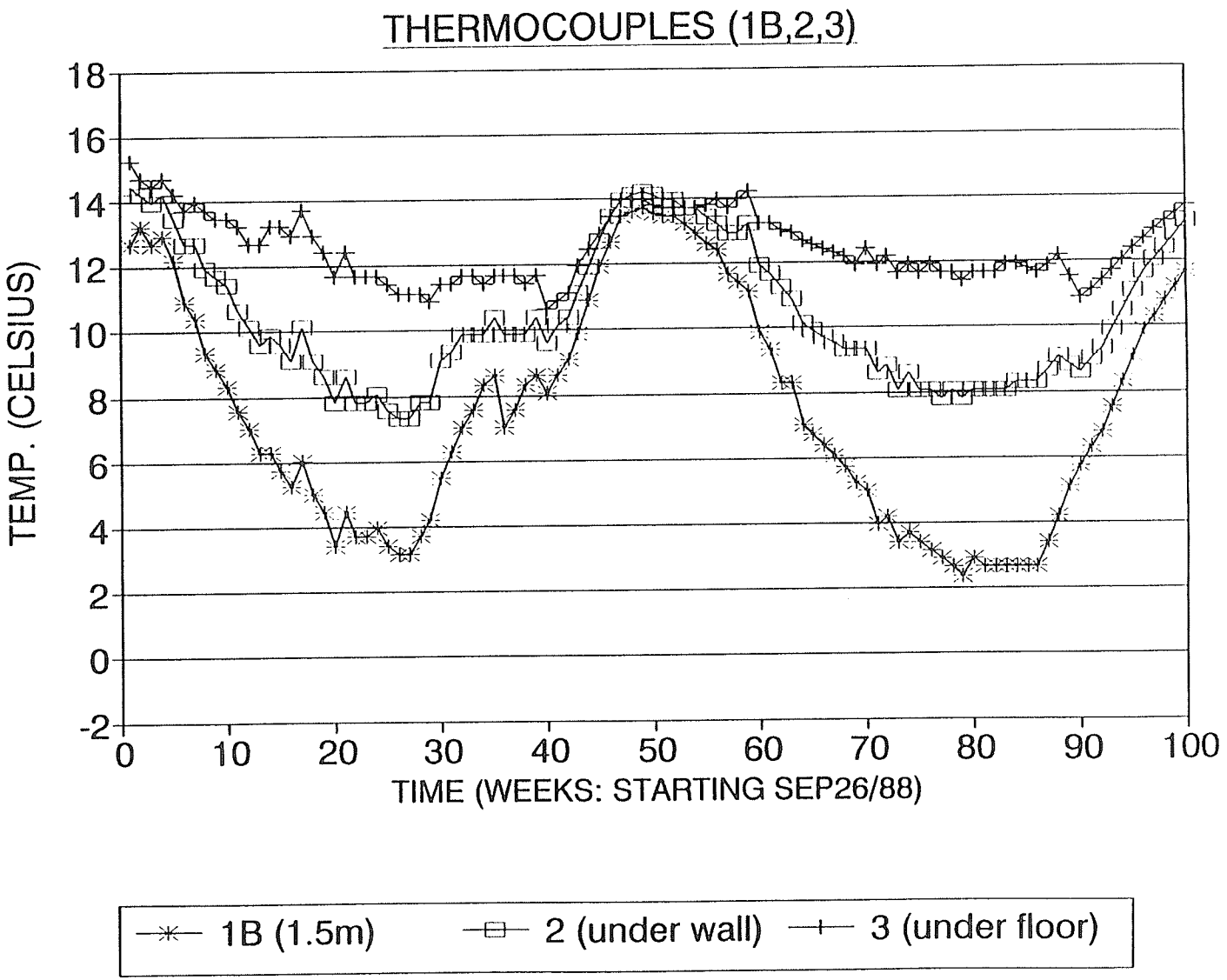

Fig.30 : Ground Temperatures at Thermocouples 1B, 2, 3.

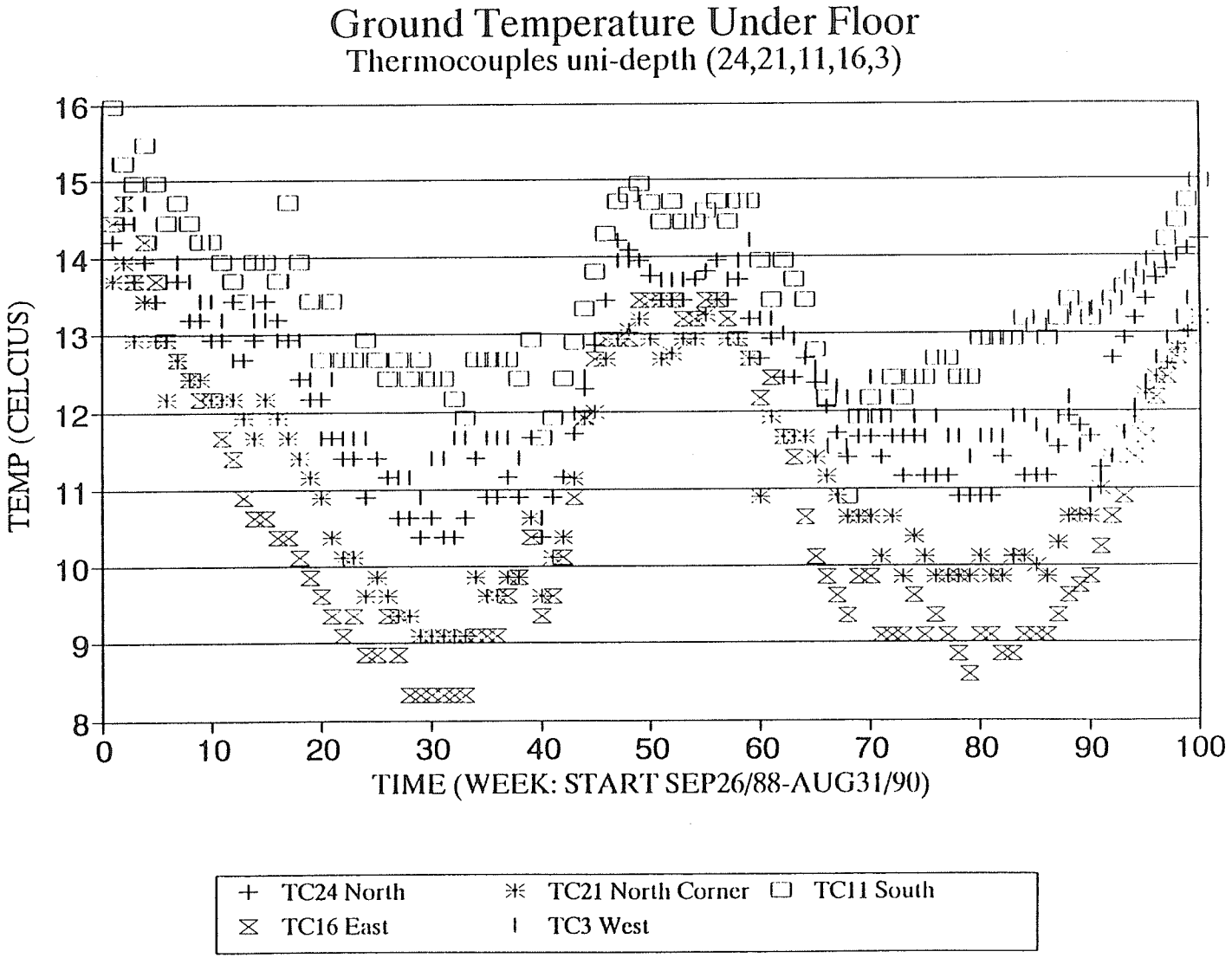

Fig.31: Ground Temperature Under the Basement Floor at Thermocouples 3, 11, 16, 21, 24

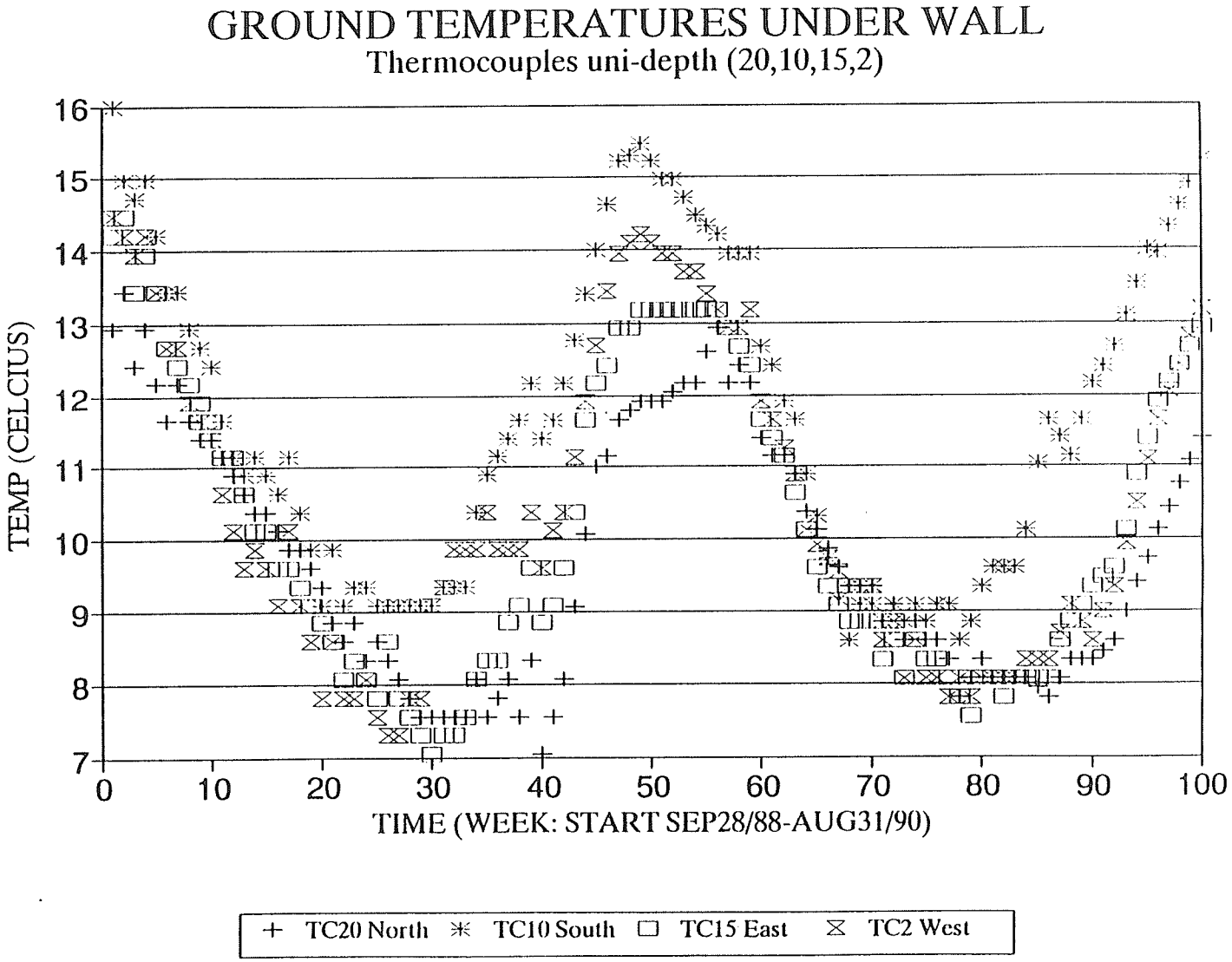

Fig.32: Ground Temperatures Under Walls Around the Residence at Thermocouples 2, 10, 15, 20.

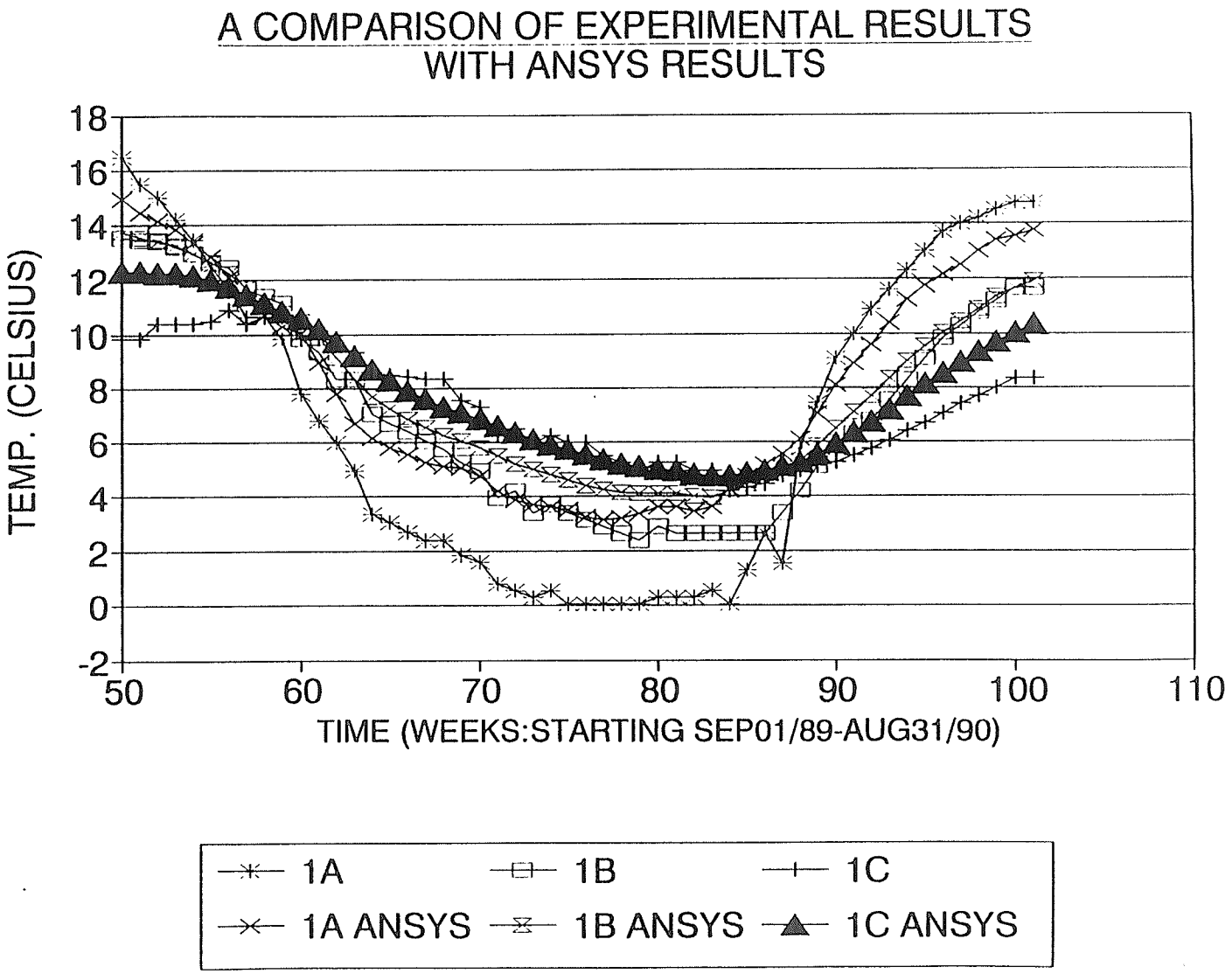

Fig.33: A Comparison of Experimental Results with ANSYS Results at Station 1.

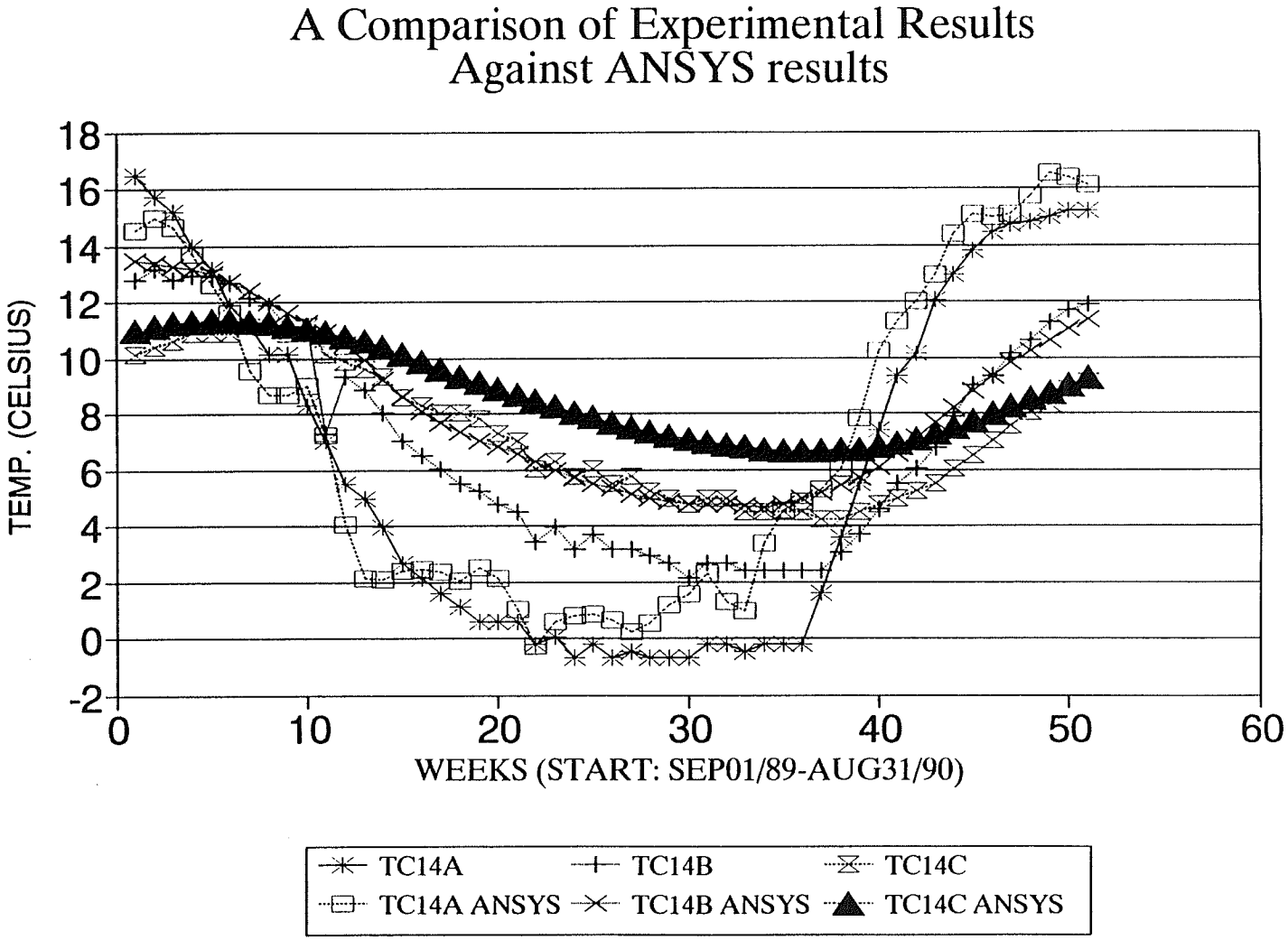

Fig.34: A Comparison of Experimental Results with ANSYS Results at Station 14.

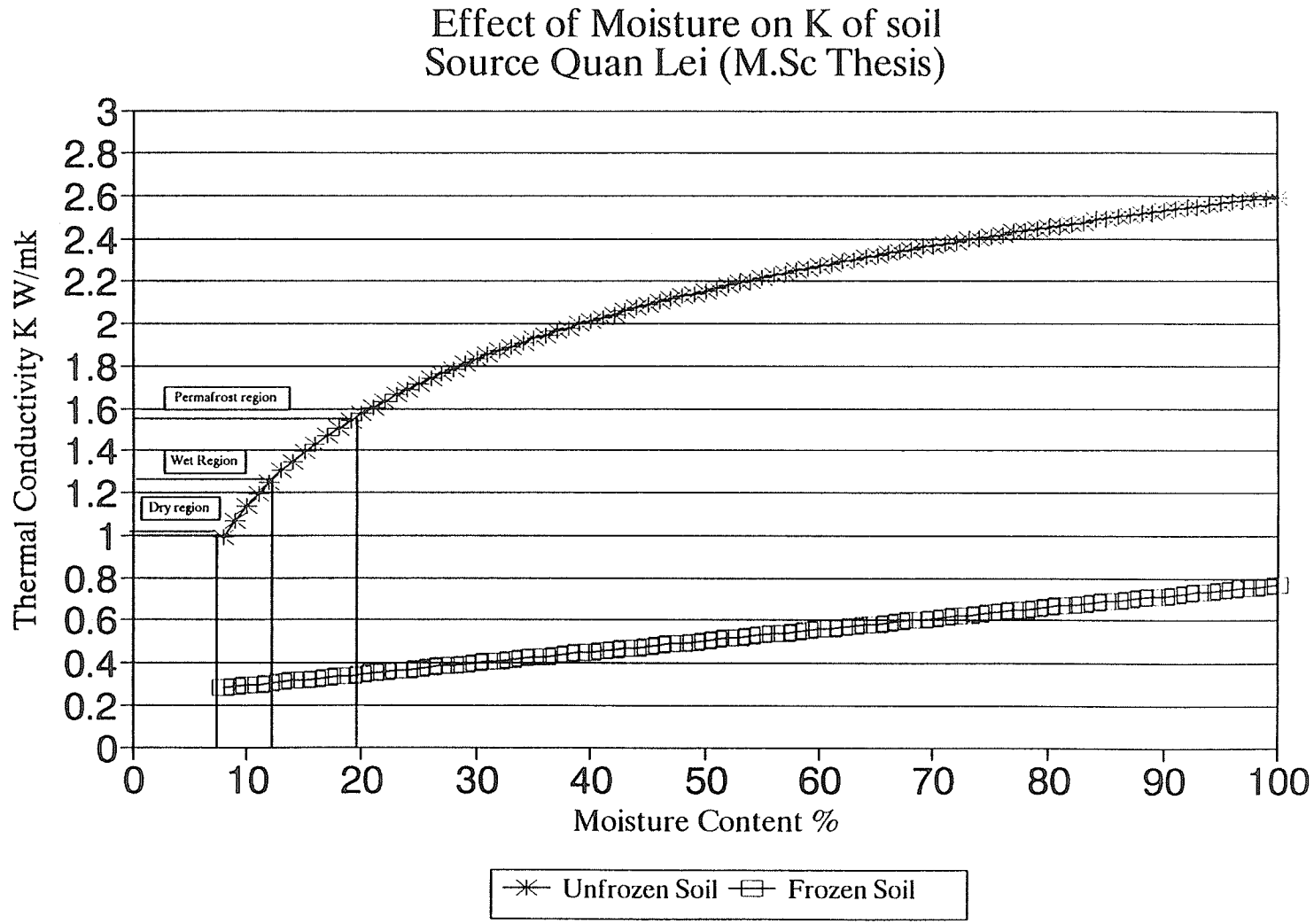

Fig.35: Effect of Moisture Content on Thermal Conductivity of Soil.

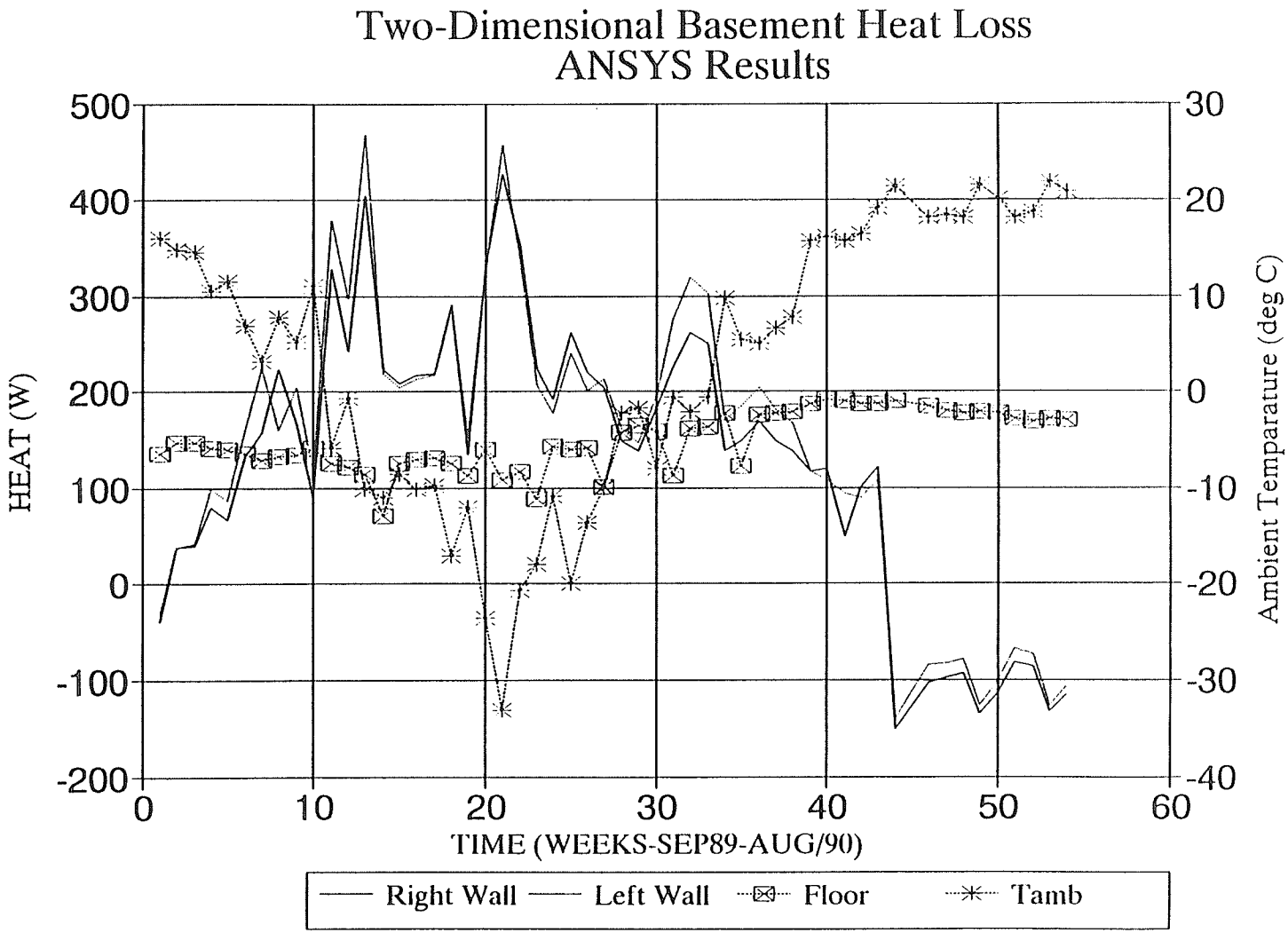

Fig.36: A Two-dimensional Basement Heat Loss Profile ANSYS Results, with Ambient Temperature from September 1989-August 1990.

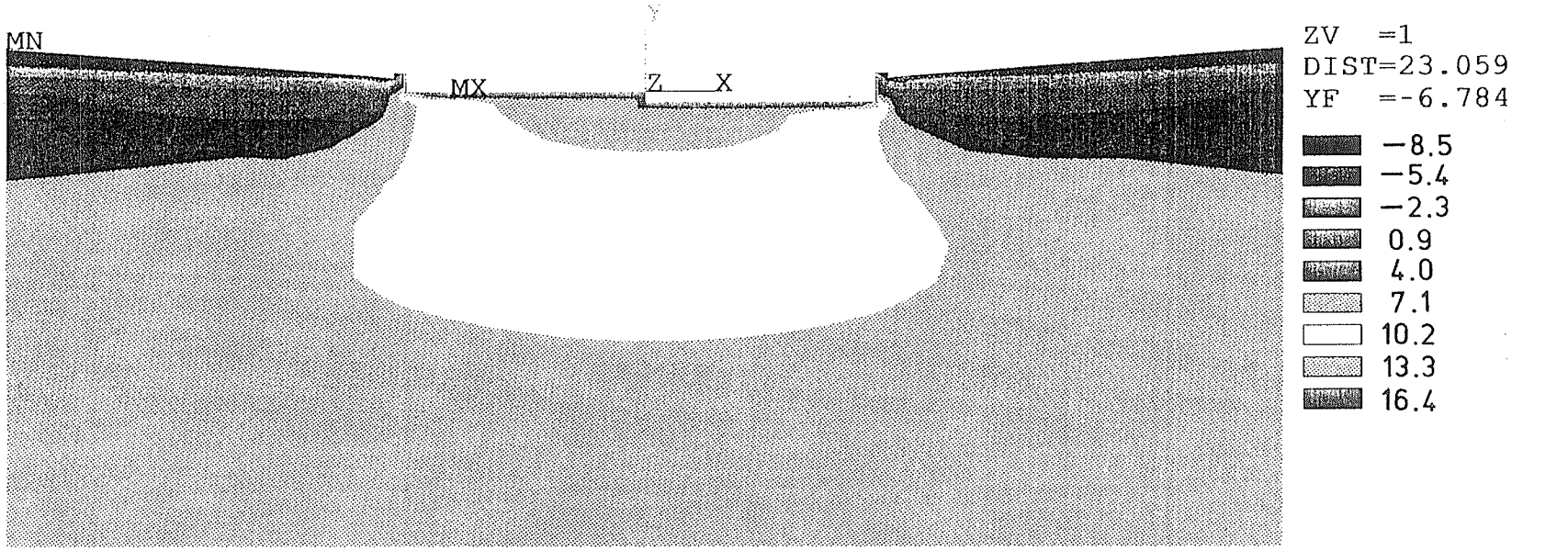

Fig. 37: Thermal Contour for Week 1/March 1990.

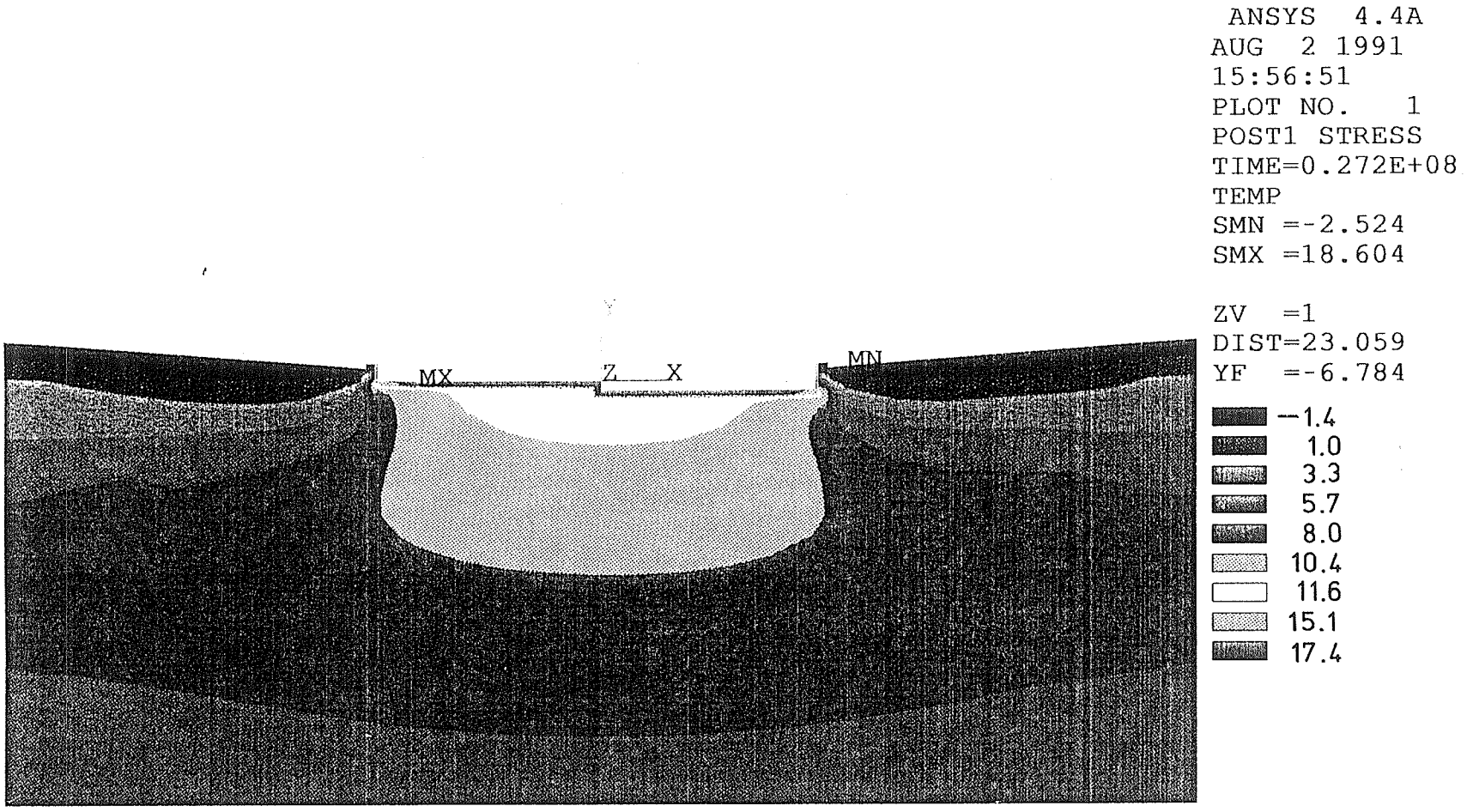

Fig. 38: Thermal Contour for Week 2/March 1990.

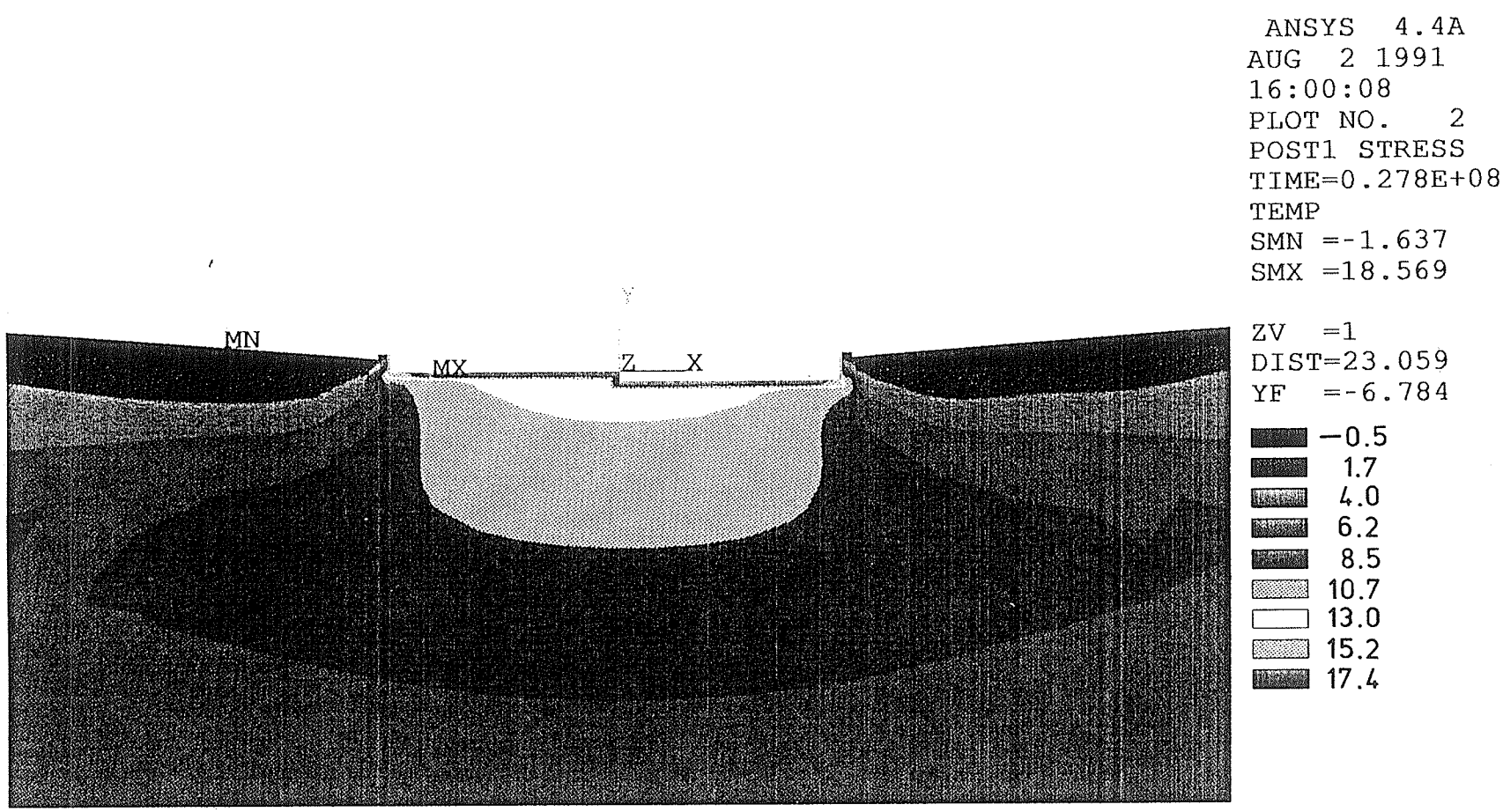

Fig. 39: Thermal Contour for Week 3/March 1990.

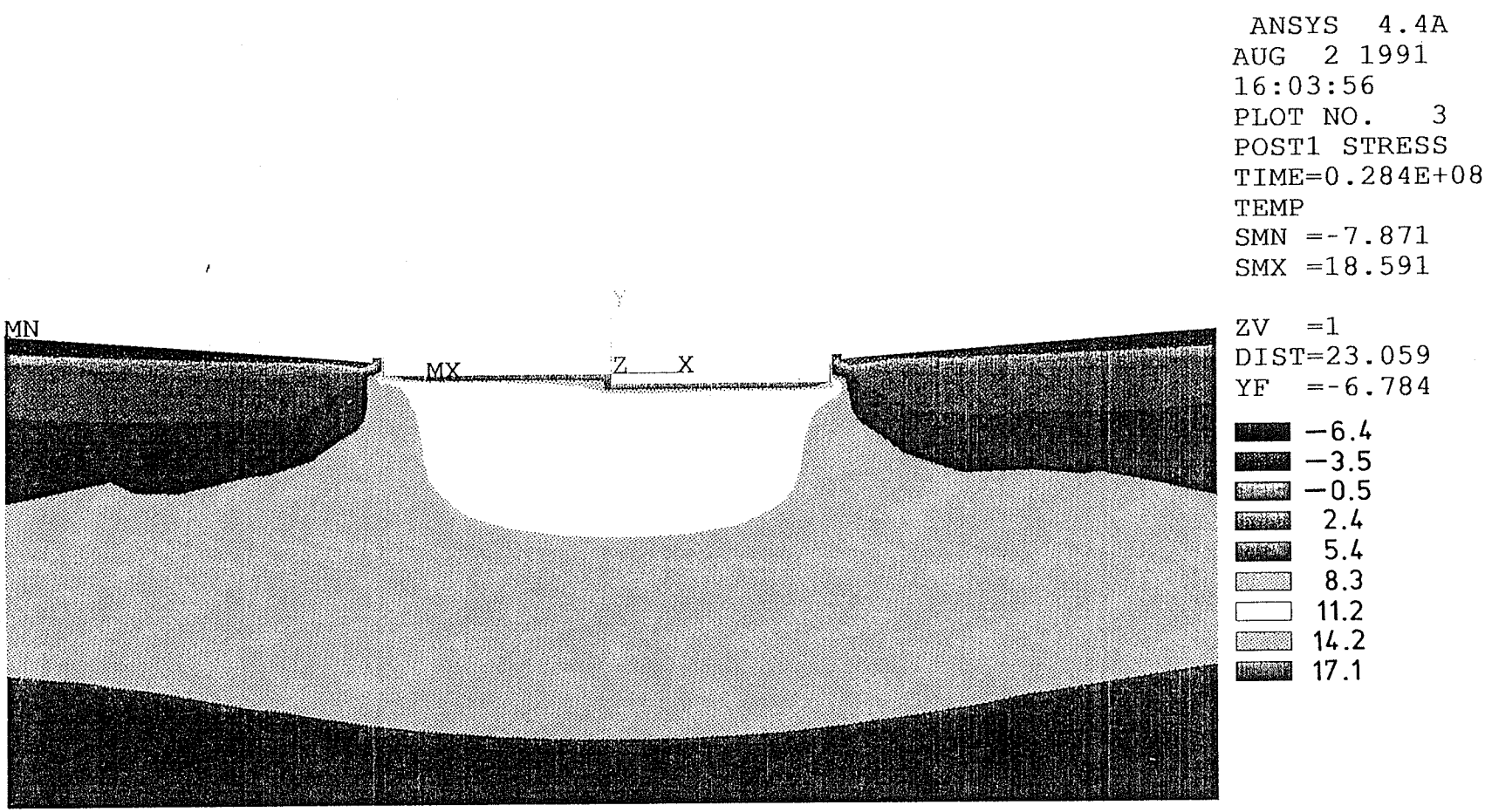

Fig. 40: Thermal Contour for Week 4/March 1990.

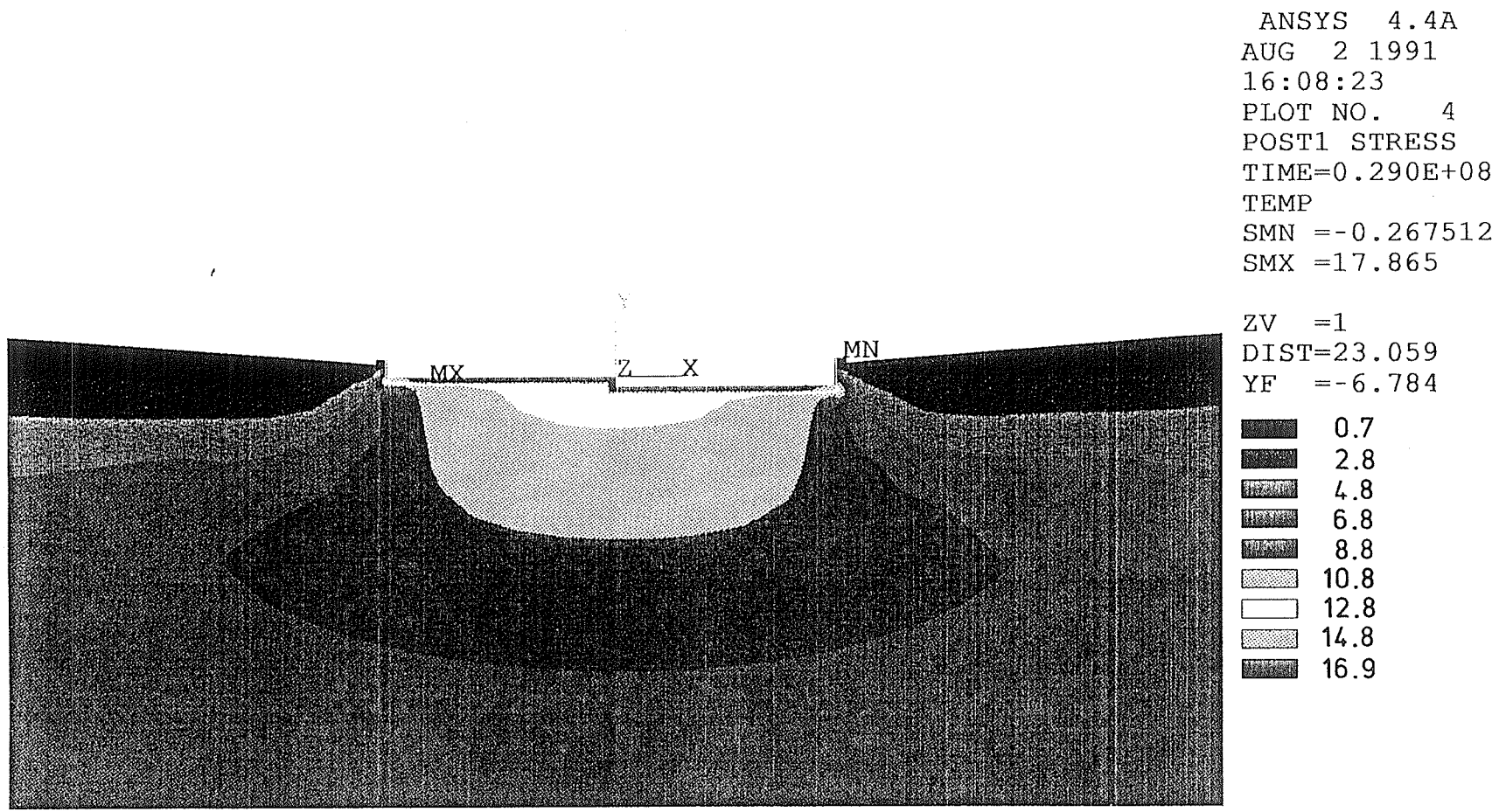

Fig. 41: Thermal Contour for Week 1/April 1990.

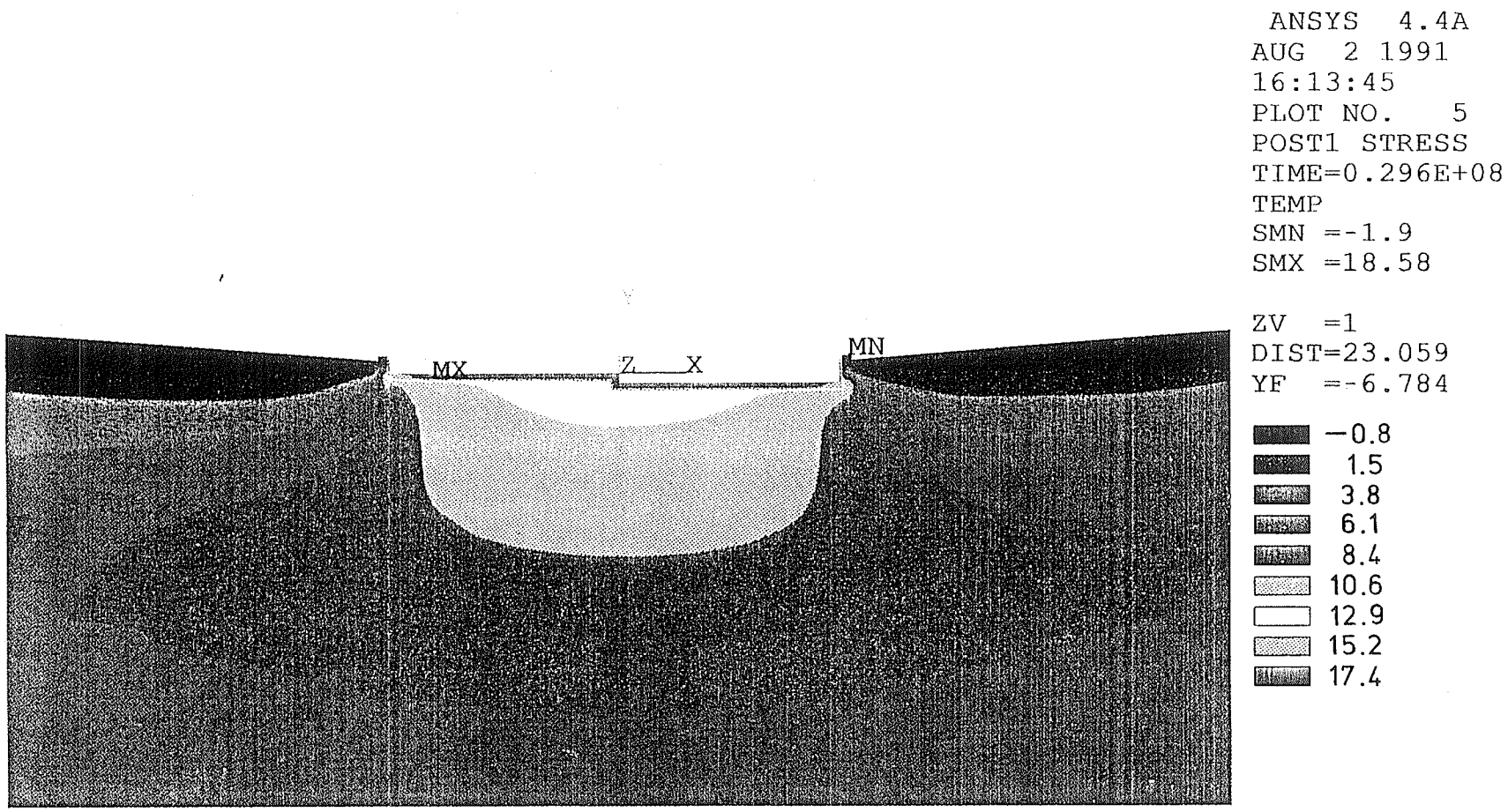

Fig. 42: Thermal Contour for Week 2/April 1990.

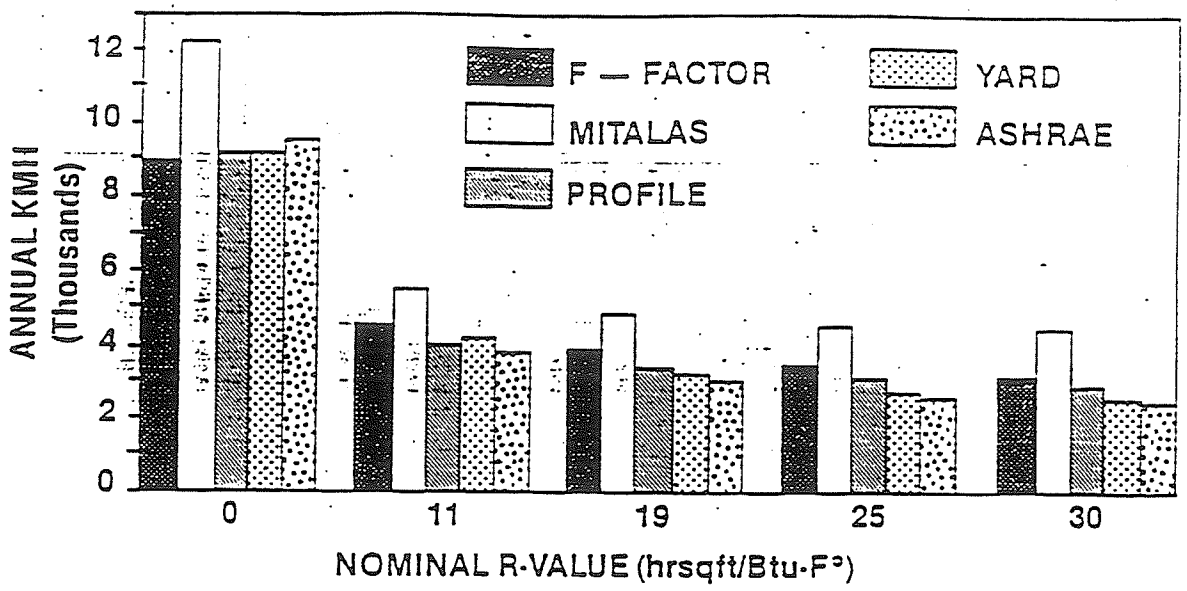

Fig.43: Estimated Heat Load for a Full Basement , Washington, D.C [13].

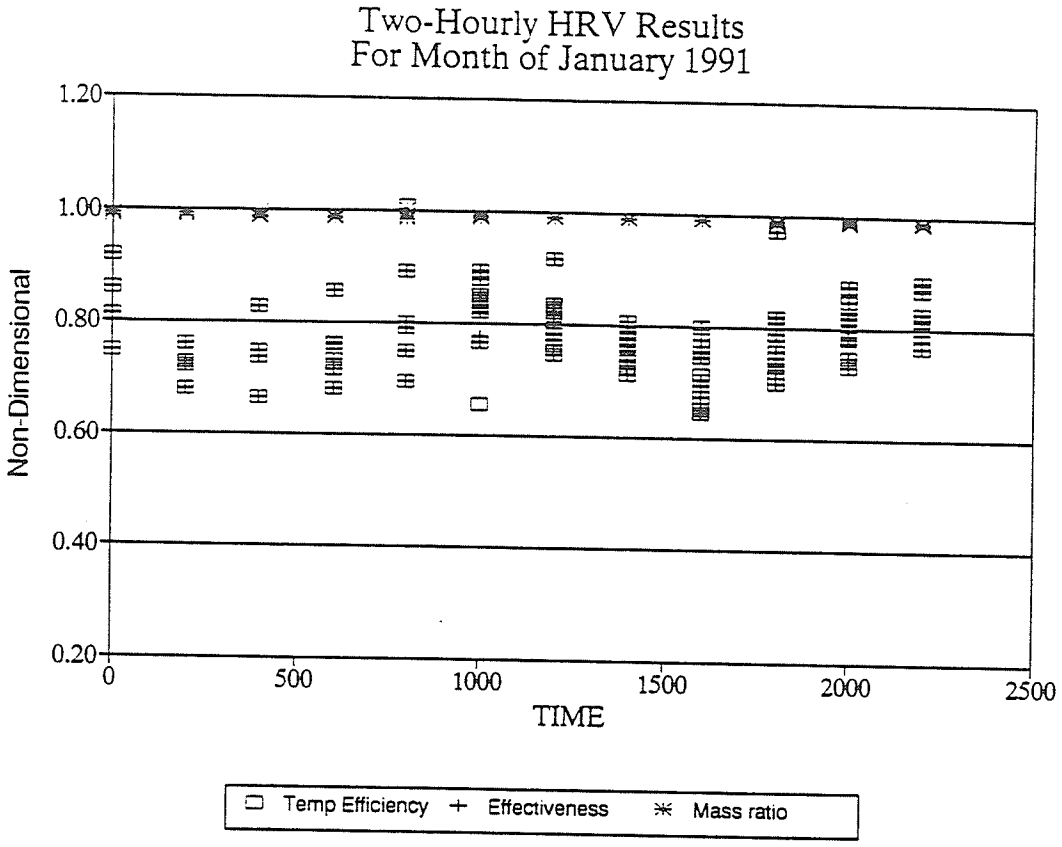

Fig.44: Two-Hourly results of HRV for Month of January 1991 under in situ Condition.

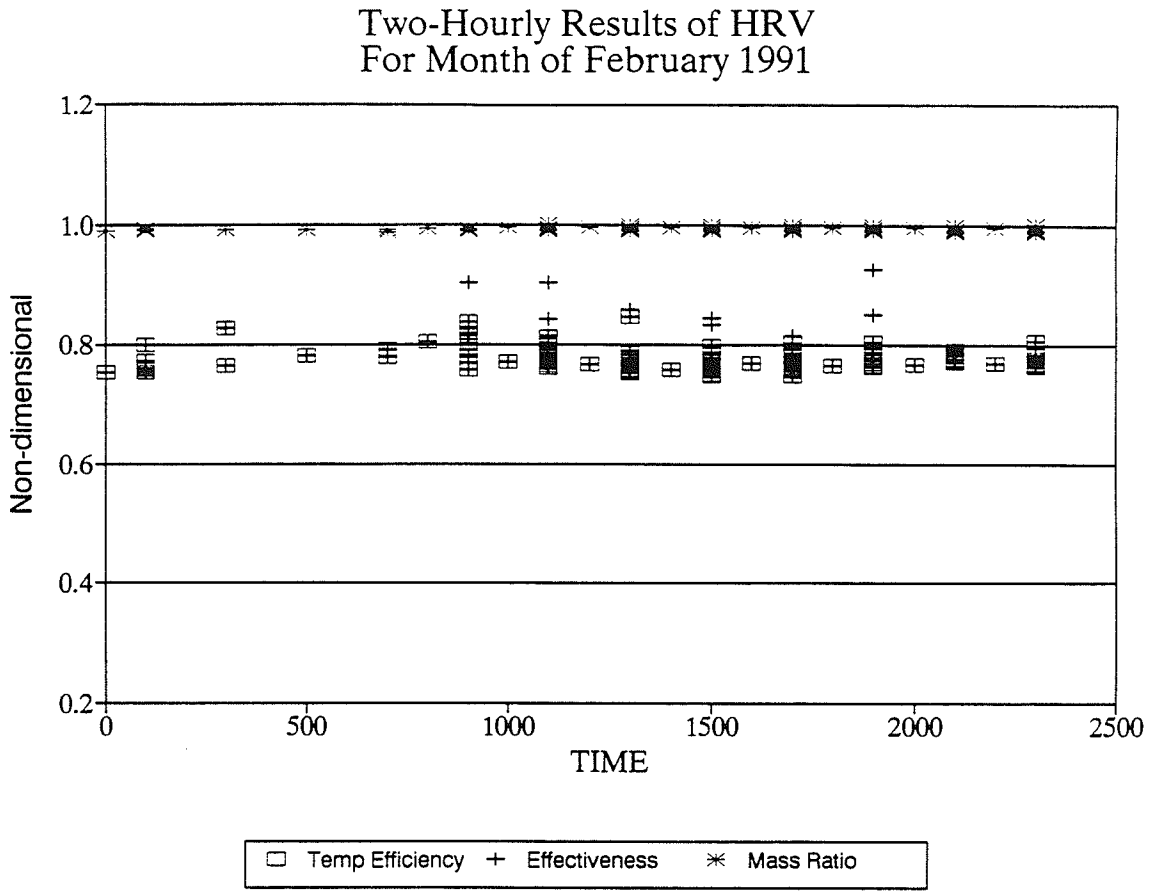

Fig.45: Two-Hourly Results of HRV for Month of February 1991 under in situ Condition.

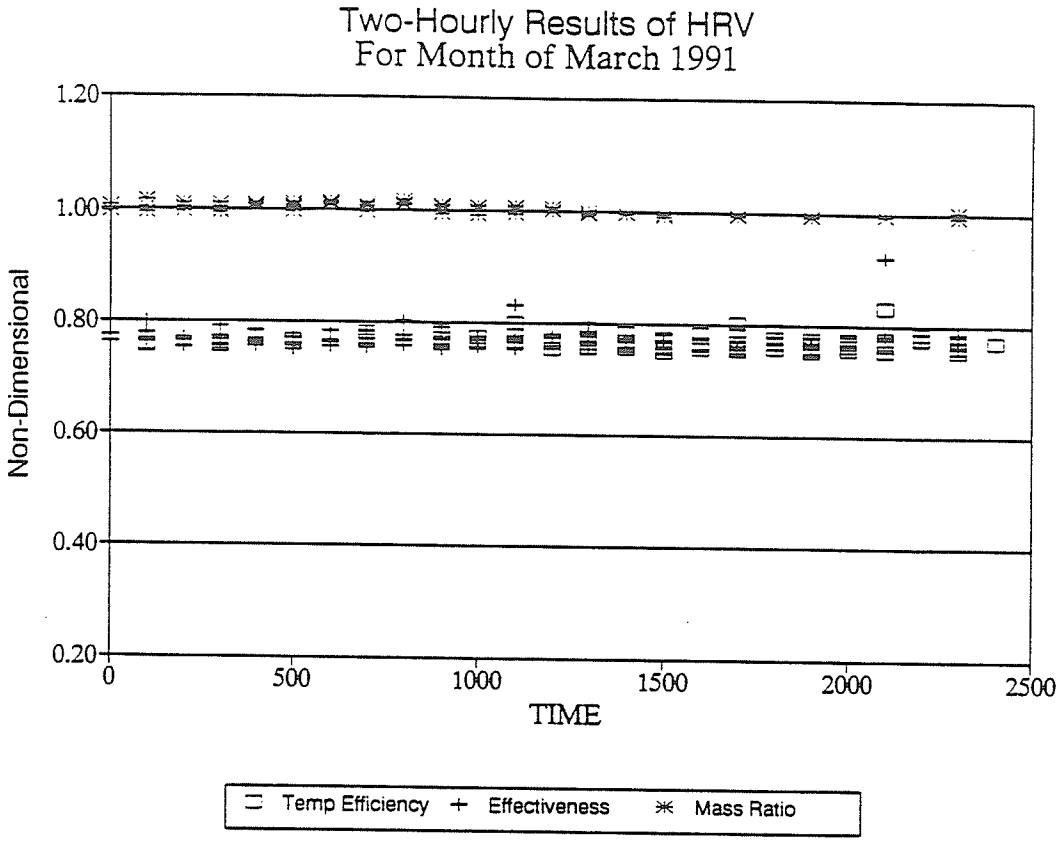

Fig.46: Two-Hourly Results of HRV for Month of March 1991 under in situ Condition.

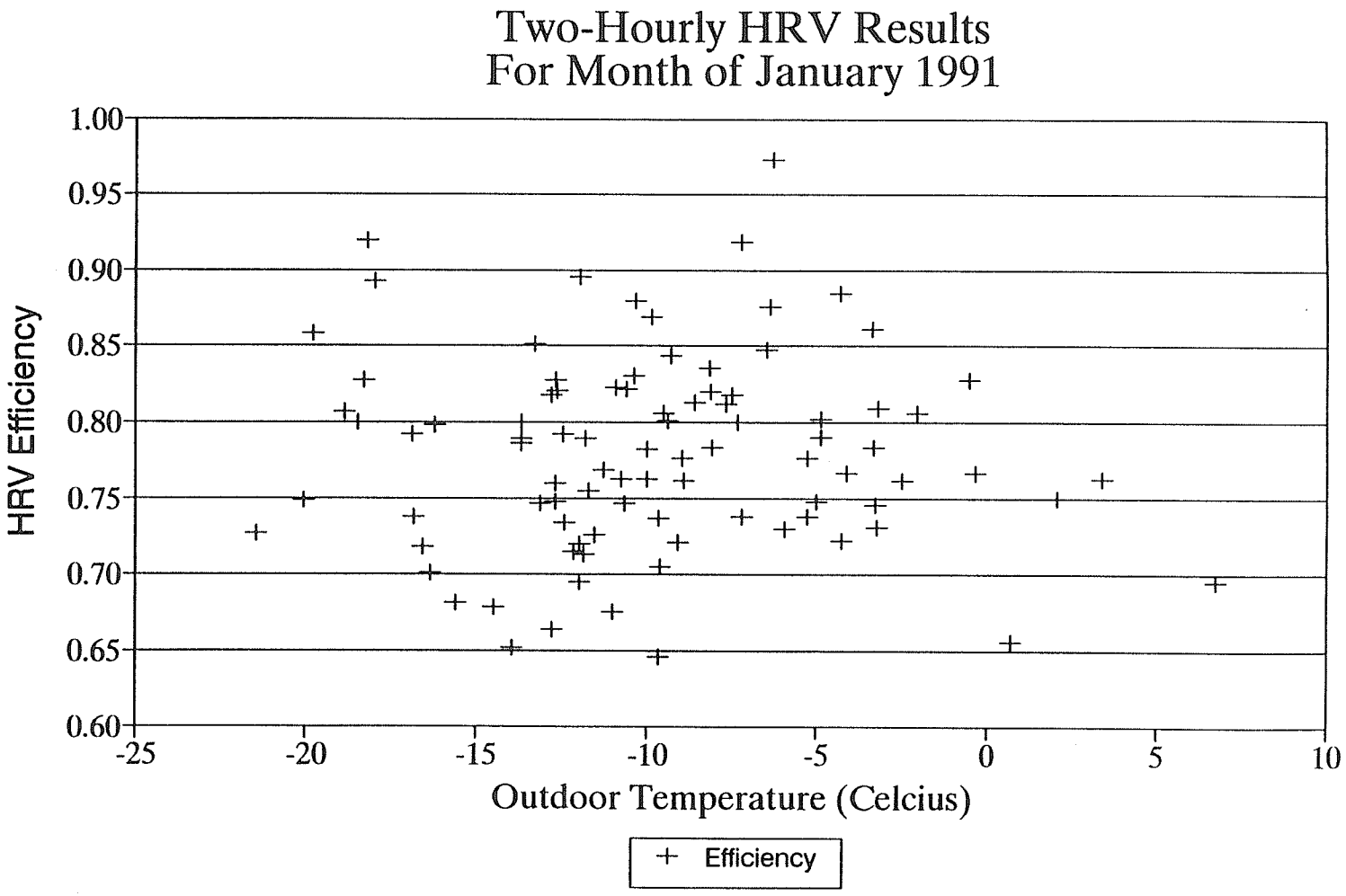

Fig.47: Two-Hourly HRV Efficiency with Outdoor Temperature: JAN 1991.

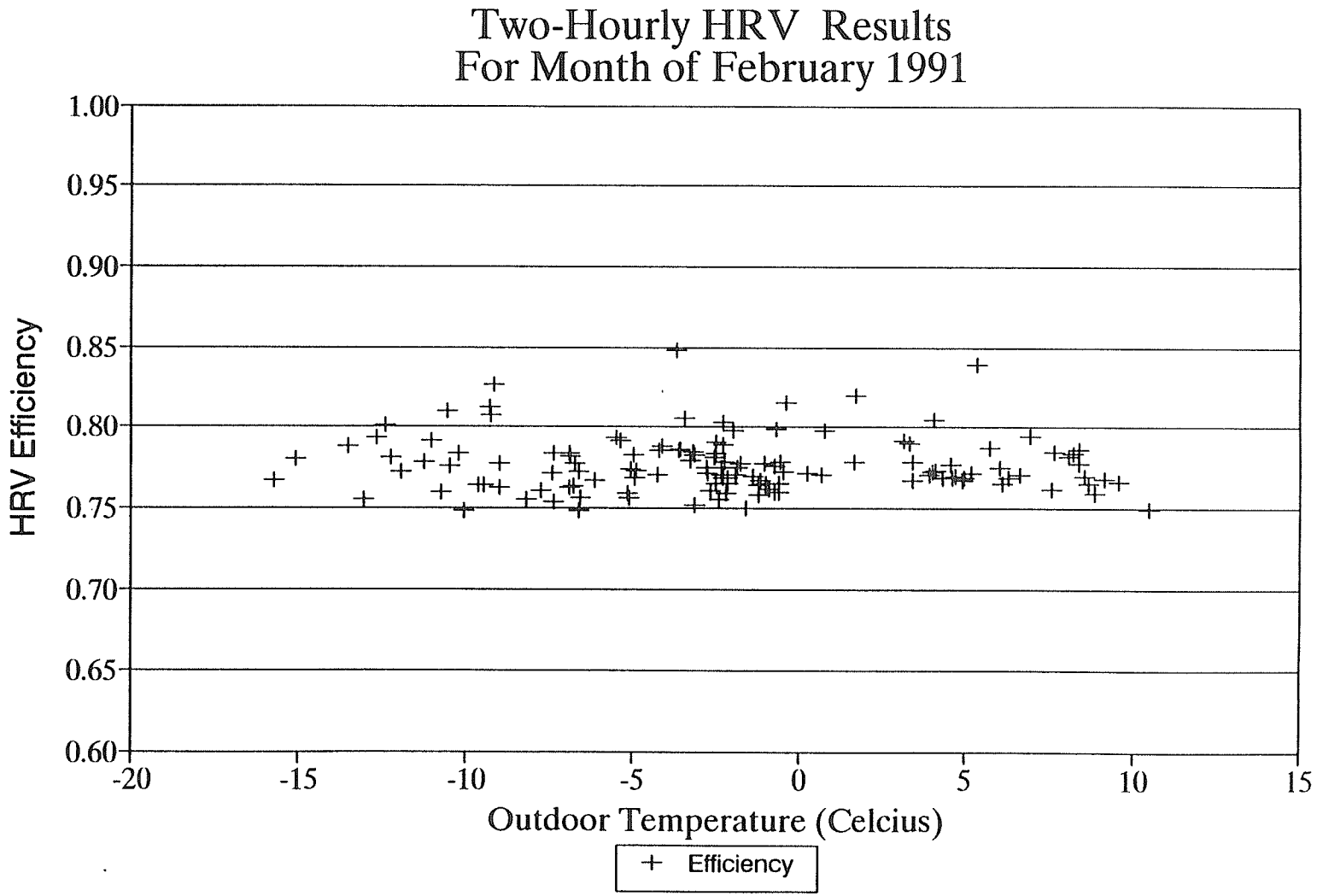

Fig.48: Two-Hourly HRV Efficiency with Outdoor Temperature: FEB 1991.

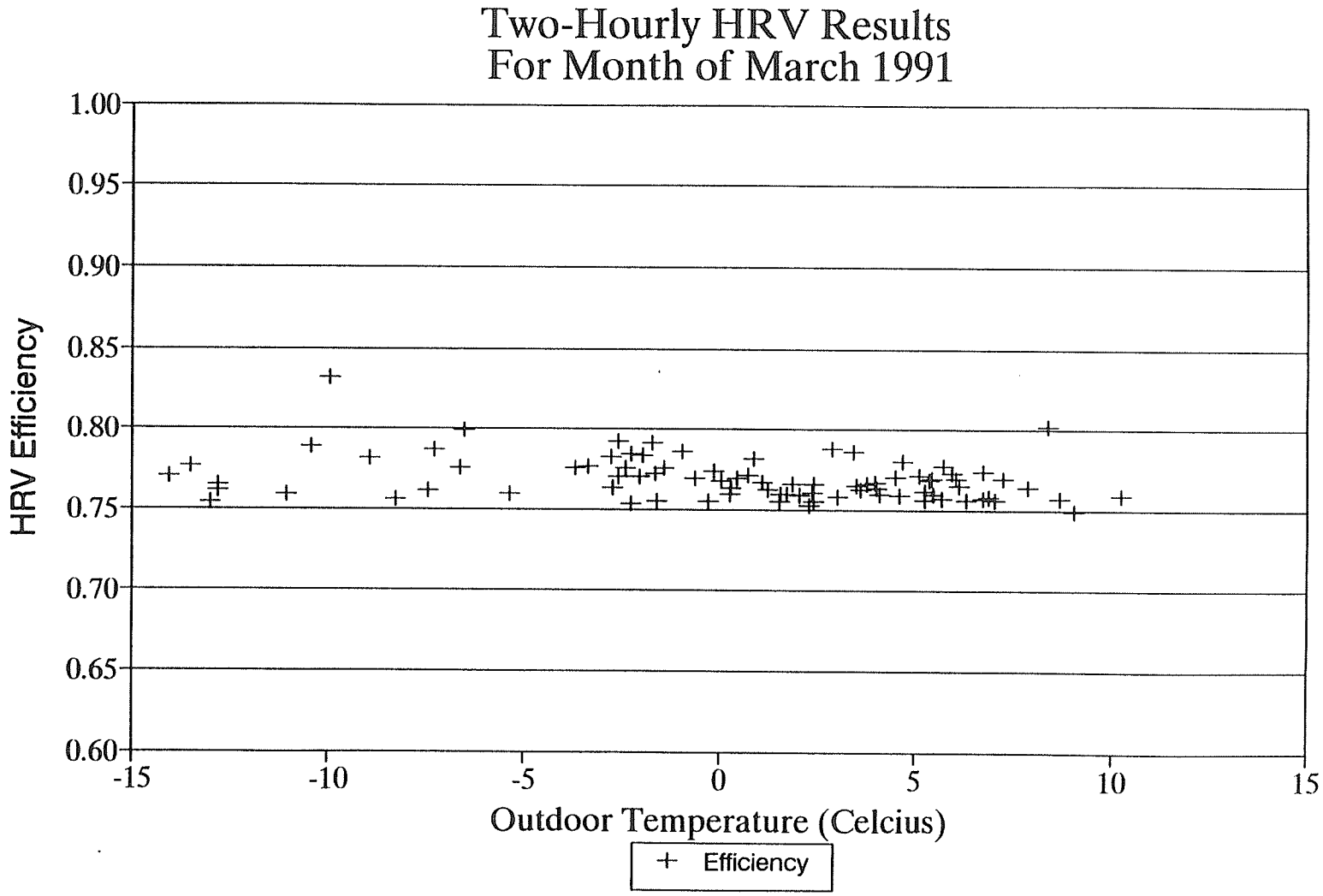

Fig.49: Two-Hourly HRV Efficiency with Outdoor Temperature: Mar 1991.

APPENDIX A

The Mitalas Sample Calculation.

The following example calculation is for the heat loss from one of the DBR/NRC test basements, that with insulation over the full height on the inside surface of the basement wall.

Step 1. The given input data are:

Basement dimensions -

length, $L = 9.2$ m

width, $W = 8.5$ m

total wall height, $H = 2.13$ m

height of wall above grade, $D = 0.38$ m

Insulation -

above grade, $1/R_T = U = 0.53$ W/(m^2 · K)

insulation resistance, $R = 1.55$ m^2 · K/W

height of insulation cover, $M = 2.13$ m (full height)

floor is uninsulated

Temperatures -

basement space temperature, $\theta_B = 21°C$

ground surface temperature (from Tab. 1)

$= \theta_G + \theta_v \cdot \sin(\omega t) = 8.9 + 11.4 \cdot \sin(30(m + 8))$

outside air temperature.[3] (For Ottawa θ_o, m = -11, -9, -3, 6, 13, 18, 21, 19, 15, 9, 2, -7°C M = 1 to 12)

Step 2. The area segments are calculated as follows:

$G_E = (4)(8.5) = 34$ m

$G_M = (2)(9.2 - 8.5) = 1.4$ m

$G = 34 + 1.4 = 35.4$ m

$A_{1E} = (34)(0.38) = 12.92$ m^2

$A_{1M} = (1.4)(0.38) = 0.53$ m^2

$A_{4E} = 34 - 4 = 30$ m^2

$A_{4M} = 1.4$ m^2

$A_{5E} = (8.5)(8.5) - 30 = 42.25$ m^2

$A_{5M} = (1.4) \times (8.5 - 3)/(2) = 4.55$ m^2

$A_{2E} = 34 \cdot 0.6 = 20.4$ m^2

$A_{2M} = (1.4)(0.6) = 0.84$ m^2

$A_{3E} = (34)(2.13 - 0.38 - 0.6) = 39.1$ m^2

$A_{3M} = (1.4)(2.13 - 0.38 - 0.6) = 1.61$ m^2

Step 3. Because the soil surrounding the basement is clay, the lower values of thermal conductivity were used to obtain the following basement factors from Tab. 2, Sect. A. For insulation system No. 3 the factors are:

Area Segment:	n = 2	n = 3	n = 4	n = 5
S	$(0.58 + 1.10R)^{-1}$	$(1.23 + 1.45R)^{-1}$	$(1.81 + 0.054R)^{-1}$	0.19
	$(0.58 + 1.12R)^{-1}$	$(1.34 + 1.55R)^{-1}$	$(2.77 - 0.11R)^{-1}$	0.07
σ	0.9	0.7	0.4	0.3
Δt	0	-1	-2	-4
C	0	0.6	2.4	0.5

Substituting R = 1.55 $m^2 \cdot K/W$ and Δt_n, and noting that $(t + \Delta t_n) = (n + 8 + \Delta t_n)$,

Area Segment:	n = 2	n = 3	n = 4	n = 5	
S	0.44	0.29	0.58	0.19	$W/(m^2 \cdot K)$
V	0.43	0.27	0.38	0.07	$W/(m^2 \cdot K)$
σ	0.9	0.7	0.4	0.3	Dimensionless
$(t + \Delta t)$	n + 8	n + 7	n + 6	n + 4	Month
C*	0	0.6 m^2	2.4 m^2	0.5	Dimensionless

* C value has different unit, as noted.

Step 4. Using the allowance factors from Tab. 2, the corner allowances, X, are:

$X_1 = X_2 = 0$

$X_3 = i \cdot C_3 = 4(0.6) = 2.4\ m^2$

$X_4 = i \cdot C_4 = 4(2.4) = 9.6\ m^2$

$X_5 = C_5 \cdot V_5 = 0.5(0.07) = 0.035\ W/(m^2 \cdot K)$

Step 5. Calculate the areas of the segments that include corner allowance factors:

$A_1 = 12.92 + 0.53 = 13.5\ m^2$

$A_2 = 20.4 + 0.84 = 21.2\ m^2$

$A_3 = 39.1 + 1.61 + 2.4 = 43.1\ m^2$

$A_{4s} = 30 + 1.4 + 9.6\ (0.38)/(0.58) = 37.7\ m^2$

$A_{4v} = 30 + 1.4 + 9.6 = 41.0\ m^2$

$A_{5s} = (42.25)\{1 + (0.035)/(0.19)\} + 4.55 = 54.6\ m^2$

$A_{5v} = (42.25)\{1 + (0.035)/(0.07)\} + 4.55 = 67.9\ m^2$

Step 6. The monthly heat loss (power) values of the five basement segments are.

$$q_{1,m} = A_1 \cdot U \cdot (\theta_B - \theta_{o,m}) = 13.5(0.53)(21-\theta_{o,m}) = 7.2(21-\theta_{o,m})$$

$$q_{2,m} = A_2[S_2 \cdot (\theta_B - \theta_G) - V_2 \cdot \sigma_2 \cdot \theta_v \cdot \sin(30(m+8))]$$

$$= 21.2[0.44(21 - 8.9) - 0.43(0.9)(11.4) \sin(30(m+8))]$$

$$= 112 - 93 \sin(30(m+8))$$

$$q_{3,m} = A_3[S_3(\theta_B - \theta_G) - V_3 \cdot \sigma_3 \cdot \theta_v \cdot \sin(30(m+7))]$$

$$= 43.1[0.29(21 - 8.9) - 0.27(0.7)(11.4) \sin(30(m+7))]$$

$$= 151 - 93 \sin(30(m+7))$$

$$q_{4,m} = A_{4s} \cdot S_4 \cdot (\theta_B - \theta_G) - A_{4v} \cdot V_4 \cdot \sigma_4 \cdot \theta_v \cdot \sin(30(m+6))$$

$$= (37.7)(0.58(21 - 8.9) - (41.0)(0.38)(0.4)(11.4) \sin(30(m+6))$$

$$= 265 - 71 \sin(30(m+6))$$

$$q_{5,m} = A_{5s} \cdot S_5 \cdot (\theta_B - \theta_G) - A_{5v} \cdot V_5 \cdot \sigma_5 \cdot \theta_v \cdot \sin(30(m+4))$$

$$= (54.6) \cdot (0.19)(21 - 8.9) - [67.9(0.07)(0.3)(11.4) \sin(30(m+4)]$$

$$= 126 - 16.3 \sin(30(m+4))$$

In summary, the monthly heat losses of the five basement segments are:

$$q_{1,m} = 7.2(21 - \theta_{o,m})$$

$$q_{2,m} = 112 - 93 \sin(30(m+8))$$

$$q_{3,m} = 151 - 93 \sin(30(m+7))$$

$$q_{4,m} = 265 - 71 \sin(30(m+6))$$

$$q_{5,m} = 126 - 16 \sin(30(m+4))$$

The average heat loss values for the five basement segments for each month of the year, the total basement average values, and the annual average values for each segment are listed in Tab. A-1.

The annual average heat loss rate was 762 W. The annual heat loss (energy) from the whole basement would be

$$\frac{762}{1000} \times 12 \times 730 = 6675 \text{ kWh} = 24 \text{ GJ}$$

As a matter of interest, the measured and calculated values are plotted in Fig. A-1 where

Curve (1) = measured energy consumption

Curve (2) = sinusoidal power curve obtained using the measured energy values

APPENDIX B
ANSYS Heat Loss Determination and Element Library
Basement Model and Load File.

4.55 2-D ISOPARAMETRIC THERMAL SOLID

This isoparametric thermal element can be used as a biaxial plane element or as an axisymmetric ring element with a two-dimensional thermal conduction capability. The element has four nodal points with a single degree of freedom, temperature, at each node.

The element is applicable to a two-dimensional, steady-state or transient, Thermal (KAN=-1) analysis. The element can also compensate for mass transport heat flow from a constant velocity field. If the model containing the isoparametric temperature element is also to be analyzed structurally, the element should be replaced by an equivalent structural element (such as STIF42), see Section 2.21, Thermal-Stress Procedure. A similar element, with mid-side node capability (STIF77), is described in Section 4.77. A similar axisymmetric element which accepts nonaxisymmetric loading (STIF75) is described in Section 4.75.

An option exists that allows the element to model nonlinear steady-state fluid flow through a porous medium. With this option the thermal parameters are interpreted as analogous fluid flow parameters.

4.55.1 Input Data

The geometry, nodal point locations, face numbers, loading, and the coordinate system for the element are shown in Figure 4.55.1. The element is defined by four node points and the orthotropic material properties. Orthotropic material directions correspond to the element coordinate directions. The element coordinate system orientation is as described in Section 4.0.12. The specific heat and the density may be assigned any values for steady-state solutions. Properties not input default as described in Section 4.0.2. An average internal heat generation rate may be applied to the element. All of the element lateral surfaces have convection capability and are numbered as shown in Figure 4.55.1.

KEYOPT(1) defines the procedure for evaluating a temperature dependent film coefficient. The nonlinear porous flow option is selected with KEYOPT(9)=1. With this option temperature boundary conditions (input with the NT command) are interpreted as pressure, and heat flow boundary conditions (input with the HFLOW command) are interpreted as mass flow rate (mass/time). A summary of the element parameters is given in Table 4.55.1. A general description of element input is given in Section 4.0.2.

4.55.2 Output Data

a) Printout - The solution printout associated with the element is in two forms: 1) the node temperatures are included in the overall nodal temperature solution printout, and 2) the element printout is as shown in Table 4.55.2. Nodal heat flows can be printed with the KRF command. For an axisymmetric analysis the face area and the heat flow rate are on a "per radian" basis. Heat flowing out of the element is considered to be positive. If KEYOPT(9)=1, the standard thermal output should be interpreted as the analogous fluid flow output. The element output directions are parallel to the element coordinate system. A general description of element printout is given in Section 4.0.3.

b) Post Data - The post data associated with the element is shown below. The data are written on File12 if requested, as described in Section 4.0.4.

1	TGSUM	9	TAVG(1)
2	TFSUM	10	TBULK(1)
3	VOL	11	HEAT RATE(1)
4	FACE NO.	12-35	4-11 @ (2,3,4)
5	AREA(1)	36	TOTAL PR GRAD
6-7	FACE NODES(1)	37-38	PRESS GRAD(X,Y)
8	HFILM(1)	39	MASS FLUX
		40	TOTAL VELOCITY
		41-42	VELOCITY(X,Y)
		43-44	TG(X,Y)
		45-46	TF(X,Y)
		3	----------

Items 5 through 11 for each face are zero unless convection is present. Items 36 through 42 are zero unless KEYOPT(9) = 1.

4.55.3 Theory

The temperature distribution for this element is obtained from the numerical solution of the following equation (for the plane analysis):

$$\rho C_p \left(\frac{\partial T}{\partial t} + v_x \frac{\partial T}{\partial x} + v_y \frac{\partial T}{\partial y}\right) = \frac{\partial}{\partial x}\left(k_{xx} \frac{\partial T}{\partial x}\right) + \frac{\partial}{\partial y}\left(k_{yy} \frac{\partial T}{\partial y}\right) + \dot{q}$$

where: ρ = density (Weight (or Mass)/Volume)

C_p = specific heat (Heat/Weight (or Mass)*Deg)

k = thermal conductivity (Heat/Length*Time*Deg)

$\dot{q}$ = internal heat generation rate (Heat/Volume*Time)

v = velocity for mass transport option (KEYOPT(8)>0 only)

For the axisymmetric analysis the equation (for constant k values) is of the form:

$$\rho C_p \left(\frac{\partial T}{\partial t} + v_x \frac{\partial T}{\partial x} + v_y \frac{\partial T}{\partial y}\right) = k_{xx}\left(\frac{1}{x}\frac{\partial T}{\partial x} + \frac{\partial^2 T}{\partial x^2}\right) + k_{yy}\frac{\partial^2 T}{\partial y^2} + \dot{q}$$

where the x-axis is in the radial direction and the y-axis is in the axial direction

The temperature functions used for the element are bilinear as described in Section 2.55 of the ANSYS Theoretical Manual (Ref. 5). A 2x2 lattice of integration points is used for the numerical (Gaussian) integration procedure.

For the nonlinear porous flow option (KEYOPT(9)=1), see Section 4.70.3 with any reference to the Z terms ignored for the analogous flow parameters.

4.55.4 Assumptions and Restrictions

The element must not have a negative or a zero area. The element must lie in a X-Y plane as shown in Figure 4.55.1 and the X-axis must be the radial direction for axisymmetric problems. Also, axisymmetric structures should be modeled in the +X quadrants. A triangular element may be formed by defining duplicate K and L node numbers as described in Section 4.0.9. The specific heat is evaluated at each

integration point to allow for abrupt changes (such as melting) within a coarse grid of elements.

If the thermal element is to be replaced by a STIF42 structural element with surface stresses requested, the thermal element should be oriented such that face 1 and/or face 3 is a free surface, see Section 2.21. A free surface of the element (i.e., not adjacent to another element and not subjected to a boundary constraint) is assumed to be adiabatic. Thermal transients having a fine integration time step and severe thermal gradient at the surface will also require a fine mesh at the surface, see Section 2.21. With the mass transport option, temperatures should be specified along the entire inlet boundary to assure a stable solution.

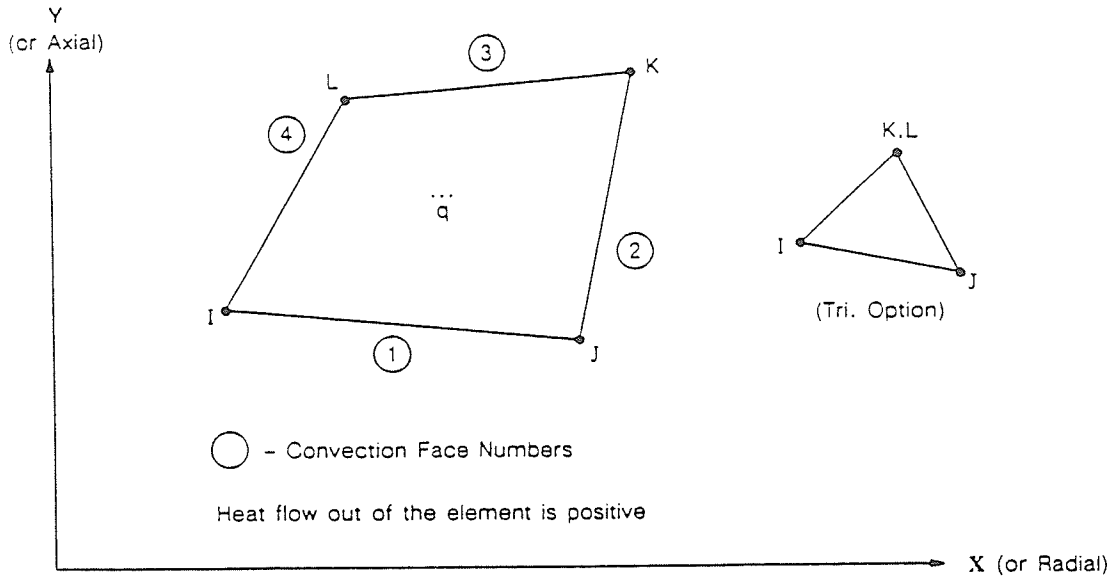

Figure 4.55.1 2-D Isoparametric Thermal Solid

Structural Point	Structural 2-D Line			
Generalized Mass	Spar	Elastic Beam	Plastic Beam	Tapered Unsymmetric Beam
				
STIF21 1 node 3-D space DOF: UX, UY, UZ, ROTX, ROTY, ROTZ	STIF1 2 nodes 2-D space DOF: UX, UY Features: P,R,S	STIF3 2 nodes 2-D space DOF: UX, UY, ROTZ Features: R,S	STIF23 2 nodes 2-D space DOF: UX, UY, ROTZ Features: P,R,S	STIF54 2 nodes 2-D space DOF: UX, UY, ROTZ Features: R,S, Offset nodes.
Structural 3-D Line				
Spar	Tension-Only Spar	Elastic Beam	Thin Walled Plastic Beam	Tapered Unsymmetric Beam
				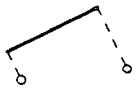
STIF8 2 nodes 3-D space DOF: UX, UY, UZ Features: P,R,S	STIF10 2 nodes 3-D space DOF: UX, UY, UZ Features: R,S,G	STIF4 2 nodes 3-D space DOF: UX, UY, UZ, ROTX, ROTY, ROTZ Features: R,S	STIF24 2 nodes 3-D space DOF: UX, UY, UZ, ROTX, ROTY, ROTZ Features: P,R,S, Arbitrary cross-section	STIF44 3 nodes 3-D space DOF: UX, UY, UZ, ROTX, ROTY, ROT Features: R,S, Offse nodes.
Elastic Straight Pipe	Elastic Pipe Tee	Curved Pipe (Elbow)	Plastic Straight Pipe	Plastic Elbow
	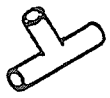			
STIF16 2 nodes 3-D space DOF: UX, UY, UZ, ROTX, ROTY, ROTZ Features: R,S	STIF17 4 nodes 3-D space DOF: UX, UY, UZ, ROTX, ROTY, ROTZ Features: R,S	STIF18 3 nodes 3-D space DOF: UX, UY, UZ, ROTX, ROTY, ROTZ Features: R	STIF20 2 nodes 3-D space DOF: UX, UY, UZ, ROTX, ROTY, ROTZ Features: P,R,S	STIF60 3 nodes 3-D space DOF: UX, UY, UZ, ROTX, ROTY, ROT Features: P,R
	Structural 2-D Solid			
Immersed Pipe	Isoparametric Solid	Axisymmetric Harmonic Stress Solid	Triangular Solid	Isoparametric Solid
	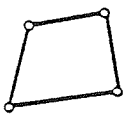	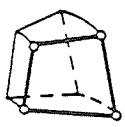	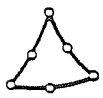	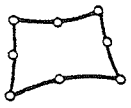
STIF59 2 nodes 3-D space DOF: UX, UY, UZ, ROTX, ROTY, ROTZ Features: R,S, Wave loading	STIF42 4 nodes 2-D space DOF: UX, UY Features: P,R,S	STIF25 4 nodes 2-D space DOF: UX, UY, UZ Features: S	STIF2 6 nodes 2-D space DOF: UX, UY Features: P,R,S	STIF82 8 nodes 2-D space DOF: UX, UY Features: P,R,S

P = Plasticity, R = Large Deflection, S = Stress Stiffening, G = Geometric Nonlinearity

Figure 4.0.1 Element Types

		Structural 3-D Solid		
Axisymmetric Harmonic Stress Solid	Hyperelastic Solid	Isoparametric Solid	Anisotropic Solid	Reinforced Solid
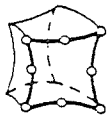	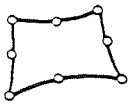	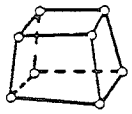	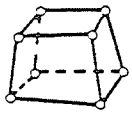	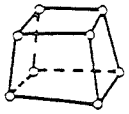
STIF83 8 nodes 2-D space DOF: UX, UY, UZ Features: S	STIF84 8 nodes 2-D space DOF: UX, UY Features: Rubber-like materials.	STIF45 8 nodes 3-D space DOF: UX, UY, UZ Features: P,R,S	STIF64 8 nodes 3-D space DOF: UX, UY, UZ Features: S, R, Anisotropic or crystalline materials.	STIF65 8 nodes 3-D space DOF: UX, UY, UZ Features: P, Concrete, rock, fiberglass, combos etc. materials.
Hyperelastic Solid	Layered Solid	Crack Tip Solid	Tetrahedral Solid	Isoparametric Solid
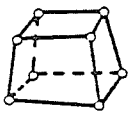		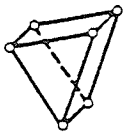	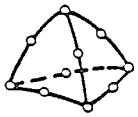	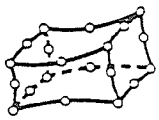
STIF86 8 nodes 3-D space DOF: UX, UY, UZ Features: Rubber-like materials.	STIF46 8 nodes 3-D space DOF: UX, UY, UZ Features: R,S	STIF85 6 nodes 3-D space DOF: UX, UY, UZ Features: P	STIF92 10 nodes 3-D space DOF: UX, UY, UZ Features: P,R,S	STIF95 20 nodes 3-D spac DOF: UX, UY, UZ Features: P,R,S
Structural 2-D Shell		Structural 3-D Shell		
Axisymmetric Harmonic Stress Shell	Plastic Axisymmetric Shell with Torsion	Quadrilateral Shell	Plastic Shell	Membrane Shell
		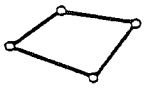	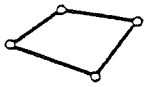	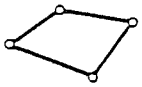
STIF61 2 nodes 2-D space DOF: UX, UY, UZ, ROTZ Features: S	STIF51 2 nodes 2-D space DOF: UX, UY, UZ, ROTZ Features: P,R,S	STIF63 4 nodes 3-D space DOF: UX, UY, UZ, ROTX, ROTY, ROTZ Features: R,S	STIF43 4 nodes 3-D space DOF: UX, UY, UZ, ROTX, ROTY, ROTZ Features: P,R,S	STIF41 4 nodes 3-D space DOF: UX, UY, UZ Features: R,S,G, Cloth-type structu
Isoparametric Shell	Layered Shell	Layered Shell		
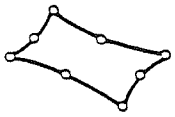	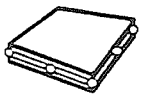	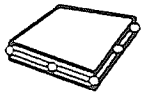		
STIF93 8 nodes 3-D space DOF: UX, UY, UZ, ROTX, ROTY, ROTZ Features: P,R,S	STIF91 8 nodes 3-D space DOF: UX, UY, UZ, ROTX, ROTY, ROTZ Features: R,S, 16 layers	STIF99 8 nodes 3-D space DOF: UX, UY, UZ, ROTX, ROTY, ROTZ Features: R,S, 100 layers.		

P = Plasticity, R = Large Deflection, S = Stress Stiffening, G = Geometric Nonlinearity

Figure 4.0.1 Element Types (continued)

Thermal Point	Thermal Line			
Lumped Thermal Mass	Thermal Bar	Thermal Bar	Convection Link	Radiation Link
				
STIF71 1 node 3-D space DOF: TEMP	STIF32 2 nodes 2-D space DOF: TEMP	STIF33 2 nodes 3-D space DOF: TEMP	STIF34 2 nodes 3-D space DOF: TEMP	STIF31 2 nodes 3-D space DOF: TEMP
Thermal 2-D Solid				
Isoparametric Thermal Solid	Axisymmetric Harmonic Thermal Solid	Triangular Thermal Solid	Isoparametric Thermal Solid	Axisymmetric Harmonic Thermal Solid
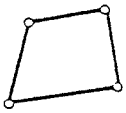	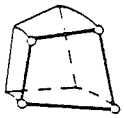	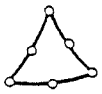	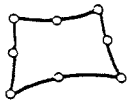	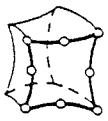
STIF55 4 nodes 2-D space DOF: TEMP	STIF75 4 nodes 2-D space DOF: TEMP	STIF35 6 nodes 2-D space DOF: TEMP	STIF77 8 nodes 2-D space DOF: TEMP	STIF78 8 nodes 2-D space DOF: TEMP
Thermal 3-D Solid			**Thermal Shell**	**Fluid**
Isoparametric Thermal Solid	Isoparametric Thermal Solid	Isoparametric Thermal Solid	Isoparametric Quadrilateral Thermal Shell	Transient Fluid Flow Thermal Pipe
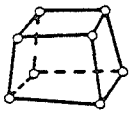	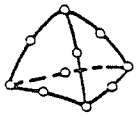	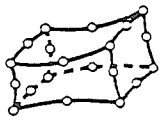	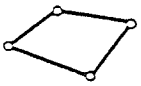	
STIF70 8 nodes 3-D space DOF: TEMP	STIF87 10 nodes 3-D space DOF: TEMP	STIF90 20 nodes 3-D space DOF: TEMP	STIF57 4 nodes 3-D space DOF: TEMP	STIF66 2 nodes 3-D space DOF: PRES, TEMP
Contained Fluid	Axisymmetric Harmonic Contained Fluid	Contained Fluid	Isoparametric Fluid Flow	Isoparametric Acoustic Fluid Flo
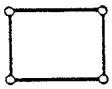	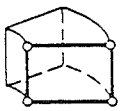	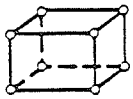	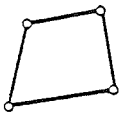	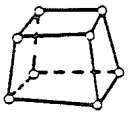
STIF79 4 nodes 2-D space DOF: UX, UY	STIF81 4 nodes 2-D space DOF: UX, UY, UZ	STIF80 8 nodes 3-D space DOF: UX, UY, UZ	STIF15 4 nodes 2-D space DOF: VX, VY, TEMP, PRES	STIF30 8 nodes 3-D spac DOF: UX, UY, UZ PRES

P = Plasticity, R = Large Deflection, S = Stress Stiffening, G = Geometric Nonlinearity

Figure 4.0.1 Element Types (continued)

Electric				
Thermal-Electric Line  STIF68 2 nodes 3-D space DOF: TEMP, VOLT	Thermal-Electric Solid 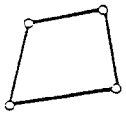 STIF67 4 nodes 2-D space DOF: TEMP, VOLT	Thermal-Electric Solid 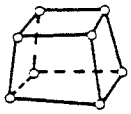 STIF69 8 nodes 3-D space DOF: TEMP, VOLT	Isoparametric Magnetic-Thermal-Electric Solid 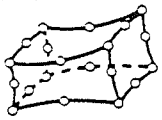 STIF97 20 nodes 3-D space DOF: TEMP, VOLT, MAG	
Multi-field			**Specialty**	
Multi-field Solid 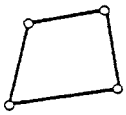 STIF13 4 nodes 2-D space DOF: UX, UY, TEMP, VOLT, MAG Features: R, S	Multi-field Solid 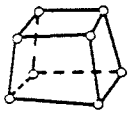 STIF5 8 nodes 3-D space DOF: UX, UY, UZ, TEMP, VOLT, MAG	Tetrahedral Multi-field Solid 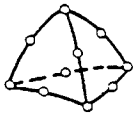 STIF98 10 nodes 3-D space DOF: UX, UY, UZ, TEMP, VOLT, MAG Features: S	Interface 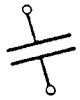 STIF12 2 nodes 2-D space DOF: UX, UY Features: G	Interface  STIF52 2 nodes 3-D space DOF: UX, UY, UZ Features: G
Spring-Damper  STIF14 2 nodes 3-D space DOF: UX, UY, UZ, ROTX, ROTY, ROTZ, PRES, TEMP	Nonlinear Force-Deflection  STIF39 2 nodes 3-D space DOF: UX, UY, UZ, ROTX, ROTY, ROTZ, PRES, TEMP Features: G	Control 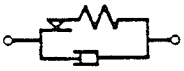 STIF37 4 nodes 3-D space DOF: UX, UY, UZ, ROTX, ROTY, ROTZ, PRES, TEMP Features: G	Combination 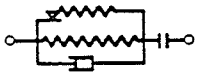 STIF40 2 nodes 3-D space DOF: UX, UY, UZ, ROTX, ROTY, ROTZ, PRES, TEMP Features: G	Contact Surface 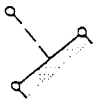 STIF26 3 nodes 2-D space DOF: UX, UY Features: R, G
Revolute Joint 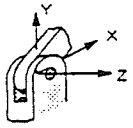 STIF7 5 nodes 3-D space DOF: UX, UY, UZ, ROTX, ROTY, ROTZ Features: R, G	Dynamic Fluid Coupling  STIF38 2 nodes 3-D space DOF: UX, UY, UZ	Stiffness, Mass or Damping Matrix 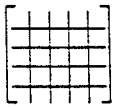 STIF27 2 nodes 3-D space DOF: UX, UY, UZ, ROTX, ROTY, ROTZ	Surface Effect 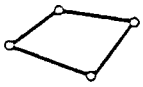 STIF6 4 nodes 3-D space DOF: UX, UY, UZ, TEMP Featues: R, S	Superelement 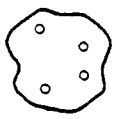 STIF50 Up to 3000+ DOF 2-D or 3-D space DOF: Any Features: Matrix of standard ANSYS elements.

P = Plasticity, R = Large Deflection, S = Stress Stiffening, G = Geometric Nonlinearity

Figure 4.0.1 Element Types (continued)

Determination of Total Heat Loss or Gain

In a thermal analysis, we often want to determine the total amount of heat loss or gain across a structure or through a portion of the structure*. This total heat flow may be obtained by integrating the local heat flux over the entire surface, as shown below:

$$\text{total heat flow} = \int_{\text{area}} (\text{heat flux}) * d(\text{area of surface})$$

or

$$q = \int_{A_s} q'' dA_s$$

* This procedure is not restricted to a steady-state analysis, however, it is presented here because it is required for your steady-state exercise.

In ANSYS, we can perform such integration using the POST1 path commands. Let's evaluate the total heat flow integral for a 2–D problem. Four steps are required:

1. Define the path (**LPATH** command)

2. Map heat flux onto the path by interpolation (**PDEF** command)

3. Integrate heat flux over area associated with the path to obtain total heat flow (**PCALC** command)

4. List and display total heat flow (**PVIEW** command)

Step 1. Define the path (**LPATH** command)

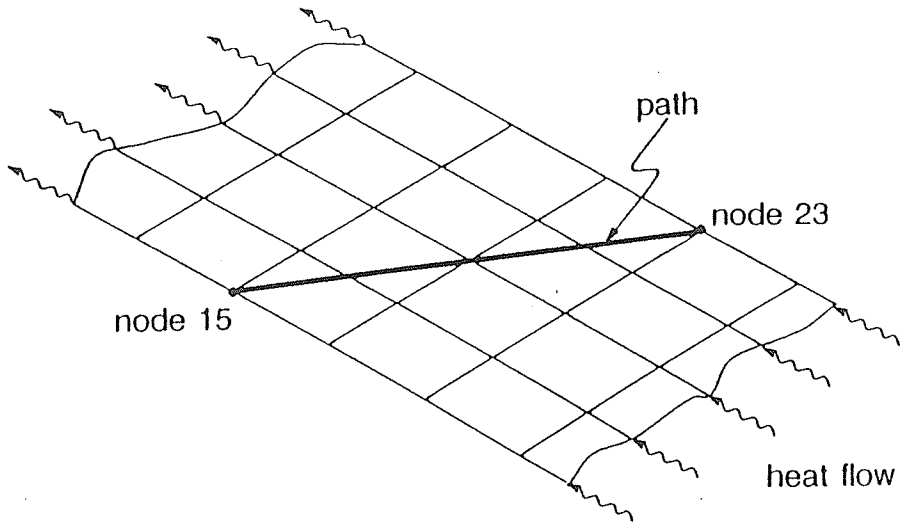

2–D model

```
LPATH,15,23
```

The **LPATH** command defines a path through a model to be used in subsequent path calculations.

LPATH, *NODE1, NODE2, . . ., NODE10*

Up to 10 node numbers used to define a path. The path between two nodes listed consecutively (*NODE1* and *NODE2*, etc.) is determined by linear interpolation.

Note: The path operations discussed in the following steps cannot be performed in non–Cartesian coordinate systems.

Step 2. Map heat flux onto the path by interpolation (PDEF command)

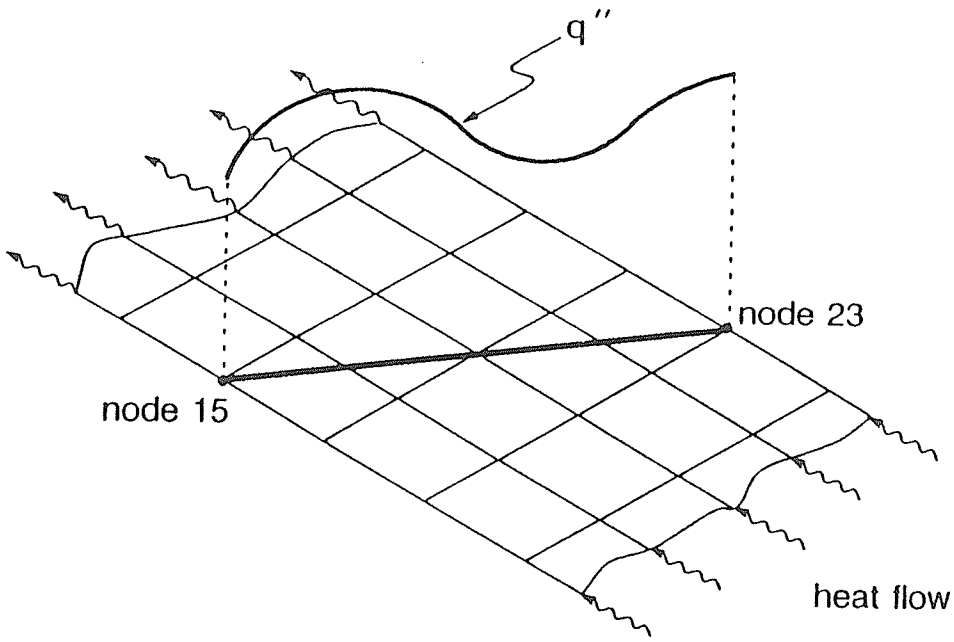


```
PDEF,INTR,FLUX,TFY
```

PDEF, INTR interpolates nodal or element data along the path.

PDEF, *INTR*, *Lab1*, *Lab2*

Lab1	*Lab2*
Arbitrary label to be assigned to the resulting path item.	Item to be interpolated along a path: "Label" — of postdata item (heat flux component) as defined by the **STRESS** command.

Note: The number of heat flux points mapped (by linear interpolation) onto the path = 48*(N–1)+1 where N is the number of nodes defining the path.

Step 3. Integrate heat flux over the area associated with the path to obtain total heat flow (**PCALC** command).

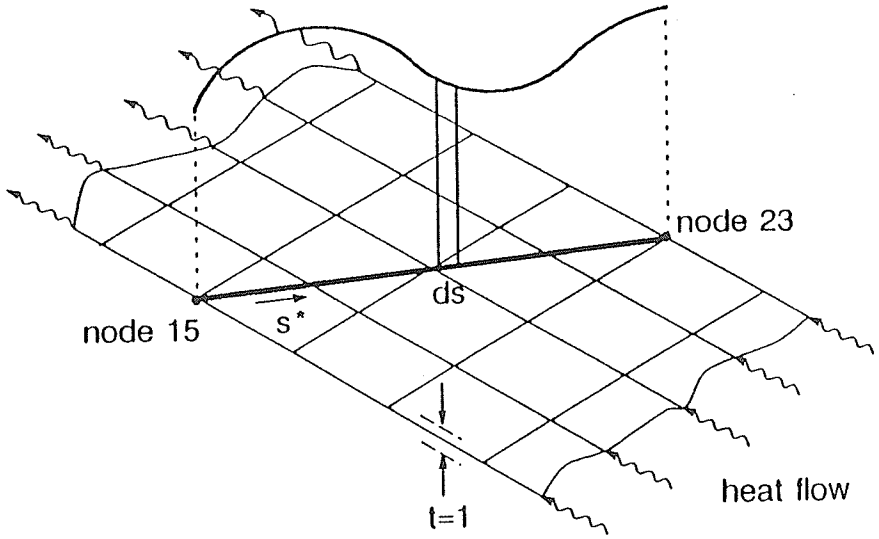


```
PCALC,INTG,FLOW,FLUX,S
```

*Path distance, s, is automatically calculated by ANSYS.

PCALC, INTG integrates a path item with respect to any other path item

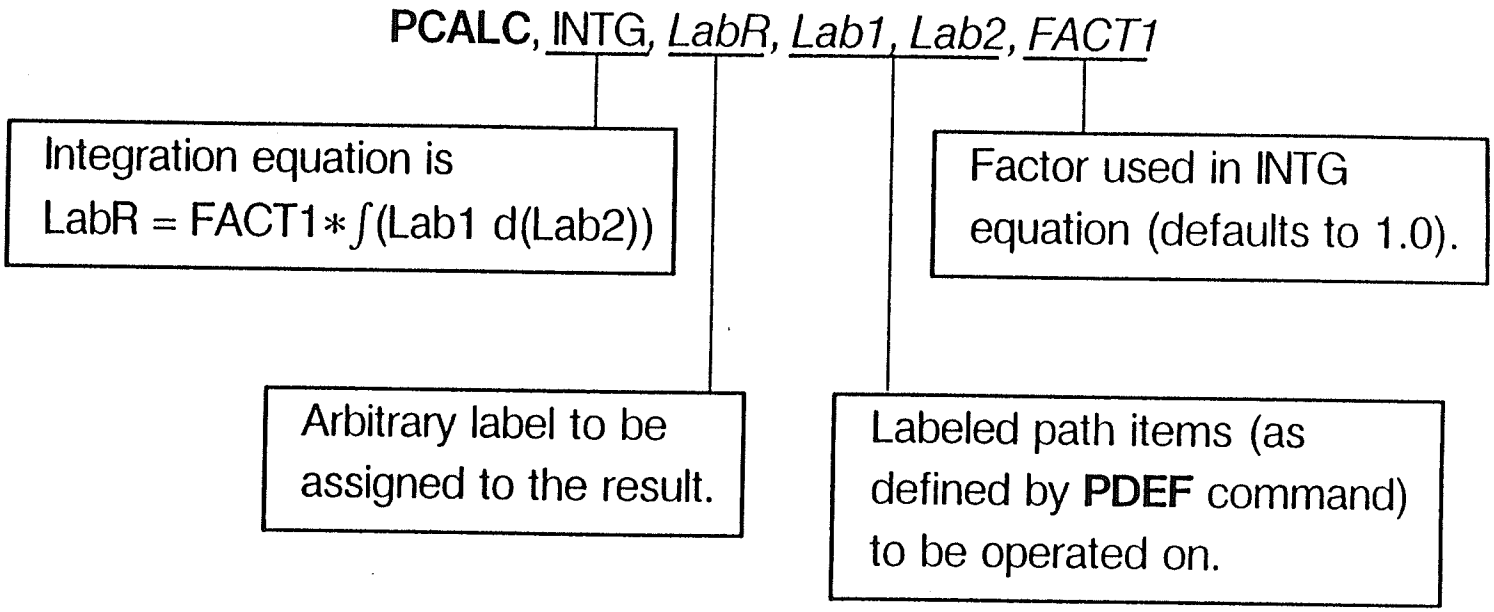

Example 4.2

Objective:

Illustrate the series of POST1 path commands required to determine the total heat flow for the 2–D problem above.

```
/POST1
STRESS,TFY,55,46          * Brings in item 46 (TFY) for STIF55 elements
SET
/PNUM,NODE,1
NPLOT                     * Displays node numbers needed for path definition
LPATH,15,23               * Defines path from node 1 to node 2
PDEF,INTR,FLUX,TFY        * Interpolates TFY onto path and calls it "FLUX".
PCALC,INTG,FLOW,FLUX,S    * Integrates FLUX with respect to S and calls it "FLOW"
PVIEW,PLOT,FLOW,FLUX      * Displays FLOW and FLUX
  .
  .
  .
```

```
$set def [seebaluk.final]
$ansys44a
*****************************************************************
*                                                               *
*  This file define the model geometry, material properties     *
*  and mesh the areas as defined.                               *
*                                                               *
*****************************************************************
/prep7
/title,BASEMENT MODEL BELOW GRADE - NEW VERSION
kan,-1  $et,1,55
mp,kxx,1,2.2     $mp,dens,1,2400      $mp,c,1,653           * Concrete floor
mp,kxx,2,0.0263 ;{A$mp,dens,2,1.1614    $mp,c,2,1007          * Void form
mp,kxx,3,0.33    $mp,dens,3,1520      $mp,c,3,800           * Compacted gravel
mp,kxx,4,2.2     $mp,dens,4,2400      $mp,c,4,653           * Concrete wall
mp,kxx,5,1.35    $mp,dens,5,1490      $mp,c,5,1770          * Unfrozen soil
mp,kxx,6,2.83    $mp,dens,6,200       $mp,c,6,800           * Base clad
mp,kxx,7,0.027   $mp,dens,7,55        $mp,c,7,1210          * Wall insulation
mp,kxx,8,0.43    $mp,dens,8,1200      $mp,c,8,1080          * Drywall
mp,kxx,9,1.115   $mp,dens,9,1920      $mp,c,9,600           * Concrete pile
mp,kxx,10,0.029 $mp,dens,10,42.5     $mp,c,10,1210         * Styrofaom ins.
mp,kxx,11,9999                                             * Snow
mp,kxx,12,1.2    $mp,dens,12,1490     $mp,c,12,1770         * Frozen soil - zor
mp,kxx,13,1.2    mp,c,13,1770         * Frozen soil - zone 2
K,4,7.582,-.344        $K,5,7.658,-.344        $K,6,7.81,-.344
K,7,7.81,-.496         $K,8,7.658,-.496        $K,9,-.152,-.496
K,10,-.152,-.152       $K,11,-7.938,-.152      $K,12,-8.09,-.152
K,13,-8.09,0           $K,14,-7.938,0          $K,15,-7.862,0
K,16,-7.846,0
1,1,2     $l,2,3     $l,3,4     $l,4,5     $l,5,6     $l,6,7     $l,7,8
1,8,9     $l,9,10    $l,10,11   $l,11,12   $l,12,13   $l,13,14   $l,15,14
1,15,16   $l,16,1    $l,14,11   $l,16,11   $l,1,10    $l,2,9     $l,3,8
1,5,8
lssel,,18,21,1 $ldvs,all,,4,3 $lsall
lssel,,5,7,1   $lsasel,,22     $lsasel,,11,13,1 $lsasel,,17 $ldvs,all,,1 $lsa
ldvs,16,,5     $ldvs,10,,5     $ldvs,1,,1       $ldvs,9,,1  $ldvs,2,,5
ldvs,8,,5      $ldvs,14,,3,2   $ldvs,4,,3,2     $ldvs,15,,2 $ldvs,3,,2
type,1
mat,1  $elsize,99,,2   $a,13,14,11,12  $amesh,1       $elsize,99
        al,17,14,15,18 $amesh,2        $elsize,99,,2
        a,16,1,10,11   $amesh,3        $a,1,2,9,10    $amesh,4
        a,2,3,8,9      $amesh,5        $elsize,99
        al,3,4,22,21   $amesh,6        $elsize,99,,2
        a,5,6,7,8      $amesh,7
 *
 * Define void form:
 *
K,17,7.658,-.648      $K,18,7.572,-.648       $K,19,-.304,-.648
K,20,-.304,-.304      $K,21,-7.85,-.304       $K,22,-7.938,-.304
l,8,17    $l,17,18  $l,18,19  $l,19,20  $l,20,21  $l,21,22  $l,11,22
l,11,21   $l,10,20  $l,9,19   $l,8,18
lssel,,25,27,1   $ldvs,all,,5  $lsall
lssel,,29,33,1   $lsas,,23     $ldvs,all,,2  $lsall
ldvs,28,,1       $ldvs,26,,1   $ldvs,24,,1
mat,2  $a,11,10,20,21  $amesh,8  $a,10,9,19,20  $amesh,9
        a,9,8,18,19    $amesh,10 $elsize,99
        al,29,30,28    $amesh,11 $al,33,23,24   $amesh,12
 *
 * Define compacted gravel:
 *
```

```
K,23,7.572,-.8    $K,24,-.456,-.8  $K,25,-.456,-.456    $K,26,-7.85,-.456
1,18,23     $1,23,24    $1,24,25    $1,25,26    $1,21,26    $1,20,25    $1,19,24
ldvs,35,,5  $ldvs,37,,5  $ldvs,36,,1
lssel,,38,40,1  $lsasel,,34  $ldvs,all,,2,1.5  $lsall
elsize,99,,2
mat,3  $a,21,20,25,26  $amesh,13  $a,20,19,24,25  $amesh,14
       a,19,18,23,24  $amesh,15
 *
 * Define left wall:
 *
k,27,-7.938,-0.456    $k,28,-8.167,-0.456  $k,29,-8.167,-0.304
k,30,-8.167,-0.152    $k,31,-8.167,0       $k,32,-8.167,0.622
k,33,-7.938,0.622     $k,34,-8.09,0.622
l,22,27  $l,27,28  $l,28,29  $l,29,30  $l,30,31  $l,31,32  $l,32,34
l,33,14  $l,31,13  $l,30,12  $l,29,22  $l,12,22  $l,13,34  $l,34,33
lssel,,43,45,1  $lsasel,,41,52,11  $ldvs,all,,1  $lsall
ldvs,46,,2      $ldvs,48,,2        $ldvs,50,,2   $ldvs,42,,2
ldvs,51,,2      $ldvs,47,,2        $ldvs,53,,2   $ldvs,54,,1
ldvs,49,,2
mat,4  $a,22,27,28,29  $amesh,16  $a,12,22,29,30  $amesh,17
       a,13,12,30,31  $amesh,18  $a,13,31,32,34  $amesh,19
       a,34,33,14,13  $amesh,20  $elsize,99
       al,11,29,52    $amesh,21
 *
 * Define right wall:
 *
k,35,7.658,-0.8     $k,36,7.887,-0.8     $k,37,7.887,-0.648
k,38,7.887,-0.496  $k,39,7.887,-0.344  $k,40,7.887,0.622
k,41,7.658,0.622    $k,42,7.81,0.622
l,17,35  $l,35,36  $l,36,37  $l,37,38  $l,38,39  $l,39,40  $l,40,42
l,42,41  $l,41,5   $l,42,6   $l,6,39   $l,7,38   $l,17,37
l,7,17
lssel,,57,59,1  $lsasel,,55  $lsasel,,68  $ldvs,all,,1  $lsall
lssel,,65,67,1  $lsasel,,56,61,5  $ldvs,all,,2 $lsall
ldvs,60,,2  $ldvs,64,,2  $ldvs,63,,2  $ldvs,62,,1
al,7,23,68     $amesh,22  $elsize,99,,2  $a,17,37,36,35  $amesh,23
a,7,38,37,17  $amesh,24   $a,6,39,38,7    $amesh,25
a,42,40,39,6  $amesh,26   $a,41,42,6,5    $amesh,27
 *
 * Define insulation and drywall:
 *
k,46,-7.862,0.622  $k,45,-7.846,0.622  $k,44,7.566,0.622  $k,43,7.582,0.622
l,46,33  $l,46,15  $l,45,46  $l,45,16  $l,43,41  $l,43,4  $l,44,43  $l,44,3
ldvs,69,,3,2  $ldvs,71,,2  $ldvs,70,,2  $ldvs,72,,2  $ldvs,73,,3,2
ldvs,75,,2    $ldvs,74,,2  $ldvs,76,,2
mat,7 $a,33,46,15,14  $amesh,28  $mat,8  $a,46,45,16,15  $amesh,29
mat,7 $a,43,41,5,4    $amesh,30  $mat,8  $a,44,43,4,3    $amesh,31
 *
 * Define baseclad:
 *
k,47,-8.243,-0.304  $k,48,-8.243         $k,49,-8.243,0.0633
k,50,-8.243,0.432   $k,51,-8.243,0.622  $k,52,7.963,-0.648
k,53,7.963          $k,54,7.963,0.063   $k,55,7.963,0.432
k,56,7.963,0.622
l,47,29  $l,48,47  $l,49,48  $l,50,49  $l,50,51  $l,51,32  $l,50,32
l,49,31  $l,52,37  $l,52,53  $l,53,54  $l,55,54  $l,56,55  $l,56,40
l,55,40  $l,54,39
lssel,,77  $lsasel,,82,84,1  $ldvs,all,,3,2  $lsall
ldvs,78,,2  $ldvs,79,,1  $ldvs,80,,2         $ldvs,81,,1
lssel,,85  $lsasel,,90,92,1  $ldvs,all,,3,2  $lsall
```

```
ldvs,86,,3  $ldvs,87,,1  $ldvs,88,,2          $ldvs,89,,1
mat,6  $a,50,32,31,49  $amesh,32  $elsize,99
        al,45,44,77,78,79,84  $amesh,33
        al,82,83,81           $amesh,34
        al,92,87,86,85,58,59  $amesh,35  $elsize,99,,2
        a,40,55,54,39         $amesh,36  $elsize,99
        al,90,89,91           $amesh,37
 *
 * Define styrofoam & gravel:
 *
k,57,-8.846,-0.152  $k,58,-8.846,-0.2153  $k,59,-8.695,-0.162
k,60,-8.556,-0.456  $k,61,-8.256,-0.456   $k,62,-8.256,-0.304
k,63,-8.256,-4      $k,64,-8.167,-3.999   $k,65,-7.938,-3.999
k,66,-7.85,-4       $k,67,8.553,-0.152    $k,68,8.553,-0.215
k,69,8.391,-0.162   $k,70,8.278,-0.8      $k,71,7.978,-0.8
k,72,7.978,-0.648   $k,73,7.978,-4        $k,74,7.887,-3.999
k,75,7.658,-3.999   $k,76,7.572,-4
l,49,57  $l,57,58  $l,58,59  $l,48,59  $l,57,59  $l,59,60  $l,60,61
l,61,62  $l,62,47  $l,62,59  $l,61,63  $l,63,64  $l,64,65  $l,65,66
l,26,66  $l,26,27  $l,28,61  $l,28,64  $l,27,65  $l,23,76  $l,76,75
l,75,74  $l,74,73  $l,71,73  $l,71,36  $l,35,23  $l,35,75  $l,36,74
l,52,72  $l,72,71  $l,71,70  $l,70,69  $l,69,72  $l,54,67  $l,67,68
l,68,69  $l,53,69  $l,67,69
ldvs,93,,3,2  $ldvs,96,,3,2  $ldvs,97,,1   $ldvs,94,,1  $ldvs,95,,1
ldvs,98,,3    $ldvs,100,,3   $ldvs,102,,2  $ldvs,99,,2  $ldvs,101,,3
lssel,,103,111,4             $lsasel,,110,119,9        $lsasel,,112,120,4
ldvs,all,,8,4 $lsall         $lssel,,104,108,2         $lsasel,,109,118,9
lsasel,,113,117,2            $ldvs,all,,1  $lsall      $lssel,,105,114,9
ldvs,all,,2  $lsall          $ldvs,121,,3  $ldvs,122,,3 $ldvs,123,,3
ldvs,124,,3  $ldvs,125,,3    $ldvs,126,,3,2$ldvs,129,,3,2$ldvs,130,,1
ldvs,127,,1  $ldvs,128,,1
elsize,99,,2
mat,10  $a,49,48,59,57  $amesh,38  $elsize,99
         al,97,95,94    $amesh,39  $elsize,99,,2
mat,5   $a,48,47,62,59  $amesh,40  $a,62,61,60,59  $amesh,41
mat,9   $elsize,99      $al,101,77,43,109,100      $amesh,42  $elsize,99,,2
         a,61,28,64,63  $amesh,43  $a,28,27,65,64  $amesh,44
         a,27,26,66,65  $amesh,45  $elsize,99
         a,22,21,26,27  $amesh,46  $a,18,17,35,23  $amesh,47  $elsize,99,,2
         a,23,35,75,76  $amesh,48  $a,35,36,74,75  $amesh,49
         a,36,71,73,74  $amesh,50  $elsize,99
         al,85,121,122,117,57       $amesh,51
mat,3   $elsize,99,,2   $a,72,69,70,71  $amesh,52  $a,53,69,72,52 $amesh,53
mat,10  $a,54,67,69,53  $amesh,54  $elsize,99    $al,130,127,128  $amesh,55
 *
 * Define surrounding soil:
 *
k,77,-20.963,1.432  $k,78,-9,0.519        $k,79,-20.963,0.432
k,80,-9,0.432       $k,81,-20.963,0.237   $k,82,-9,0.237
k,83,-8.35,0.237    $k,84,-20.963,0.043   $k,85,-9,0.043
k,86,-8.35,0.043    $k,87,-20.963,-0.152  $k,88,-9,-0.152
k,89,-8.846,-1      $k,90,-20.963,-15     $k,91,-8.556,-5
k,92,-8.846,-15     $k,93,-7.85,-15       $k,94,-7.85,-5.5
k,95,-7.5,-0.8      $k,96,-0.456,-4       $k,97,-0.456,-5.5
k,98,-0.456,-15     $k,99,7.572,-5.5      $k,100,7.572,-15
k,101,8.553,-15     $k,102,8.278,-5       $k,103,20.963,-15
k,104,8.553,-1.3    $k,105,8.7,-0.152     $k,106,20.963,-0.152
k,107,8.1,0.043     $k,108,8.7,0.043      $k,109,20.963,0.043
k,110,8.1,0.237     $k,111,8.7,0.237      $k,112,20.963,0.237
k,113,8.7,0.432     $k,114,20.963,0.432   $k,115,8.7,0.516
```

```
k,116,20.963,1.432
l,50,78 $l,50,80 $l,83,82 $l,86,85 $l,55,115 $l,55,113 $l,110,111
l,107,108 $l,50,83 $l,49,86 $l,55,110 $l,54,107 $l,78,77 $l,80,79
l,82,81 $l,85,84 $l,88,87 $l,89,90 $l,91,92 $l,94,93 $l,97,98
l,99,100 $l,102,101 $l,104,103 $l,105,106 $l,108,109 $l,111,112
l,113,114 $l,115,11+16 $l,77,79 $l,78,80 $l,115,113 $l,116,114 $l,79,81
l,80,82 $l,113,111 $l,114,112 $l,81,84 $l,82,85 $l,83,86 $l,110,107
l,111,108 $l,112,109 $l,84,87 $l,85,88 $l,85,57 $l,108,67 $l,108,105
l,109,106 $l,87,90 $l,88,89 $l,105,104 $l,106,103 $l,90,92 $l,89,91
l,104,102 $l,103,101 $l,92,93 $l,94,91 $l,102,99 $l,101,100 $l,93,98
l,94,97 $l,66,96 $l,95,24 $l,76,96 $l,99,97 $l,100,98 $l,95,66
l,66,94 $l,96,97 $l,76,99 $l,91,63 $l,73,102 $l,60,89 $l,61,89
l,70,104 $l,71,104 $l,57,88 $l,67,105 $l,24,96 $l,26,95
lssel,,131,138,1 $ldvs,all,,3,2 $lsall $lssel,,139,141,2 $ldvs,all,,3,2 $lsa
lssel,,140,142,2 $ldvs,all,,2   $lsall $lssel,,143,159,1 $ldvs,all,,8   $lsa
lssel,,160,167,1 $ldvs,all,,3   $lsall $lssel,,168,179,1 $ldvs,all,,2   $lsa
lssel,,180,183,1 $ldvs,all,,3   $lsall $lssel,,184,187,1 $ldvs,all,,2   $lsa
lssel,,188,191,1 $ldvs,all,,2   $lsall $lssel,,192,198,1 $ldvs,all,,5   $lsa
ldvs,199,,8      $lssel,,200,202,1
ldvs,all,,2      $lsall          $lssel,,203,208,1 $ldvs,all,,3  $lsall
ldvs,209,,2      $ldvs,210,,2    $ldvs,211,,8      $ldvs,212,,1
mat,11 $elsize,99,,2    $a,77,78,80,79 $amesh,56 $elsize,99
        al,131,132,161  $amesh,57  $al,135,162,136  $amesh,58  $elsize,99,,2
        a,115,116,114,113 $amesh,59
mat,12 $a,79,80,82,81 $amesh,60 $a,80,50,83,82 $amesh,61
       a,55,113,111,110 $amesh,62 $a,113,114,112,111 $amesh,63
mat,13 $a,81,82,85,84    $amesh,64 $a,82,83,86,85     $amesh,65
        a,110,111,108,107 $amesh,66 $a,111,112,109,108 $amesh,67
mat,14 $a,84,85,88,87     $amesh,68 $elsize,99
        a,85,86,49,57     $amesh,69 $a,107,108,67,54   $amesh,70
        elsize,99,,2      $a,108,109,106,105           $amesh,71
        elsize,99         $al,175,176,209              $amesh,72
        al,139,80,140,170 $amesh,73  $al,141,171,142,88 $amesh,74
        al,177,178,210    $amesh,75
mat,5  $al,209,94,95,98,205,181 $amesh,76 $al,205,99,206 $amesh,77
        al,104,105,106,200,189,203    $amesh,78
        al,202,113,114,115,204,190
        amesh,79 $al,123,207,208   $amesh,80 $al,207,124,128,127,210,182
        amesh,81 $al,107,212,199   $amesh,82 $elsize,99,,2
        a,87,88,89,90     $amesh,83   $elsize,99 $a,90,89,91,92 $amesh,84
        a,89,61,63,91     $amesh,85
        elsize,99,,2      $a,91,94,93,92 $amesh,86  $elsize,99
        a,26,25,24,95     $amesh,87
        elsize,99,,2      $a,95,24,96,66  $amesh,88
        a,66,96,97,94     $amesh,89 $a,94,97,98,93 $amesh,90
        a,24,23,76,96     $amesh,91 $a,96,76,99,97 $amesh,92
        a,97,99,100,98    $amesh,93 $a,99,102,101,100 $amesh,94
        a,102,73,71,104   $elsize,99 $amesh,95 $a,102,104,103,101
        amesh,96          $a,104,105,106,103 $amesh,97
finish
/eof
```

```
$set def [seebaluk.final]
$ansys44a

*****************************************************************
*                                                               *
*  This file contains the load for the basement model from      *
*  May 1989 to August 1990.                                     *
*                                                               *
*****************************************************************
/prep7
resume
kbc,0          $tref,5          $tunif,5   $nsel,y,-15   $nt,all,temp,6.1
               nall
time,0    $iter,7,,0          $lssel,,81,89,8          $lsasel,,131,135,4
lsasel,,143,159,16      $lcvsf,all,22.62,6.51         $lsall $lssel,,1,2,1
               lsasel,,16       $lsasel,,72,76,4      $lcvsf,all,10,18.3
               lsall            $lwrite    *1.step1
time,604800     $iter,7,,-1 $lssel,,81,89,8          $lsasel,,131,135,4
lsasel,,143,159,16      $lcvsf,all,22.62,18.7     $lsall $lssel,,1,2,1
               lsasel,,16       $lsasel,,72,76,4      $lcvsf,all,10,18.3
               lsall            $lwrite    *1.step2
time,1209600    $iter,7,,-1 $lssel,,81,89,8          $lsasel,,131,135,4
lsasel,,143,159,16      $lcvsf,all,21.53,16.8     $lsall $lssel,,1,2,1
               lsasel,,16       $lsasel,,72,76,4      $lcvsf,all,10,18.3
               lsall            $lwrite    *1.step3
time,1814400    $iter,7,,-1 $lssel,,81,89,8          $lsasel,,131,135,4
lsasel,,143,159,16      $lcvsf,all,22.62,10.84    $lsall $lssel,,1,2,1
               lsasel,,16       $lsasel,,72,76,4      $lcvsf,all,10,18.3
               lsall            $lwrite    *1.step4
time,2419200    $iter,7,,-1 $lssel,,81,89,8          $lsasel,,131,135,4
lsasel,,143,159,16      $lcvsf,all,24.72,14.08    $lsall $lssel,,1,2,1
               lsasel,,16       $lsasel,,72,76,4      $lcvsf,all,10,18.3
               lsall            $lwrite    *1.step5
time,3024000    $iter,7,,-1 $lssel,,81,89,8          $lsasel,,131,135,4
lsasel,,143,159,16      $lcvsf,all,18.43,13.33    $lsall $lssel,,1,2,1
               lsasel,,16       $lsasel,,72,76,4      $lcvsf,all,10,18.3
               lsall            $lwrite    *1.step6
time,3628800    $iter,7,,-1 $lssel,,81,89,8          $lsasel,,131,135,4
lsasel,,143,159,16      $lcvsf,all,17.9,17.64     $lsall $lssel,,1,2,1
               lsasel,,16       $lsasel,,72,76,4      $lcvsf,all,10,18.3
               lsall             $lwrite    *1.step7
time,4233600    $iter,7,,-1 $lssel,,81,89,8          $lsasel,,131,135,4
lsasel,,143,159,16      $lcvsf,all,25,18.4        $lsall $lssel,,1,2,1
               lsasel,,16       $lsasel,,72,76,4      $lcvsf,all,10,18.3
               lsall             $lwrite    *1.step8
time,4838400    $iter,7,,-1 $lssel,,81,89,8          $lsasel,,131,135,4
lsasel,,143,159,16      $lcvsf,all,26.9,21.8      $lsall $lssel,,1,2,1
               lsasel,,16       $lsasel,,72,76,4      $lcvsf,all,10,18.3
               lsall             $lwrite    *1.step9
time,5443200    $iter,7,,-1 $lssel,,81,89,8          $lsasel,,131,135,4
lsasel,,143,159,16      $lcvsf,all,26.9,22.14     $lsall $lssel,,1,2,1
               lsasel,,16       $lsasel,,72,76,4      $lcvsf,all,10,18.3
               lsall             $lwrite    *1.step10
time,6048000    $iter,7,,-1 $lssel,,81,89,8          $lsasel,,131,135,4
lsasel,,143,159,16      $lcvsf,all,20,20.94       $lsall $lssel,,1,2,1
               lsasel,,16       $lsasel,,72,76,4      $lcvsf,all,10,18.3
               lsall             $lwrite    *1.step11
time,6652800    $iter,7,,-1 $lssel,,81,89,8          $lsasel,,131,135,4
lsasel,,143,159,16      $lcvsf,all,13.15,21.14    $lsall $lssel,,1,2,1
               lsasel,,16       $lsasel,,72,76,4      $lcvsf,all,10,18.3
```

```
              lsall                $lwrite     *1.step12
time,7257600     $iter,7,,-1 $lssel,,81,89,8          $lsasel,,131,135,4
lsasel,,143,159,16       $lcvsf,all,20,24.54        $lsall $lssel,,1,2,1
              lsasel,,16         $lsasel,,72,76,4       $lcvsf,all,10,18.3
              lsall                $lwrite     *1.step13
time,7862400     $iter,7,,-1 $lssel,,81,89,8          $lsasel,,131,135,4
lsasel,,143,159,16       $lcvsf,all,20,21.46        $lsall $lssel,,1,2,1
              lsasel,,16         $lsasel,,72,76,4       $lcvsf,all,10,18.3
              lsall                $lwrite     *1.step14
time,8467200     $iter,7,,-1 $lssel,,81,89,8          $lsasel,,131,135,4
lsasel,,143,159,16       $lcvsf,all,17.32,21.73     $lsall $lssel,,1,2,1
              lsasel,,16         $lsasel,,72,76,4       $lcvsf,all,10,18.3
              lsall                $lwrite     *1.step15
time,9072000     $iter,7,,-1 $lssel,,81,89,8          $lsasel,,131,135,4
lsasel,,143,159,16       $lcvsf,all,19.91,20.7      $lsall $lssel,,1,2,1
              lsasel,,16         $lsasel,,72,76,4       $lcvsf,all,10,18.3
              lsall                $lwrite     *1.step16
time,9676800     $iter,7,,-1 $lssel,,81,89,8          $lsasel,,131,135,4
lsasel,,143,159,16       $lcvsf,all,23.16,18.2      $lsall $lssel,,1,2,1
              lsasel,,16         $lsasel,,72,76,4       $lcvsf,all,10,18.3
              lsall                $lwrite     *1.step17
time,10281600    $iter,7,,7 $lssel,,81,89,8          $lsasel,,131,135,4
lsasel,,143,159,16       $lcvsf,all,17.5,19.3      $lsall $lssel,,1,2,1
              lsasel,,16         $lsasel,,72,76,4       $lcvsf,all,10,18.3
              lsall                $lwrite     *1.step18
lsall
afwrite
finish
/input,27
finish
/eof
$rename file12.dat file39.dat
$ansys44a
/prep7        $resume          $krstrt,18   $nsel,y,-15  $nt,all,temp,6.1
              nall
time,10886400    $iter,7,,0     $lssel,,81,89,8          $lsasel,,131,135,4
lsasel,,143,159,16       $lcvsf,all,23.16,16          $lsall $lssel,,1,2,1
              lsasel,,16         $lsasel,,72,76,4       $lcvsf,all,10,18.3
              lsall                $lwrite     *1.step19
time,11491200    $iter,7,,0      $lssel,,81,89,8          $lsasel,,131,135,4
lsasel,,143,159,16       $lcvsf,all,17.7,14.9     $lsall $lssel,,1,2,1
              lsasel,,16         $lsasel,,72,76,4       $lcvsf,all,10,18.3
              lsall                $lwrite     *1.step20
time,12096000    $iter,7,,0      $lssel,,81,89,8          $lsasel,,131,135,4
lsasel,,143,159,16       $lcvsf,all,26.7,14.48    $lsall $lssel,,1,2,1
              lsasel,,16         $lsasel,,72,76,4       $lcvsf,all,10,18.3
              lsall                $lwrite     *1.step21
time,12700800    $iter,7,,0      $lssel,,81,89,8          $lsasel,,131,135,4
lsasel,,143,159,16       $lcvsf,all,26.8,10.58    $lsall $lssel,,1,2,1
              lsasel,,16         $lsasel,,72,76,4       $lcvsf,all,10,18.3
              lsall                $lwrite     *1.step22
time,13305600    $iter,7,,0      $lssel,,81,89,8          $lsasel,,131,135,4
lsasel,,143,159,16       $lcvsf,all,24.38,11.6    $lsall $lssel,,1,2,1
              lsasel,,16         $lsasel,,72,76,4       $lcvsf,all,10,18.3
              lsall                $lwrite     *1.step23
time,13910400    $iter,7,,0      $lssel,,81,89,8          $lsasel,,131,135,4
lsasel,,143,159,16       $lcvsf,all,20.83,7       $lsall $lssel,,1,2,1
              lsasel,,16         $lsasel,,72,76,4       $lcvsf,all,10,18.3
              lsall                $lwrite     *1.step24
time,14515200    $iter,7,,0      $lssel,,81,89,8          $lsasel,,131,135,4
```

```
lsasel,,143,159,16      $lcvsf,all,18.35,3.25   $lsall $lssel,,1,2,1
                lsasel,,16      $lsasel,,72,76,4      $lcvsf,all,10,18.3
                lsall            $lwrite     *1.step25
time,15120000    $iter,7,,0      $lssel,,81,89,8          $lsasel,,131,135,4
lsasel,,143,159,16      $lcvsf,all,18.59,7.74   $lsall $lssel,,1,2,1
                lsasel,,16      $lsasel,,72,76,4      $lcvsf,all,10,18.3
                lsall            $lwrite     *1.step26
time,15724800    $iter,7,,0      $lssel,,81,89,8          $lsasel,,131,135,4
lsasel,,143,159,16      $lcvsf,all,19.55,5.15   $lsall $lssel,,1,2,1
                lsasel,,16      $lsasel,,72,76,4      $lcvsf,all,10,18.3
                lsall            $lwrite     *1.step27
time,16329600    $iter,7,,0      $lssel,,81,89,8          $lsasel,,131,135,4
lsasel,,143,159,16      $lcvsf,all,22.31,11.11  $lsall $lssel,,1,2,1
                lsasel,,16      $lsasel,,72,76,4      $lcvsf,all,10,18.3
                lsall            $lwrite     *1.step28
time,16934400    $iter,7,,0      $lssel,,81,89,8          $lsasel,,131,135,4
lsasel,,143,159,16      $lcvsf,all,20.4,-5.8    $lsall $lssel,,1,2,1
                lsasel,,16      $lsasel,,72,76,4      $lcvsf,all,10,18.3
                lsall            $lwrite     *1.step29
time,17539200    $iter,7,,0      $lssel,,81,89,8          $lsasel,,131,135,4
lsasel,,143,159,16      $lcvsf,all,22.35,-.073  $lsall $lssel,,1,2,1
                lsasel,,16      $lsasel,,72,76,4      $lcvsf,all,10,18.3
                lsall            $lwrite     *1.step30
time,18144000    $iter,7,,7      $lssel,,81,89,8          $lsasel,,131,135,4
lsasel,,143,159,16      $lcvsf,all,24.45,-10.2  $lsall $lssel,,1,2,1
                lsasel,,16      $lsasel,,72,76,4      $lcvsf,all,10,18.3
                lsall            $lwrite     *1.step31
afwrite
finish
/input,27
finish
/eof
$rename file12.dat file40.dat
$ansys44a
/prep7
resume
krstrt,31
mp,kxx,12,.3    $mp,dens,12,1490    $mp,c,12,1770
mp,kxx,11,.19   $mp,dens,11,500     $mp,c,11,500000  *for dec1-dec31/89
nsel,y,-15          $nt,all,temp,6.1
nall
time,18748800   $iter,7,,0  $lssel,,81,89,8          $lsasel,,131,135,4
lsasel,,143,159,16          $lcvsf,all,19.52,-11    $lsall $lssel,,1,2,1
                lsasel,,16      $lsasel,,72,76,4      $lcvsf,all,10,18.3
                lsall            $lwrite    *1.step32
time,19353600   $iter,7,,0   $lssel,,81,89,8          $lsasel,,131,135,4
lsasel,,143,159,16    $      $lcvsf,all,17.2,-8.6    $lsall $lssel,,1,2,1
                lsasel,,16      $lsasel,,72,76,4      $lcvsf,all,10,18.3
                lsall            $lwrite    *1.step33
time,19958400   $iter,7,,0   $lssel,,81,89,8          $lsasel,,131,135,4
lsasel,,143,159,16          $lcvsf,all,16.7,-10.2   $lsall $lssel,,1,2,1
                lsasel,,16      $lsasel,,72,76,4      $lcvsf,all,10,18.3
                lsall            $lwrite    *1.step34
time,20563200   $iter,7,,0   $lssel,,81,89,8          $lsasel,,131,135,4
lsasel,,143,159,16          $lcvsf,all,21.8,-9.7    $lsall $lssel,,1,2,1
                lsasel,,16      $lsasel,,72,76,4      $lcvsf,all,10,18.3
                lsall            $lwrite    *1.step35
time,21168000   $iter,7,,0   $lssel,,81,89,8          $lsasel,,131,135,4
lsasel,,143,159,16          $lcvsf,all,22.1,-17.1   $lsall $lssel,,1,2,1
                lsasel,,16      $lsasel,,72,76,4      $lcvsf,all,10,18.3
```

```
              lsall                $lwrite    *1.step36
lsall
afwrite
finish
/input,27
finish
/eof
$rename file12.dat file41.dat
$ansys44a
/prep7
resume
krstrt,36
mp,kxx,13,.3     $mp,dens,13,1490     $mp,c,13,1770     *for Jan1-jan31/91
nsel,y,-15            $nt,all,temp,6.1
nall
time,21772800    $iter,7,,0    $lssel,,81,89,8          $lsasel,,131,135,4
                lsasel,,16       $lsasel,,72,76,4       $lcvsf,all,10,18.3
                lsall             $lwrite    *1.step37
time,22377600    $iter,7,,0    $lssel,,81,89,8          $lsasel,,131,135,4
lsasel,,143,159,16             $lcvsf,all,22.27,-23.6  $lsall $lssel,,1,2,1
                lsasel,,16       $lsasel,,72,76,4       $lcvsf,all,10,18.3
                lsall             $lwrite    *1.step38
time,22982400    $iter,7,,0    $lssel,,81,89,8          $lsasel,,131,135,4
lsasel,,143,159,16             $lcvsf,all,21.5,-33     $lsall $lssel,,1,2,1
                lsasel,,16       $lsasel,,72,76,4       $lcvsf,all,10,18.3
                lsall             $lwrite    *1.step39
time,23587200    $iter,7,,0    $lssel,,81,89,8          $lsasel,,131,135,4
lsasel,,143,159,16             $lcvsf,all,21.5,-20.7   $lsall $lssel,,1,2,1
                lsasel,,16       $lsasel,,72,76,4       $lcvsf,all,10,18.3
                lsall             $lwrite    *1.step40
lsall
afwrite
finish
/input,27
finish
/eof
$rename file12.dat file42.dat
$ansys44a
/prep7
resume
krstrt,40
mp,kxx,14,.3     $mp,dens,14,1490     $mp,c,14,1770     *for feb90
nsel,y,-15            $nt,all,temp,6.1
nall
time,24192000    $iter,7,,0   $lssel,,81,89,8          $lsasel,,131,135,4
lsasel,,143,159,16             $lcvsf,all,19.23,-17.9  $lsall $lssel,,1,2,1
                lsasel,,16       $lsasel,,72,76,4       $lcvsf,all,10,18.3
                lsall             $lwrite    *1.step41
time,24796800    $iter,7,,0    $lssel,,81,89,8          $lsasel,,131,135,4
lsasel,,143,159,16             $lcvsf,all,21.81,-10.9  $lsall $lssel,,1,2,1
                lsasel,,16       $lsasel,,72,76,4       $lcvsf,all,10,18.3
                lsall             $lwrite    *1.step42
time,25401600    $iter,7,,0    $lssel,,81,89,8          $lsasel,,131,135,4
lsasel,,143,159,16             $lcvsf,all,22.27,-20    $lsall $lssel,,1,2,1
                lsasel,,16       $lsasel,,72,76,4       $lcvsf,all,10,18.3
                lsall             $lwrite    *1.step43
time,26006400    $iter,7,,0    $lssel,,81,89,8          $lsasel,,131,135,4
lsasel,,143,159,16             $lcvsf,all,23.5,-13.6   $lsall $lssel,,1,2,1
                lsasel,,16       $lsasel,,72,76,4       $lcvsf,all,10,18.3
                lsall             $lwrite    *1.step44
```

```
lsall
afwrite
finish
/input,27
finish
/eof
$rename file12.dat file43.dat
$ansys44a
/prep7
resume
krstrt,44
mp,kxx,12,1.35     $mp,dens,12,1490  $mp,c,12,1770
mp,kxx,14,1.35     $mp,dens,14,1499  $mp,c,14,1770     *for mar90
nsel,y,-15            $nt,all,temp,6.1
nall
time,26611200    $iter,7,,0  $lssel,,81,89,8          $lsasel,,131,135,4
lsasel,,143,159,16            $lcvsf,all,23.42,-10.1  $lsall $lssel,,1,2,1
                lsasel,,16      $lsasel,,72,76,4       $lcvsf,all,10,18.3
                lsall            $lwrite    *1.step45
time,27216000    $iter,7,,0   $lssel,,81,89,8          $lsasel,,131,135,4
lsasel,,143,159,16            $lcvsf,all,28.62,-2.2   $lsall $lssel,,1,2,1
                lsasel,,16      $lsasel,,72,76,4       $lcvsf,all,10,18.3
                lsall            $lwrite    *1.step46
time,27820800    $iter,7,,0   $lssel,,81,89,8          $lsasel,,131,135,4
lsasel,,143,159,16            $lcvsf,all,26.33,-1.66  $lsall $lssel,,1,2,1
                lsasel,,16      $lsasel,,72,76,4       $lcvsf,all,10,18.3
                lsall            $lwrite    *1.step47
time,28425600    $iter,7,,0   $lssel,,81,89,8          $lsasel,,131,135,4
lsasel,,143,159,16            $lcvsf,all,17.69,-7.97  $lsall $lssel,,1,2,1
                lsasel,,16      $lsasel,,72,76,4       $lcvsf,all,10,18.3
                lsall            $lwrite    *1.step48
lsall
afwrite
finish
/input,27
finish
/eof
$rename file12.dat file44.dat
$ansys44a
/prep7
resume
krstrt,48
mp,kxx,13,1.35     $mp,dens,13,1490  $mp,c,13,1770
mp,kxx,11,9999                                        *for april90
nsel,y,-15            $nt,all,temp,6.1
nall
time,29030400    $iter,7,,0  $lssel,,81,89,8          $lsasel,,131,135,4
lsasel,,143,159,16            $lcvsf,all,24.53,-.57   $lsall $lssel,,1,2,1
                lsasel,,16      $lsasel,,72,76,4       $lcvsf,all,10,18.3
                lsall            $lwrite    *1.step49
time,29635200    $iter,7,,0   $lssel,,81,89,8          $lsasel,,131,135,4
lsasel,,143,159,16            $lcvsf,all,21.6,-2.1    $lsall $lssel,,1,2,1
                lsasel,,16      $lsasel,,72,76,4       $lcvsf,all,10,18.3
                lsall            $lwrite    *1.step50
time,30240000    $iter,7,,0   $lssel,,81,89,8          $lsasel,,131,135,4
lsasel,,143,159,16            $lcvsf,all,27.03,-.61   $lsall $lssel,,1,2,1
                lsasel,,16      $lsasel,,72,76,4       $lcvsf,all,10,18.3
                lsall            $lwrite    *1.step51
time,30844800    $iter,7,,0   $lssel,,81,89,8          $lsasel,,131,135,4
lsasel,,143,159,16            $lcvsf,all,29,9.78      $lsall $lssel,,1,2,1
```

```
              lsasel,,16        $lsasel,,72,76,4       $lcvsf,all,10,18.3
              lsall               $lwrite    *1.step52
lsall
afwrite
finish
/input,27
finish
/eof
$rename file12.dat file45.dat
$ansys44a
/prep7
resume
krstrt,52
mp,kxx,12,.8     $mp,dens,12,1490     $mp,c,12,1770
mp,kxx,13,1.2    $mp,dens,13,1490     $mp,c,13,1770
mp,kxx,14,1.2    $mp,dens,14,1490     $mp,c,14,1770     *for may90-aug90
nsel,y,-15            $nt,all,temp,6.1
nall
time,31449600    $iter,7,,0    $lssel,,81,89,8          $lsasel,,131,135,4
lsasel,,143,159,16             $lcvsf,all,17.94,5.44    $lsall $lssel,,1,2,1
               lsasel,,16        $lsasel,,72,76,4       $lcvsf,all,10,18.3
               lsall               $lwrite    *1.step53
time,32054400    $iter,7,,0    $lssel,,81,89,8          $lsasel,,131,135,4
lsasel,,143,159,16             $lcvsf,all,21.9,5.08     $lsall $lssel,,1,2,1
               lsasel,,16        $lsasel,,72,76,4       $lcvsf,all,10,18.3
               lsall               $lwrite    *1.step54
time,32659200    $iter,7,,0    $lssel,,81,89,8          $lsasel,,131,135,4
lsasel,,143,159,16             $lcvsf,all,23.81,6.68    $lsall $lssel,,1,2,1
               lsasel,,16        $lsasel,,72,76,4       $lcvsf,all,10,18.3
               lsall               $lwrite    *1.step55
time,33264000    $iter,7,,0    $lssel,,81,89,8          $lsasel,,131,135,4
lsasel,,143,159,16             $lcvsf,all,19.92,7.86    $lsall $lssel,,1,2,1
               lsasel,,16        $lsasel,,72,76,4       $lcvsf,all,10,18.3
               lsall               $lwrite    *1.step56
time,33868800    $iter,7,,0    $lssel,,81,89,8          $lsasel,,131,135,4
lsasel,,143,159,16             $lcvsf,all,28.68,15.74   $lsall $lssel,,1,2,1
               lsasel,,16        $lsasel,,72,76,4       $lcvsf,all,10,18.3
               lsall               $lwrite    *1.step57
time,34473600    $iter,7,,0    $lssel,,81,89,8          $lsasel,,131,135,4
lsasel,,143,159,16             $lcvsf,all,21.82,16.12   $lsall $lssel,,1,2,1
               lsasel,,16        $lsasel,,72,76,4       $lcvsf,all,10,18.3
               lsall               $lwrite    *1.step58
time,35078400    $iter,7,,0    $lssel,,81,89,8          $lsasel,,131,135,4
lsasel,,143,159,16             $lcvsf,all,21.1,15.63    $lsall $lssel,,1,2,1
               lsasel,,16        $lsasel,,72,76,4       $lcvsf,all,10,18.3
               lsall               $lwrite    *1.step59
time,35683200    $iter,7,,0    $lssel,,81,89,8          $lsasel,,131,135,4
lsasel,,143,159,16             $lcvsf,all,15,16.4       $lsall $lssel,,1,2,1
               lsasel,,16        $lsasel,,72,76,4       $lcvsf,all,10,18.3
               lsall               $lwrite    *1.step60
time,36288000    $iter,7,,0    $lssel,,81,89,8          $lsasel,,131,135,4
lsasel,,143,159,16             $lcvsf,all,15.31,19.1    $lsall $lssel,,1,2,1
               lsasel,,16        $lsasel,,72,76,4       $lcvsf,all,10,18.3
               lsall               $lwrite    *1.step61
time,36892800    $iter,7,,0    $lssel,,81,89,8          $lsasel,,131,135,4
lsasel,,143,159,16             $lcvsf,all,19.64,21.47   $lsall $lssel,,1,2,1
               lsasel,,16        $lsasel,,72,76,4       $lcvsf,all,10,18.3
               lsall               $lwrite    *1.step62
time,37497600    $iter,7,,0    $lssel,,81,89,8          $lsasel,,131,135,4
lsasel,,143,159,16             $lcvsf,all,16.7,18.07    $lsall $lssel,,1,2,1
```

```
                lsasel,,16          $lsasel,,72,76,4        $lcvsf,all,10,18.3
                lsall                $lwrite    *l.step63
time,38102400    $iter,7,,0     $lssel,,81,89,8            $lsasel,,131,135,4
lsasel,,143,159,16              $lcvsf,all,17.12,18.4      $lsall $lssel,,1,2,1
                lsasel,,16          $lsasel,,72,76,4        $lcvsf,all,10,18.3
                lsall                $lwrite    *l.step64
time,38707720    $iter,7,,0     $lssel,,81,89,8            $lsasel,,131,135,4
lsasel,,143,159,16              $lcvsf,all,21.26,18.2      $lsall $lssel,,1,2,1
                lsasel,,16          $lsasel,,72,76,4        $lcvsf,all,10,18.3
                lsall                $lwrite    *l.step65
time,39312000    $iter,7,,0     $lssel,,81,89,8            $lsasel,,131,135,4
lsasel,,143,159,16              $lcvsf,all,19.64,21.57     $lsall $lssel,,1,2,1
                lsasel,,16          $lsasel,,72,76,4        $lcvsf,all,10,18.3
                lsall                $lwrite    *l.step66
time,39916800    $iter,7,,0     $lssel,,81,89,8            $lsasel,,131,135,4
lsasel,,143,159,16              $lcvsf,all,18.71,20.14     $lsall $lssel,,1,2,1
                lsasel,,16          $lsasel,,72,76,4        $lcvsf,all,10,18.3
                lsall                $lwrite    *l.step67
time,40521600    $iter,7,,0     $lssel,,81,89,8            $lsasel,,131,135,4
lsasel,,143,159,16              $lcvsf,all,23.04,18.11     $lsall $lssel,,1,2,1
                lsasel,,16          $lsasel,,72,76,4        $lcvsf,all,10,18.3
                lsall                $lwrite    *l.step68
time,41126400    $iter,7,,0     $lssel,,81,89,8            $lsasel,,131,135,4
lsasel,,143,159,16              $lcvsf,all,19.12,18.7      $lsall $lssel,,1,2,1
                lsasel,,16          $lsasel,,72,76,4        $lcvsf,all,10,18.3
                lsall                $lwrite    *l.step69
time,41731200    $iter,7,,0     $lssel,,81,89,8            $lsasel,,131,135,4
lsasel,,143,159,16              $lcvsf,all,31.41,21.81     $lsall $lssel,,1,2,1
                lsasel,,16          $lsasel,,72,76,4        $lcvsf,all,10,18.3
                lsall                $lwrite    *l.step70
time,42336000    $iter,7,,0     $lssel,,81,89,8            $lsasel,,131,135,4
lsasel,,143,159,16              $lcvsf,all,18.99,20.92     $lsall $lssel,,1,2,1
                lsasel,,16          $lsasel,,72,76,4        $lcvsf,all,10,18.3
                lsall                $lwrite    *l.step71
lsall
afwrite
finish
/input,27
finish
/eof
$rename file12.dat file46.dat
$show time
$logoff
```

APPENDIX C
Infiltration Calculation and Theory.

TABLE 1

SYMBOLS

Quantity Symbol	Quantity Definition	SI Unit	Unit Symbol
C, C_r	a regression coefficient; a constant used to determine Q_r (Appendix C)	litres/second·Pascal^n	L/s·Pa^n
ELA	equivalent leakage area	metre^2	m^2
NLA	normalized leakage area	$\frac{\text{centimetre}^2}{\text{metre}^2}$	cm^2/m^2
n	a regression coefficient; flow exponent; a constant used to determine ELA (Appendix C)	–	–
P_a	ambient atmospheric pressure	kilopascals	kPa
$\Delta P_{o,i}$	initial pressure difference across the building envelope with the fan(s) not operating and sealed	Pascals	Pa
$\Delta P_{o,f}$	final pressure difference across the building envelope with the fan(s) not operating and sealed	Pascals	Pa
ΔP_m	measured pressure difference across the building envelope	Pascals	Pa
ΔP	corrected pressure difference across the building envelope	Pascals	Pa
P_r	barometric pressure under reference conditions (101.325 kPa)	kilopascals	kPa
Q_a	corrected volumetric air flow rate into the building at outdoor test conditions	litres/second	L/s
Q_m	measured air flow rate indicated by the flow measuring device before any corrections for the difference in the operating temperature and the calibration temperature	litres/second	L/s
Q, Q_r	corrected air flow rate (Appendix C)	litres/second	L/s
$\hat{Q}$	estimated air flow rate (Appendix C)	litres/second	L/s
r	correlation coefficient (Appendix C)	–	–
R	gas constant for air (0.287055 J/g·K)	joules/gram·Kelvin	J/g·K
t_o	outdoor air temperature	degrees Celsius	°C
t_i	intake air temperature at the fan	degrees Celsius	°C
t_r	reference temperature of outside ambient air (20°C)	degrees Celsius	°C
ρ_r	density of air at reference conditions	kilograms/metre^3	kg/m^3

AIR FLOW CORRECTIONS

D-1 GENERAL THEORY

The measured air flow rates (Q_m) need to be corrected for the differences in air density (ρ) between

a. the reference and calibration conditions, and

b. the indoor air moving out through the measuring device and the outdoor air moving in through the leaks in building envelope (the air flow of interest).

---

a. In mass flow measuring devices (orifice plates, nozzles, venturis, pitot tubes, etc.):

$$Q \propto 1.\sqrt{\rho}$$ (see Appendix B-1, par. 6).

Because the calibration curve from Appendix B was used to obtain Q_m from the measuring device output:

$$Q_m = \frac{\text{constant}}{\sqrt{\rho_C}}$$

where ρ_C is the calibration air density.

The true air flow rate through the measuring device is

$$Q_i = \frac{\text{constant}}{\sqrt{\rho_i}}$$

where ρ_i is the indoor air density

Thus $Q_i = Q_m\sqrt{\frac{\rho_C}{\rho_i}}$

b. Continuity of mass for compressible flow means

ρQ = constant

Thus, the in-leakage air flow rate,

$$Q = Q_i \frac{\rho_i}{\rho_o}$$

where ρ_o is the outdoor air density

From par 7.7.1:

$$\rho \propto \frac{p}{t + 273.15}$$

Now the indoor and outdoor atmospheric pressures are essentially the same. Thus the full correction to Q_m to give Q_a is:

$$Q_a = Q_m \frac{(t_o + 273.15)}{(t_i + 273.15)}\sqrt{\frac{P_C}{P_a}\frac{(t_i + 273.15)}{(t_C + 273.15)}}$$

where Q_a is the corrected outside volumetric air flow rate into the building at outdoor test conditions, L/s

Q_m is the measured air flow rate indicated by the flow measuring device before any correction for difference in the operating temperature and the calibration temperature, L/s, from par. 6.2.6

t_o is the outdoor air temperature, °C, from par. 6.1.1

t_i is the indoor air temperature, °C, from par. 6.2.6

t_C is the calibration air temperature, °C, from Appendix B

P_C is the calibration atmospheric pressure, kPa, from Appendix B

P_a is the ambient atmospheric pressure, kPa.

Q_a, as determined using the formula derived in D-1 above is corrected to reference conditions of $t_i = t_o = 20°C$ and $P_a = 101.325$ kPa and yields Q_r as follows:

From D-1:

$$Q_a = Q_m \frac{(t_o + 273.15)}{(t_i + 273.15)} \sqrt{\frac{P_c}{P_a} \cdot \frac{(t_i + 273.15)}{(t_c + 273.15)}}$$

Deriving Q_r for estimating ELA:

$$Q_r = Qa \sqrt{\frac{P_a\,(20 + 273.15)}{101.325\,(t_o + 273.15)}}$$

Thus:

$$Q_r = Q_m \frac{(t_o + 273.15)}{(t_i + 273.15)} \sqrt{\frac{P_c}{P_a} \cdot \frac{(t_i + 273.15)}{(t_c + 273.15)}} \sqrt{\frac{P_a}{101.325} \cdot \frac{(20 + 273.15)}{(t_o + 273.15)}}$$

Simplifying:

$$Q_r = Q_m \sqrt{\frac{(t_o + 273.15)}{(t_i + 273.15)} \cdot \frac{P_c}{101.325} \cdot \frac{(20 + 273.15)}{(t_c + 273.15)}}$$

Note that this can be reduced to:

$$Q_r = Q_m \sqrt{\frac{(t_o + 273.15)}{(t_i + 273.15)}} \times \text{constant for any given fan}$$

where Q_a, Q_m, t_o, t_i, t_c and P_a and P_c are as defined in D-1.

7.6 **Determination of Correlation Coefficient** – Applying the procedure described in Appendix C to the corr data, fit a curve of the form:

$$Q_r = C_r (\Delta P)^n$$

where: Q_r, C_r and ΔP are as defined in par. 7.1.2

n is the flow exponent and is dimensionless.

7.7 **Calculation of Equivalent Leakage Area**

7.7.1 The density of air at the reference conditions of t_r = 20°C and P_r = 101.325 kPa, ρ_r, is:

$$\rho_r = \frac{P_r}{R\,(t_r + 273.15)}$$

where: ρ_r is in units of kg/m³

R = gas constant for air = 0.287055 J/g·K

P_r = barometric pressure under reference conditions (kPa)

t_r = reference temperature of outside ambient air (°C)

Therefore:

$$\rho_r = \frac{101.325}{.287055 \times 293.15} = 1.204097$$

7.7.2 Calculate the equivalent leakage area, ELA, using the following equation:

$$ELA = .001157\ \sqrt{\rho_r} \cdot C_r \cdot 10^{n-0.5}$$

where ELA is in units of m²

ρ_r is the air density at reference conditions, as provided in par. 7.7.1

C_r and n are determined in accordance with par. 7.6.

The above equation is based on the assumption that the leakage openings in the building envelope can be com and represented by a single sharp-edged orifice.

7.8 **Calculation of Normalized Leakage Area**

When the purpose of the test is to compare the ELA of different buildings, it is recommended that the norma leakage area, NLA, should be used. To calculate NLA, use the following equation:

$$NLA = \frac{ELA}{\left(\text{Area of the Building Envelope}\right)} \times 10\,000$$

where: NLA is in units of cm²·m²

ELA is in units of m²

Area of the Building Envelope is in units of m².

8. **TEST REPORT**

8.1 The test report shall include the following information:

a. The name and address of the company which conducted the test

b. The name of the tester

c. The address of the building under test

d. The date of test and the date of the report

e. The test conditions which include the outdoor temperature in degrees Celsius, comments on the wind st direction and variability

f. A description of the building envelope

g. The area in square metres of the building envelope

6.2.12 *Completion of the Test* — After the test:

a. remove all seals applied in accordance with Table 2;

b. reopen dampers as necessary;

c. relight the gas pilot light.

7. CALCULATIONS

7.1 General Description

7.1.1 This method gives an equivalent leakage area (ELA), a C_r value (often used to obtain forced-air change rates) and an air flow rate which are constant for all test ambient conditions.

7.1.2 ΔP, C_r and Q_r are defined as follows:

ΔP is the corrected pressure difference across the building envelope and is in units of Pa.

C_r is a constant used to determine Q_r.

Q_r is a constant used to determine ELA.

7.1.3 The method described in this standard should be used to determine ELA, a constant C_r value and air change rates. If the actual outside air flow under test conditions is required, it can be determined using the following:

$$Q_a = C_r \sqrt{\frac{101.325}{P_a} \frac{(t_o + 273.15)}{(20 + 273.15)}}$$

where: Q_a is the corrected outside volumetric air flow rate into the building at outdoor test conditions (L/s)

Q_r is as defined above (L/s)

P_a is the ambient atmospheric pressure (kPa) from par. 6.1.2

t_o is the outdoor air temperature (°C) from par. 6.1.1.

7.2 Determination of the Area of the Building Envelope

7.2.1 Use interior dimensions when determining the area of the building envelope.

7.2.2 Include all ceilings (flat or sloping), floors and walls (including doors and windows) that are correspondingly below, above and adjacent to unheated spaces and spaces heated to less than 10°C. For example, include:

a. ceilings below unheated attics and roofs;

b. basement floors and floors above unheated basements (or unheated portions thereof), cellars, crawl spaces, cold storage rooms, garages and floors exposed to the ambient environment such as floors above carports, floors of bay windows and floors of buildings (or parts thereof) supported above grade;

c. exterior above grade and below grade walls and walls adjacent to unheated portions of basements, cellars, crawl spaces, cold storage rooms, unheated porches, garages and stairwells to basement entrances.

7.2.3 The area of the building envelope is the total area of all eligible ceilings, floors and walls.

7.3 **Determination of the Interior Volume Enclosed by the Building Envelope** — It is recommended that the interior volume enclosed by the building envelope be determined and recorded. Include the total volume of all rooms specified in accordance with par. 6.1.3.

7.4 **Correction of Air Flow Readings** — Correct each air flow reading for differences in the indoor, outdoor and calibration air temperatures in accordance with Appendix D.

7.5 **Correction of Pressure Difference Readings** — Using the following equation, correct each pressure difference reading, ΔP_m.

$$\Delta P = \Delta P_m \cdot \frac{(\Delta P_{C,i} + \Delta P_{O,i})}{2}$$

APPENDIX D
Calibration of Equipment.

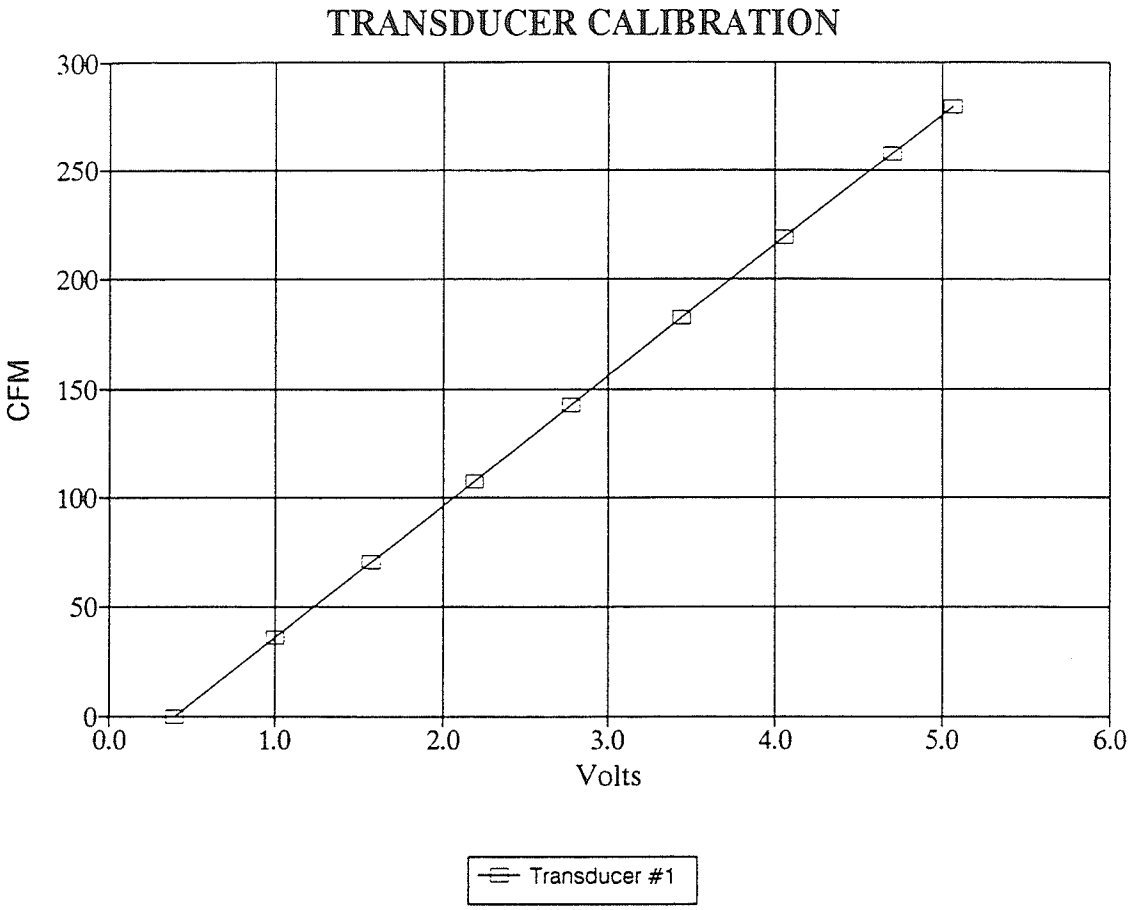
TRANSDUCER CALIBRATION
CFM
300
250
200
150
100
50
0
0.0
1.0
2.0
3.0
4.0
5.0
6.0
Volts
Transducer #1

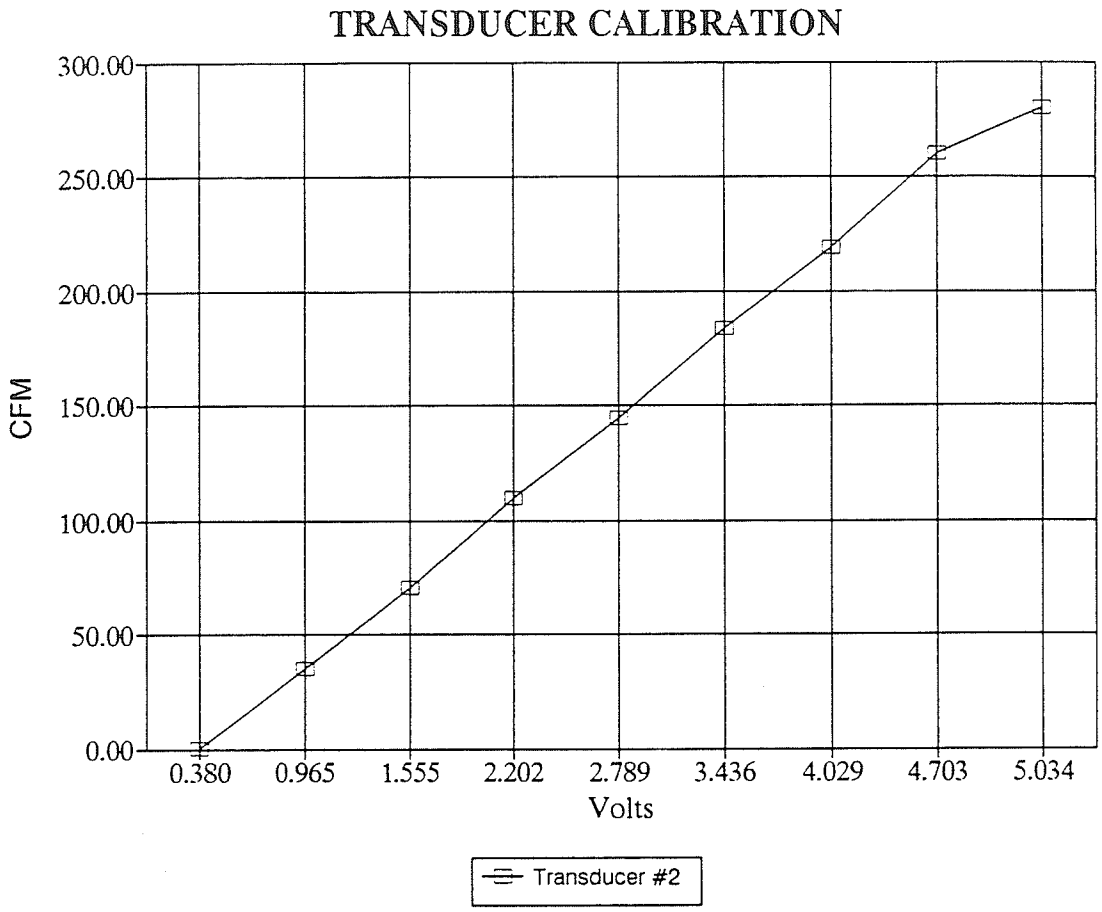
TRANSDUCER CALIBRATION
300.00
250.00
200.00
150.00
100.00
50.00
0.00
CFM
0.380
0.965
1.555
2.202
2.789
3.436
4.029
4.703
5.034
Volts
Transducer #2

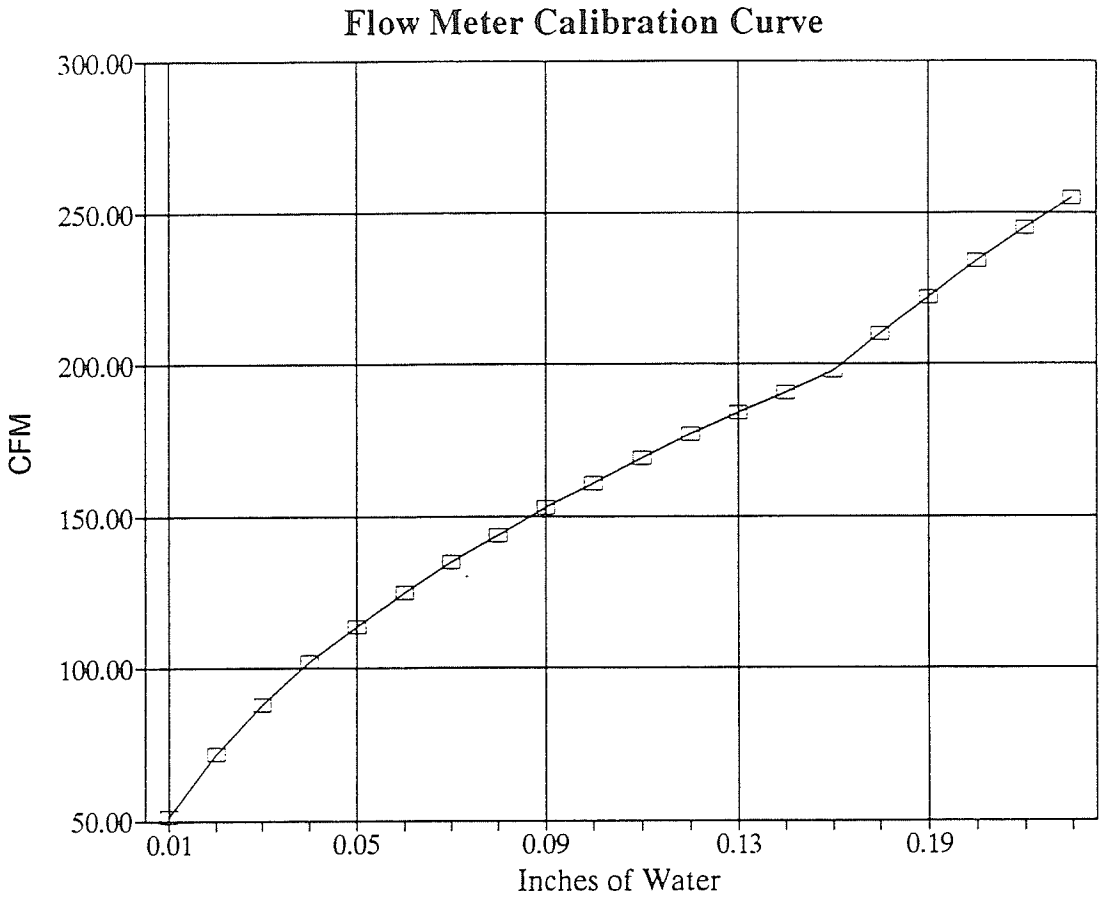
Flow Meter Calibration Curve
300.00
250.00
200.00
150.00
100.00
50.00
CFM
0.01
0.05
0.09
0.13
0.19
Inches of Water

APPENDIX E
HOT-2000 Energy Analysis Output.

```
*****************************************
*                                       *
*              Hot-2000                 *
*        Fortran Version 5.06           *
*  Energy, Mines and Resources CANADA   *
*             Mar 31, 1989              *
*                                       *
*****************************************
```

Builder Code =rec

CLIENT NAME: WELCH
ADDRESS : BOX37, GRP.11, RR 1, ST NORB.

House Data Filename=C:\HOT\WELCH.HDF

Weather Data is for WINNIPEG, MANITOBA

*** TEMPERATURE AND BUILDING MASS ***

Heating Temperatures	Main Floor	= 66.9 F
	Basement	= 65.0 F
	TEMP. Swing from 66.9 F	= 6.0 F

SOIL TYPE: Normal Conductivity: dry sand, loam, clay, low water table

HOUSE THERMAL MASS LEVEL: (1) Wood frame construction, 0.5 in. gyproc walls and ceiling, wooden floor

*** FOUNDATION CONSTRUCTION CHARACTERISTICS ***

Foundation Construction	Attachment Sides	Insulation Placement
Shallow Basement	1 Side	Exterior
Full Basement	1 Side	Exterior

*** WINDOW/GLAZING CHARACTERISTICS ***

Orientation	Average # Glazings	Average Transmission Coefficient	Average Window Height Ft	Average Overhang Width Ft	Average Header Height Ft
South	3.00	.64	5.25	4.53	.30
East	3.00	.64			
North	3.00	.64			
West	3.00	.64			

Component	Area Ft2	R	Heat Loss Mil.BTU	% Annual Heat Loss
Above Grade Components				
Ceiling				
	1528.77	56.00		
	5.69	3.50		
	72.44	31.00		
TOTAL:	1606.90	51.40	8.588	7.42
Main Walls (Less windows and doors)				
	1551.48	24.00		
TOTAL:	1551.48	24.00	16.588	14.32
Doors (Less windows)				
	42.00	12.00		
	8.85	12.00		
TOTAL:	50.85	12.00	1.164	1.01
Exposed or overhanging floors				
	16.00	29.00		
	44.00	26.50		
	64.00	29.00		
TOTAL:	124.00	28.06	1.102	.95
Basement walls above grade				
	396.19	34.50		
	70.00	24.00		
TOTAL:	466.19	32.37	3.716	3.21
Shallow Basement Area				
Basement walls below grade				
	472.54	19.48		
TOTAL:	472.54	19.48	3.707	3.20
Perimeter area				
	159.24	8.69		
TOTAL:	159.24	8.69	1.646	1.42
Centre area				
	706.17	1.14		
TOTAL:	706.17	.00	7.087	6.12
Full Basement Area				
Upper Basement Walls				
	47.50	19.50		
TOTAL:	47.50	19.50	.386	.33
Lower basement walls				
	142.50	19.50		
TOTAL:	142.50	19.50	1.166	1.01

Component		Area Ft2	R	Heat Loss Mil.BTU	% Annual Heat Loss
Perimeter area					
		102.76	8.71		
	TOTAL:	102.76	8.71	1.559	1.58
Centre area					
		102.76	1.14		
	TOTAL:	102.76	1.14	.713	.72

WINDOWS

Orientation		Glazing Area(Ft2)	R Glazing (Shutter)	Heat Loss Mil.BTU	% Annual Heat Loss
South					
		58.70	4.35		
		79.10	4.35		
		74.26	4.35		
		49.13	4.35		
		18.20	4.35		
		44.54	4.35		
		45.94	4.35		
	TOTAL:	369.87	4.35	23.359	23.72
East					
		47.90	4.35		
		8.25	4.35		
	TOTAL:	56.15	4.35	3.546	3.60
North					
		93.02	4.35		
		4.11	4.35		
	TOTAL:	97.13	4.35	6.134	6.23
West					
		47.34	4.35		
		8.91	4.35		
	TOTAL:	56.25	4.35	3.552	3.61

Ventilation

House Volume	Air Change	Heat Loss Mil.BTU	% Annual Heat Loss
18626.5 Ft3	.50 ACH	9.856	10.01

*** AIR LEAKAGE AND VENTILATION ***

Building Envelope Surface Area	=	6112.3 Ft2
Air Leakage Test Results at 50 Pa.(0.2 in H2O)	=	.05 ACH
Equivalent Leakage Area	=	45.8 in2
Building Envelope is Not Sheltered from the Wind.		
R-2000 Normalized Leakage Area Limit	=	.01 in2/ft2
Estimated Airflow to cause a 10 Pa Pressure Difference	=	89 cfm
Estimated Airflow to cause a 20 Pa Pressure Difference	=	135 cfm

R-2000 VENTILATION REQUIREMENTS:

Kitchen,living,dining:	3 rooms @ 10 cfm	= 30 cfm
Bedrooms:	1 rooms @ 10 cfm	= 10 cfm
Bedrooms:	2 rooms @ 10 cfm	= 20 cfm
Bathrooms:	3 rooms @ 10 cfm	= 30 cfm
Utility rooms:	1 rooms @ 20 cfm	= 20 cfm
Other habitable rooms:	2 rooms @ 10 cfm	= 20 cfm

Required continuous ventilation rate	=	130 cfm (.44ACH)
Required Ventilation Capacity (Additional 50 cfm)	=	180 cfm (.61 ACH
Average Ventilation Rate (Balanced)	=	.45 ACH (132 cfm

Ventilation System is : Heat recovery ventilator (HRV)
Manufacturer: LIFEBREATH
Model Number: 195

Fan and Preheater Power at 32 F	=	117. Watts
Fan and Preheater Power at -13 F	=	123. Watts
PreHeater Capacity:	=	0. Watts
Heat Recovery Efficiency at 32 F	=	80. %
Heat Recovery Efficiency at -13 F	=	77. %
Low Temperature Ventilation Reduction	=	1. %
Low Temperature Ventilation Reduction: Airflow Adjustment	=	164 cfm (126%)
Gross Air Leakage and Ventilation Energy Load	=	44.39 Mil.BTU
Seasonal Heat Recovery Ventilator Efficiency	=	78 %
Estimated Ventilation Electrical Load: Heating Hours	=	3.088 Mil.BTU
Estimated Ventilation Electrical Load: Non-Heating Hours	=	.436 Mil.BTU
Net Air Leakage and Ventilation Energy Load	=	11.39 Mil.BTU

*** SPACE HEATING SYSTEM ***

Primary Space Heating Fuel : Natural Gas
Space Heating Equipment : Condensing or pulse furnace/boiler

Space Heating Equipment Manufacturer	:	LENNOX
Space Heating Equipment Model	:	60000
Space Heating System Output Capacity	=	60053.7 BTU/hr
Average Seasonal Efficiency	=	90 %

*** ANNUAL SPACE HEATING SUMMARY ***

Design Heat Loss at -27.4 F	= 42869 BTU/hr
Gross Space Heating Load	= 97.66 Mil.BTU
Sensible Daily Heat Gain From Occupants	= 2.00 kWh/day
Usable Internal Gains	= 14.22 Mil.BTU
Usable Internal Gains Fraction	= 15 %
Usable Solar Gains	= 35.52 Mil.BTU
Usable Solar Gains Fraction	= 36 %
Auxiliary Energy Required	= 47.93 Mil.BTU
Ventilation Equipment Electrical Contribution	= 1.54 Mil.BTU
Furnace/Boiler Annual Energy Consumption	= 51.54 Mil.BTU

*** DOMESTIC WATER HEATING SYSTEM ***

PRIMARY Water Heating Fuel : Electricity
Water Heating Equipment : Electric tank

Water Heating Equipment Manufacturer	:	
Water Heating Equipment Model	:	
Water Heating Equipment Tank Capacity	=	40.0 Imp. Gal
Seasonal Efficiency	=	93 %

*** ANNUAL DOMESTIC WATER HEATING SUMMARY ***

Daily Hot Water Consumption	= 41.0 Imp. Gal/day
Estimated Domestic Water Heating Load	= 12.824 Mil.BTU
PRIMARY Domestic Water Heating Energy Consumption	= 13.790 Mil.BTU

*** LIGHTING AND APPLIANCES SUMMARY ***

Daily Electrical Load	= 9.0 kWh/day
Estimated Annual Energy Consumption	= 3285. kWh

*** R-2000 HOME PROGRAM ENERGY CONSUMPTION SUMMARY REPORT ***

Estimated Annual Space Heating Energy Consumption	=54376 MJ = 15104 kWh
Ventilator Electrical Consumption: Heating Hours	= 3258 MJ = 905.1 kWh
Estimated Annual DHW Heating Energy Consumption	=14549 MJ = 4041 kWh
ESTIMATED ANNUAL SPACE + DHW ENERGY CONSUMPTION	= 72182MJ = 20051 kWh
ANNUAL R-2000 SPACE + DHW ENERGY CONSUMPTION TARGET	= 74361MJ = 20655.9 kWh
Estimated Annual Base Electrical Energy Consumption	= 11826MJ = 3285 kWh
Ventilator Electrical Consumption: Non Heating Hours	= 461MJ = 128 kWh

*** ESTIMATED ANNUAL FUEL CONSUMPTION SUMMARY ***

FUEL	SPACE HEATING	+ DHW HEATING	+ APPLIANCES	= TOTAL
Natural Gas (MCF)	52	.0	.0	52 MCF
Electricity (kWh)	905.1	4041.3	3412.6	8359.1 kWh

**** R-2000 MONTHLY TABLES ***

*** MONTHLY ENERGY PROFILE ***

Month	Energy Load Mil.BTU	Internal Gains Mil.BTU	Solar Gains Mil.BTU	Aux Energy Req Mil.BTU	HRV Eff. %
Jan	21.200	1.225	5.729	14.247	74.6
Feb	17.507	1.106	5.771	10.630	75.1
Mar	15.329	1.225	5.900	8.203	75.7
Apr	8.592	1.185	3.380	4.027	75.4
May	4.946	1.225	2.232	1.489	73.2
Jun	2.345	1.183	1.161	.000	67.7
Jul	1.511	1.090	.421	.000	64.4
Aug	1.910	1.181	.729	.000	67.1
Sep	4.035	1.185	1.955	.894	72.0
Oct	7.164	1.225	2.897	3.042	74.8
Nov	12.839	1.185	3.791	7.863	76.2
Dec	18.427	1.225	4.697	12.505	75.2

****

Energy units: MIL.BTU = Million British Thermal Units (3413 BTU = 1 kWh)

The calculated heat losses and energy consumptions are only estimates, based upon the data entered and assumptions within the program. Actual energy consumption and heat losses will be influenced by construction practices, localized weather, equipment characteristics and the lifestyle of the occupants.

1

```
*****************************************
*                                       *
*              Hot-2000                 *
*         Fortran Version 5.06          *
*  Energy, Mines and Resources CANADA   *
*             Mar 31, 1989              *
*                                       *
*****************************************
```

CLIENT NAME: WELCH
ADDRESS : BOX37, GRP.11, RR 1, ST NORB.

House Data Filename=C:\HOT\STORMON2.HDF

Weather Data is for WINNIPEG, MANITOBA

*** TEMPERATURE AND BUILDING MASS ***

Heating Temperatures	Main Floor	= 19.4 C
	Basement	= 18.3 C
	TEMP. Swing from 19.4 C	= 3.3 C

SOIL TYPE: Normal Conductivity: dry sand, loam, clay, low water table

HOUSE THERMAL MASS LEVEL: (1) Wood frame construction, 12.5 mm gyproc walls and ceiling, wooden floor

*** FOUNDATION CONSTRUCTION CHARACTERISTICS ***

Foundation Construction	Attachment Sides	Insulation Placement
Shallow Basement	1 Side	Interior
Full Basement	1 Side	Interior

*** WINDOW/GLAZING CHARACTERISTICS ***

Orientation	Average # Glazings	Average Transmission Coefficient	Average Window Height m	Average Overhang Width m	Average Header Height m
South	3.00	.64	1.60	1.38	.09
East	3.00	.64			
North	3.00	.64			
West	3.00	.64			

*** BUILDING PARAMETERS ***

Component	Area m2	RSI	Heat Loss MJ	% Annual Heat Loss
Above Grade Components				
Ceiling	142.03	9.86		
	.53	.62		
	6.73	5.46		
TOTAL:	149.29	9.05	9061.3	7.50
Main Walls (Less windows and doors)	144.14	4.23		
TOTAL:	144.14	4.23	17501.1	14.49
Doors (Less windows)	3.90	2.11		
	.82	2.11		
TOTAL:	4.72	2.11	1228.2	1.02
Exposed or overhanging floors	1.49	5.11		
	4.09	4.67		
	5.95	5.11		
TOTAL:	11.52	4.94	1163.2	.96
Basement walls above grade	36.81	6.08		
	6.50	4.23		
TOTAL:	43.31	5.70	3921.1	3.25
Shallow Basement Area				
Basement walls below grade	43.90	3.43		
TOTAL:	43.90	3.43	4151.6	3.44
Perimeter area	14.79	1.53		
TOTAL:	14.79	1.53	1860.4	1.54
Centre area	65.61	.20		
TOTAL:	65.61	.20	6260.0	5.18
Full Basement Area				
Upper Basement Walls	4.41	3.43		
TOTAL:	4.41	3.43	406.9	.34
Lower basement walls	13.24	3.43		
TOTAL:	13.24	3.43	1135.9	.94

Component		Area m2	RSI	Heat Loss MJ	% Annual Heat Loss
Perimeter area					
		9.55	1.53		
	TOTAL:	9.55	1.53	1200.3	.99
Centre area					
		9.55	.20		
	TOTAL:	9.55	.20	866.7	.72

WINDOWS

Orientation		Glazing Area(m2)	RSI Glazing (Shutter)	Heat Loss MJ	% Annual Heat Loss
South					
		34.36	.70		
	TOTAL:	34.36	.70	26971.7	22.32
East					
		5.22	.70		
	TOTAL:	5.22	.70	4094.6	3.39
North					
		9.02	.70		
	TOTAL:	9.02	.70	7082.9	5.86
West					
		5.23	.70		
	TOTAL:	5.23	.70	4101.9	3.39

Ventilation

House Volume	Air Change	Heat Loss MJ	% Annual Heat Loss
795.00 m3	.65 ACH	30062.0	24.88

*** AIR LEAKAGE AND VENTILATION ***

Building Envelope Surface Area	=	567.9 m2
Air Leakage Test Results at 50 Pa.(0.2 in H2O)	=	3.02 ACH
Equivalent Leakage Area	=	896.60 cm2
Building Envelope is Sheltered from the Wind.		
R-2000 Normalized Leakage Area Limit	=	.70 cm2/m2
Estimated Airflow to cause a 10 Pa Pressure Difference	=	134 L/s
Estimated Airflow to cause a 20 Pa Pressure Difference	=	204 L/s

R-2000 VENTILATION REQUIREMENTS:

Kitchen,living,dining:	3 rooms @ 5 L/s	= 15 L/s
Bedrooms:	1 rooms @ 10 L/s	= 10 L/s
Bedrooms:	2 rooms @ 5 L/s	= 10 L/s
Bathrooms:	3 rooms @ 5 L/s	= 15 L/s
Utility rooms:	1 rooms @ 5 L/s	= 5 L/s
Other habitable rooms:	2 rooms @ 5 L/s	= 10 L/s
Basement:	1 rooms @ 10 L/s	= 10 L/s

Required continuous ventilation rate = 75 L/s (.34 AC
Average Ventilation Rate (Balanced) = .48 ACH (106 L/

Ventilation System is : Heat recovery ventilator (HRV)
Manufacturer: LIFEBREATH
Model Number: 195

Fan and Preheater Power at 0 C = 117. Watts
Fan and Preheater Power at -25 C = 123. Watts
PreHeater Capacity: = 0. Watts
Heat Recovery Efficiency at 0 C = 78. %
Heat Recovery Efficiency at -25 C = 74. %
Low Temperature Ventilation Reduction = 1. %
Low Temperature Ventilation Reduction: Airflow Adjustment = 0 L/s (00.0

Gross Air Leakage and Ventilation Energy Load =85387.6 MJ
Seasonal Heat Recovery Ventilator Efficiency = 76.1 %
Estimated Ventilation Electrical Load: Heating Hours = 3258.5 MJ
Estimated Ventilation Electrical Load: Non-Heating Hours = 459.5 MJ
Net Air Leakage and Ventilation Energy Load =31691.3 MJ

*** SPACE HEATING SYSTEM ***

Primary Space Heating Fuel : Natural Gas
Space Heating Equipment : Condensing or pulse furnace/boiler

Space Heating Equipment Manufacturer : LENNOX
Space Heating Equipment Model : 60000
Space Heating System Output Capacity = 17.6 kW
SGUE Seasonal Efficiency = 89 %

*** ANNUAL SPACE HEATING SUMMARY ***

Design Heat Loss at -33.0 C	= 16587. Watts
Gross Space Heating Load	=120821. MJ
Sensible Daily Heat Gain From Occupants	= 2.00 kWh/day
Usable Internal Gains	= 14984. MJ
Usable Internal Gains Fraction	= 12.4 %
Usable Solar Gains	= 46514. MJ
Usable Solar Gains Fraction	= 38.5 %
Auxiliary Energy Required	= 59324. MJ
Ventilation Equipment Electrical Contribution	= 1629. MJ
Furnace/Boiler Annual Energy Consumption	= 64825. MJ

*** DOMESTIC WATER HEATING SYSTEM ***

PRIMARY Water Heating Fuel : Electricity
Water Heating Equipment : Electric tank

Water Heating Equipment Manufacturer	:	
Water Heating Equipment Model	:	
Water Heating Equipment Tank Capacity	=	.0 Litres
Seasonal Efficiency	=	93 %

*** ANNUAL DOMESTIC WATER HEATING SUMMARY ***

Daily Hot Water Consumption	= 186.4 Litres /
Estimated Domestic Water Heating Load	= 13530. MJ
PRIMARY Domestic Water Heating Energy Consumption	= 14549. MJ

*** LIGHTING AND APPLIANCES SUMMARY ***

Daily Electrical Load	= 9.0 kWh/day
Estimated Annual Energy Consumption	= 3285. kWh

*** R-2000 HOME PROGRAM ENERGY CONSUMPTION SUMMARY REPORT ***

Estimated Annual Space Heating Energy Consumption	= 64825. MJ	= 18007.0	kW
Ventilator Electrical Consumption: Heating Hours	= 3258. MJ	= 905.1	kW
Estimated Annual DHW Heating Energy Consumption	= 14549. MJ	= 4041.3	kW
ESTIMATED ANNUAL SPACE + DHW ENERGY CONSUMPTION	= 82632. MJ	= 22953.5	kW
ANNUAL R-2000 SPACE + DHW ENERGY CONSUMPTION TARGET	= 102767. MJ	= 28546.4	kW
Estimated Annual Base Electrical Energy Consumption=	11826. MJ	= 3285.0	kW
Ventilator Electrical Consumption: Non Heating Hours=	459. MJ	= 127.6	kW

*** ESTIMATED ANNUAL FUEL CONSUMPTION SUMMARY ***

FUEL	SPACE HEATING	+ DHW HEATING	+ APPLIANCES	= TOTAL
Natural Gas (m3)	1739.2	.0	.0	1739.2 m3
Electricity (kWh)	905.1	4041.3	3412.6	8359.1 kWh

**** R-2000 MONTHLY TABLES ***

*** MONTHLY ENERGY PROFILE ***

Month	Energy Load MJ	Internal Gains MJ	Solar Gains MJ	Aux Energy Req MJ	HRV Eff. %
Jan	22222.0	1292.3	7011.6	13918.1	75.0
Feb	18270.4	1167.2	6058.8	11044.5	75.9
Mar	15891.9	1292.3	6166.5	8433.2	77.0
Apr	9037.4	1250.6	4615.0	3171.8	77.6
May	5158.8	1292.3	3177.3	689.3	76.2
Jun	2388.8	1245.8	1142.9	.0	72.4
Jul	1507.7	1121.4	386.3	.0	70.1
Aug	1955.5	1236.0	719.5	.0	72.0
Sep	4253.1	1250.6	2763.4	239.1	75.4
Oct	7596.4	1292.3	4035.6	2268.5	77.2
Nov	13295.2	1250.6	4752.9	7291.8	77.9
Dec	19244.2	1292.3	5684.6	12267.3	76.0

****

Energy units: MJ = Megajoules (3.6 MJ = 1 kWh)

The calculated heat losses and energy consumptions are only estimates, based upon the data entered and assumptions within the program. Actual energy consumption and heat losses will be influenced by construction practices, localized weather, equipment characteristics and the lifestyle of the occupants.